POTENTIAL FOR POTASSIUM RECOVERY AS K-STRUVITE

by

Aline Miriam Bennett

B.Eng. (Bioresource), McGill University, 2010

A THESIS SUBMITTED IN PARTIAL FULFILLMENT OF

THE REQUIREMENTS FOR THE DEGREE OF

MASTER OF APPLIED SCIENCE

in

THE FACULTY OF GRADUATE AND POSTDOCTORAL STUDIES

(Civil Engineering)

THE UNIVERSITY OF BRITISH COLUMBIA

(Vancouver)

July 2015

ABSTRACT

Crystallization of NH_4-struvite ($MgNH_4PO_4:6H_2O$) pellets has proven to be a successful method of recovering nitrogen and phosphorus from wastewaters. Thus far, little work has been done on potassium recovery since it is not considered a water pollutant, nor do we face potassium shortages. However, potassium is an essential plant macronutrient and we are seeing worldwide imbalances in nutrient and fertilizer use, as well as a need for a slow release potassium fertilizer. Development of a full complement NPK fertilizer with NH_4-struvite and K-struvite components may have great potential. Given this, research into potassium recovery through crystallization of K-struvite ($MgKPO_4: 6H_2O$) is relevant and complements previous work done with NH_4-struvite.

The goals of this research were to develop fundamental understanding of K-struvite formation as the first step to recovering potassium, and eventually produce a full complement NPK slow-release fertilizer from wastewaters. This required the determination of new solubility product values for K-struvite at different temperatures, followed by bench-scale experiments to assess K-struvite synthesis under various solution conditions. A model to simulate each batch experiment and to predict optimal supersaturation conditions for K-struvite precipitation was developed using PHREEQC, aqueous equilibrium modelling software. Finally, initial experiments in the UBC fluidized bed reactor (UBC-FBR) were undertaken to assess the pelletization potential of K-struvite.

New solubility product values for K-struvite indicate that it is less soluble than previously reported, and the values determined at 10, 25 and 35°C fit the Van't Hoff model. Optimal Mg:K:P molar ratio for synthesis of pure K-struvite was found to be approximately 3:50:1 in a wastewater matrix with pH 8, $P-PO_4$ concentration of 8 mM and a Mg:P ratio of 3:1. These concentrations were used in the UBC-FBR to assess the pelletization potential of K-struvite. These initial reactor runs were inconclusive due to an inability to stabilize the reactor without seeding. It would be recommended to seed the reactor during start-up in order to be able to compare process performance with the NH_4-struvite crystallization process in the UBC-FBR.

This study showed that formation of pure K-struvite is possible given the right supersaturation conditions in solution, requiring high potassium concentrations.

PREFACE

This thesis is composed of original research performed by the author. Dr. Sergey Lobanov performed the data modeling for $K_{sp\text{-}K}$ determination described in Chapter 5.

TABLE OF CONTENTS

LIST OF TABLES

LIST OF FIGURES

LIST OF ABBREVIATIONS AND SYMBOLS

CRT	Crystal retention time
EC	Electrical conductivity
FBR	Fluidized bed reactor
HRT	Hydraulic retention time
K-struvite	$MgKPO_4:6H_2O$
$K_{sp,}$	Solubility product
K_{sp-K}	Solubility product of K-struvite
NPK	Nitrogen, phosphorus and potassium
NH_4-struvite	$MgNH_4PO_4:6H_2O$
pK_{sp}	$-log_{10}(K_{sp})$
pK_{sp-K}	$-log_{10}(K_{sp-K})$
OF	Objective function, Equation 44
PHREEQC	Aqueous equilibrium modelling software developed by the US Geological Survey
S	Supersaturation ratio
S_K	K-struvite supersaturation ratio, Equation 34
SI	Saturation index
UBC	University of British Columbia
WWTP	Wastewater treatment plant
μ	Ionic strength
USD	US dollars
XRD	X-ray diffraction

ACKNOWLEDGEMENTS

This work is dedicated to all those working towards
a world where wastewater is a resource.

CHAPTER 1
INTRODUCTION

Potassium is an essential plant macronutrient with no known substitutes. In 2014, thirty one million tonnes of potassium fertilizer (as K_2O) were applied worldwide, with that demand expected to increase by about 3% per year (FAO 2015). Potassium fertilizers are mined from potash deposits and currently there are no established methods for recovery of potassium.

Drivers for nutrient recovery research have transitioned from practical concerns around struvite scale removal in wastewater treatment plants to global concerns around water quality, nutrient cycling, and food security. Nutrient recovery work has focused primarily on phosphorus, because of supply and water quality issues, and to a lesser extent, nitrogen. As mentioned above, potassium is an essential plant macronutrient, along with nitrogen and phosphorus and the majority of potassium used in agriculture is derived from mined potash (Jasinski 2012). Little work has been done on potassium recovery since it is not considered a water pollutant nor are we facing potassium shortages. However, we know that massive soil potassium deficiencies exist (Römheld and Kirkby 2010; Smil 1999), that there are global imbalances in soil nutrients and fertilizer use (MacDonald et al. 2011), and there is a need for a slow release potassium fertilizer (Adeoye et al., 2001; Manning 2011).

The major driver for this research is the potential to produce a full complement fertilizer, one that includes nitrogen, phosphorus and potassium (NPK) fertilizer entirely from wastes. A pelletized product incorporating both struvite and K-struvite would provide the nitrogen, phosphorus and potassium components of traditional fertilizers. Given the high cost of conventional fertilizers, such a product could have significant market value (Manning 2011).

This thesis explores the beginnings of research on potassium recovery. The questions: (a) why recover potassium? (b) how does one recover potassium? and (c) from where is potassium recovered? were considered through this work. The general goal of this thesis is to provide a comprehensive overview, based on the current state of knowledge, of the potential for recovering potassium through crystallization as magnesium potassium phosphate hexahydrate, or as it is more commonly known, K-struvite.

Recovery of nutrients through crystallization has become one of the more promising methods of extracting valuable nutrients from wastewaters. Where conventional wastewater treatment technologies are able to remove nitrogen and phosphorus from wastewater streams, most of them are not efficient enough or applicable for beneficial reuse and recovery. Crystallization of NH_4-struvite has been successful in this regard, at recovering nitrogen and phosphorus for beneficial reuse as fertilizer (Bhuiyan et al. 2008; Britton et al. 2005; Fattah 2004). Potassium is found in high concentrations in animal manures, and applying those to land is a form of nutrient recovery. However, manures can only be transported a short distance economically, often leading to nutrient overload to the receiving land base. Potassium recovery through

crystallization offers an opportunity to recover the valuable nutrients from wastes in a concentrated, easily transported form.

A handful of papers have been published on recovery of potassium through crystallization as K-struvite. Work by a few researchers, such as Zeng & Li (2006), Wilsenach (2007), Satoshi et al., (2013) have indicated that it is possible. Important takeaways from their research indicate the need for a high K:N ratio in solution for successful K-struvite formation.

In this current work, it became important, given the limited information in the literature, to take a step back and to learn more about the fundamental properties of K-struvite, which are important in predicting how K-struvite will form and behave. Therefore, the goals of this research were to develop fundamental understanding of K-struvite formation as the first step to recovering potassium, and eventually producing a full complement NPK slow-release fertilizer from liquid wastes. This resulted in (a) the determination of new solubility product (K_{sp}) values for K-struvite at different temperatures, followed by (b) bench-scale batch experiments to assess K-struvite synthesis under various solution conditions. A model to simulate each batch experiment for K-struvite precipitation was developed using PHREEQC, aqueous equilibrium modelling software. Finally, (c) initial experiments in the UBC fluidized bed reactor (FBR) were performed to assess the pelletization potential of K-struvite.

CHAPTER 2
BACKGROUND & CONTEXT FOR RESEARCH

Recovery of potassium is interesting for a few reasons; the expected long-term increase in demand for potassium-based fertilizers coupled with high prices could make a product like K-struvite a valuable commodity. However, perhaps a more compelling reason for interest in K-struvite may be its potential for creating a slow-release full complement NPK fertilizer. As well, potash production is concentrated in Canada and Russia, making potash fertilizers expensive for the agriculture economies of developing nations, leading to potassium deficiencies, evident in crop productivity (Adeoye et al., 2001; Sheldrick et al., 2003). Nations without potash or phosphate rock deposits may one day benefit from the development of this kind of technology, by allowing for self sufficiency in fertilizer production.

2.1 Potassium in nature and agriculture

The potassium story differs from the phosphorus story in that it has not been found to cause any environmental or water quality issues when found in excess in watercourses. It is not toxic and does not cause eutrophication; therefore, there is no guideline in Canada for its levels in water or soils (Canadian Council of Ministers of the Environment 2014).

Potassium plays a specific ecological role in nature. It is one of the most important nutrients in plant and animal health, being third most likely, after nitrogen and phosphorous to limit plant productivity. Potassium is not actually incorporated into the structure of organic compounds, rather it remains in its ionic form, and acts as an activator for over 80 different cellular enzymes (Brady and Weil 2008). It has been found that good potassium nutrition in plants is linked to improved drought tolerance, improved winter hardiness, better resistance to disease and greater tolerance to insect pests. There are no substitutes for potassium as an essential plant nutrient and nutritional requirement for humans and animals (Brady and Weil 2008).

Three primary issues are associated with potassium and soil fertility. First, potassium is found in relatively high concentrations in soils; however, much of this is not available to plants. The majority of potassium is bound up in the non-exchangeable soil layer, leaving only 1-2% available as exchangeable potassium, available to dissolve into the soil solution (Brady and Weil 2008). Secondly, potassium is quite readily lost from soils to leaching. Far more potassium is lost to leaching than phosphorus. Lastly, removal of potassium by plants is very high. When excess quantities of potassium are applied, this has been shown to lead to 'luxury consumption' by crops (Brady and Weil 2008).

The 'luxury consumption' of potassium by grasses and other crops introduces new challenges into nutrient management. It has been found that dairy cattle can experience problems when

foraging on grasses undergoing luxury uptake because the excess potassium in their diet interferes with uptake of calcium and magnesium, which then causes problems in calving and milking (Schmidt et al., 2010).

Further to this, high potassium levels in the soils can be an indicator that farms do not have adequate land base for the amount of manure generated. These farms often import feed, bringing more potassium onto the farm and further exacerbating the issue. Additionally, little potassium is lost during storage and application of manures, and soils have a high capacity to hold potassium. Breaking the cycle of excess potassium is a challenging cycle to break and one that requires a complete reorganization of nutrient management at the farm level; typically by bringing in low potassium feed which can be expensive.

Excessive potassium in soils can be an issue, though the real cause for concern are soil potassium deficits, which is the norm across much of the world, with potassium fertilizer being applied at a far lower rate than its nitrogen and phosphorus counterparts. Manning (2011) notes that '*recently published assessments of nutrient budgets on a national basis have shown that potassium deficits for developing countries are so substantial that a doubling of world production of potash fertilisers would be required to balance inputs and offtake, simply to meet demands in Africa alone.*' On average, potassium fertilizers are applied at a rate that replenishes only 35% of the potassium removed primarily because fertilizers are expensive and because many agriculturalists often do not have access to them (Smil 1999).

Shown in Figure 1 is a striking example of potassium deficits in China, which shows China's potassium deficit increasing from 2.9 million tonnes in 1961 to 8.3 million tones in 1997 due to low application rates of potassium fertilizer. The large potassium deficit poses a threat to China's future food production. Sheldrick et al., (2003) estimate that an increase in potassium fertilizer use of more than 8% per year would be necessary to increase annual food production growth rates and to achieve potassium balance. Unfortunately, this situation seems to be common amongst several agrarian nations.

This has lead to some researchers calling for alternate forms of potassium fertilizers that might be less expensive, or more geographically available than potash based potassium fertilizers (Manning 2011). Development of K-struvite recovery technology may be one method of addressing this issue.
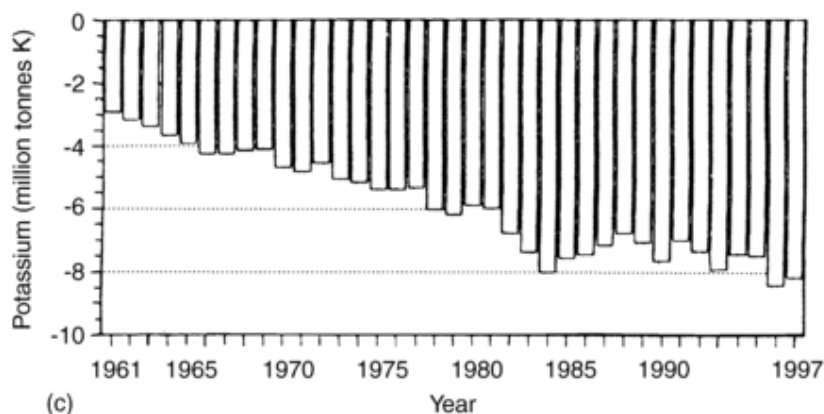
Figure 1 - Potassium balance in China between 1961 and 1997 (Sheldrick et al., 2003)

2.2 Global outlooks for potassium fertilizers

Production of phosphorus and potassium rely on mining ore deposits from the earth's crust, whereas production of nitrogen fertilizers relies on fixing elemental nitrogen from the atmosphere through the Haber-Bosch process. The majority of potassium applied to crops is applied as potash, which is derived from sylvinite ores, and applied as potassium chloride (KCl). About 93% of potash consumed globally is used as fertilizer for food, animal feed, fibers and biofuels, with the remainder used to produce potassium based chemicals (Jasinski 2010).

Canada, Russia, Belarus and China are the world's major producers of potash, with Canada and Russia holding the lion's share, approximately 80% of the world's reserves (Jasinski 2012, 2015b). Figures put Canada at producing approximately 11,200,000 tonnes per year of potash (as K_2O), which accounts for 30% of the world's yearly global supply. Canada's reserves are estimated at about 4,700 million tonnes (Jasinski 2015b), which, at current production rates will last for approximately 400 years.

In contrast, the major phosphate rock producers in order of production are China, Morocco, and the United States accounting for 70% of global production (Jasinski 2015a); Canada is simply a bit player contributing about 0.1% to global supply (Jasinski 2015a; Mavinic 2015). Morocco and the western Sahara hold the majority of the world's reserves, accounting for as much as 75% of the world's highest quality P_2O_5 reserves. The next largest holder of phosphate rock reserves is China with 5% of the world's reserves (Jasinski 2014), but exports are no longer allowed (Mavinic 2015).

Current population projections estimate the world population to reach between 9 and 10 billion by 2050 (Pew Research Center 2014; UN News Centre 2013). Among other things, this will mean increases in food production to feed the growing population. Commercial fertilizers play an important role in our food system, and the majority of our phosphorus and potassium based fertilizers are derived from mined sources. Population increases will be seen primarily in South

East Asia, India, China and on the African continent (Pew Research Center 2014); where the bulk of food production will need to increase. However, most of the world's potash is applied to land in developed countries such as Canada, the United States and countries in Europe due to cost constraints for cash-strapped farmers. The UN Food and Agriculture Organization estimates that over half of the increase in demand for potash ores will be Asia, specifically China and India (FAO 2015).

Potash ores have limited distribution globally partly because potassium fertilizers saw a price increase of as much as four times during the period from 2007-2009 (Manning 2011). Shown in Figure 2, prices have since decreased and hover around $300 per metric tonne (USD), which is still greater than prices prior to 2007. For food production to increase to required levels in Asia, India, China and Africa, supplies of fertilizer to developing nations must increase. However, based on current usage patterns and population projections, world potash production is expected to increase by about 3-4% per year (FAO 2015; Jasinski 2012).

Within Canada, there does not seem to be a strong business case to promote potassium recovery as potassium reserves in Canada are sufficient for long term use. Shifting to a global perspective, and reiterating the conclusion from the previous section, K-struvite technology could promote self-sufficiency for nations without access to potash reserves.
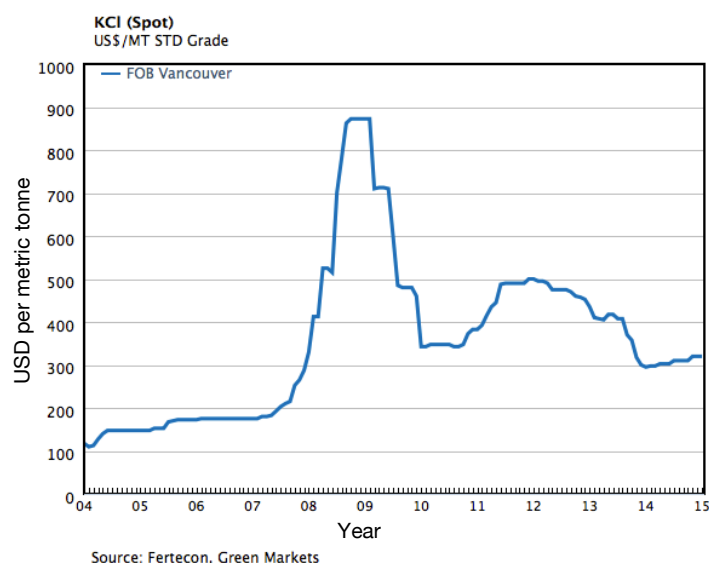
Figure 2 - Potash prices from 2004 to 2014
(http://www.potashcorp.com/customers/markets/market_data/prices/)

2.3 K-struvite as a fertilizer

In terms of the efficacy of K-struvite as a fertilizer, Salutsky et al., (1964) report good response for tomatoes, rye grass and other crops fertilized with K-struvite. The response depended on

the granule size and they suggest that K-struvite was well suited to supplying nutrients close to the plants in direct seeded crops. It was also reported that nutrient release occurs at a different rate than regular NH_4-struvite because of different solubilities and the effect of nitrifying bacteria acting on the regular struvite.

This was the only study found on the effectiveness of K-struvite as a plant fertilizer, although there have been many studies done with NH_4-struvite, which have found it to be an effective slow release fertilizer (Cerrillo et al. 2014; Lunt, Kofranek, and Clark 1964).

2.4 Driving forces for potassium recovery as K-struvite

Based on understanding potassium needs in agriculture and the economics of potash fertilizers, it seems that primary drivers for potassium recovery as K-struvite include (a) the potential to create a full complement NPK fertilizer from wastes (b) the need for a slow-release potassium fertilizer and (c) its estimated future market potential (though there are no readily available numbers for the market value of K-struvite). Secondary drivers would include (a) K-struvite production as a way to remove potassium from waste streams on farms and restore balance in the potassium cycle, and (b) the need to find other sources of potassium fertilizers besides potash due to its high price and limited distribution worldwide.

As mentioned previously, soil potassium depletion is prevalent in many agricultural areas, due to low fertilizer application, but also due to potassium's high mobility and prevalence for leaching. With large areas of agricultural land deficient in potassium, three quarters of paddy soils in China and two thirds of the Southern Australian wheat belt, and much of India (Römheld and Kirkby 2010), a slow release potassium fertilizer could potentially reduce the rate of potassium being leached away. However, more study would be needed to confirm this hypothesis.

Another potential driver for K-struvite production may be its ability to mitigate or reduce salt buildup in salt affected soils. Potash, the most prevalent potassium based fertilizer is a potassium chloride, KCl which has a high salt index according to Braunschweig (1986). Saline soils are found in arid and semi-arid regions as a result of low rainfall and poor irrigation practices resulting in salt buildup and affecting crop productivity. The use of potassium chloride fertilizers is not recommended in these areas because of the problems caused by additional salinity. In these situations, fertilizers in which the anion and cation is taken up by the plant, such as KNO_3, K_2SO_4 or K-struvite may be preferable. Salutsky (1964) found that soluble salt levels decreased with K-struvite use, which helps to support the statement above.

In terms of potential to offset potash mining, there are no readily available numbers for potassium, so presented are estimates for phosphorus recovery's potential to offset phosphate rock mining. Table 1 gives estimates for the potential reduction in phosphorus mining if the entire world's population was connected to wastewater treatment plants and phosphorus recovery was 100%. These figures, given their set of assumptions, estimates that between 7-

9% of mined phosphate rock could be offset through phosphorus recovery from wastewater. The situation for potassium would likely be quite different, as potassium would likely be recovered from agricultural wastewater (the numbers in Table 1 do not include agricultural wastewaters) which are orders of magnitude greater than human wastewater production. For example, in Canada it is estimated that over 180 million tonnes of manure from livestock is produced every year (Statistics Canada 2013). Using the value for potassium and phosphorus concentration in dairy manure given in Table 2, and doing some crude calculations, this represents approximately 450,000 tonnes of potassium and 100,000 tonnes of phosphorus. If 100% of this potassium were recovered, it would account for approximately 4% of Canada's potash fertilizer output. There have not been any studies on the cost-benefit ratio of recovering potassium as fertilizer as of yet, thus more study would be needed.

Table 1 - Contribution of recovered phosphorus from WWTPs worldwide to the reduction in phosphate rock mining (Shu et al. 2006)

Population billions	Recovered P_2O_5/yr (million tons)	kg/ha/yr of P_2O_5 from recovered phosphorus	% reduction in rock mining
6	2.31	1.25	5.76
7	2.69	1.45	6.72
8	3.07	1.66	7.68
9	3.46	1.87	8.64
10	3.84	2.08	9.60

Assume the entire world population is connected to WWTPs and phosphorus recovery is 100%. Assume at present, P_2O_5 consumption = 40 million tons/yr and 80% of it is used as fertilizer. World arable land 1.48 billion ha.

2.5 Potential wastes for potassium recovery

Recovery of potassium in agricultural wastes such as dairy, swine or poultry waste has been suggested by several researchers (Salutsky and Steiger 1964; Satoshi et al. 2013; Schuiling and Andrade 1999; Wilsenach et al. 2007; Zhang 2013). Agricultural waste streams have the advantage of all K-struvite constituents being present already, so there is no need for additional chemicals, except to adjust pH.

Potash brine, tailings from potash processing operations, is an interesting source of potassium for K-struvite production, though phosphorus and magnesium would have to be supplemented, making the process less attractive. It is important to keep in mind that phosphorus recovery remains the global priority over potassium recovery. However, using potash brine to supplement an existing phosphorus and magnesium rich waste could be effective. Concentrates from membrane processes such as those generated from treating

landfill leachates with membranes have been suggested by (Li et al. 2015; Wang et al. 2012) although these wastes are quite low in phosphorus and magnesium. Municipal wastewater, as anaerobic digester centrate has quite a low potassium concentration, meaning potassium would have to be supplemented to achieve the necessary K:P ratio. Human urine, though more concentrated in nutrients than diluted wastewater, is generally difficult to separate from the waste stream. As well, many of these wastes have relatively high concentrations of nitrogen as ammonium, which is not conducive to K-struvite formation (though it is conducive to NH_4-struvite formation). Palm oil mill effluent as described by Ahmad et al., (2009) has a Mg:K:P ratio of 4.4 : 10 : 1 with 2.5 mM of ammoniacal nitrogen present, making it one of the more promising wastes for producing K-struvite.

Based on the literature reviewed, it seems there is no 'perfect' waste for producing K-struvite and a combination of processes would have to be employed to produce a feed solution with the appropriate nutrient ratios. Perhaps a process which denitrifies the waste and concentrates the nutrients, followed by addition of potash brine could achieve appropriate solution conditions. There are likely multiple permutations, and will inevitably be dictated by local availabilities of waste products and local economics.

Table 2 gives average nutrient concentrations of various wastes, which might be considered for potassium recovery through crystallization of K-struvite.

Table 2 - Average nutrient concentrations in wastes with potential for K-struvite production

Waste material	N-NH$_4$ (mg/L)	P-PO$_4$ (mg/L)	K (mg/L)	Mg (mg/L)	pH	Reference
Anaerobic digester centrate	1290	108	150	1	-	Bhuiyan et al. 2007
Potash tailings brine*	-	-	~42,000	-	-	Godwin 2014
Membrane concentrate from landfill leachate treatment	44.7	-	2806	-	7.7	Wang et al., 2012
Untreated swine manure	2342	969	2342	565	7.5	American Society of Agricultural Engineers, 2003
Untreated dairy manure	700	540	2569	629	7.0	
Untreated chicken manure	3183	1394	4547	2122	6.9	
Concentrate from beet processing	3.7 g organic N/100g solids	-	9.0 g/100g solids K$_2$O	0.03 g/100g solids	-	Decloux et al., 2002
Human urine (synthetic)	266	633	1642	78	5.8	Tilley et al. 2008
Palm oil mill effluent	35	180	2270	615	4.7	Ahmad and Chan, 2009

*see calculation for potassium concentration in potash brine in Appendix C

2.6 Nutrient recovery research at UBC

Nutrient recovery research started within the Environmental Engineering group at UBC in 1999 with a grant from BC Hydro. This work was tasked to find a way to fertilise oligotrophic streams; streams that no longer had enough nutrient inputs to sustain returning salmon populations. Struvite scale build-up in wastewater treatment plants was also becoming an increasingly costly issue to deal with, but was also recognized as an excellent slow release fertilizer with a Mg:N:P ratio of 1:1:1, perfect to use in the stream fertilization project. Bench scale studies led to the development of the UBC-FBR NH_4-struvite crystallizer. Pilot studies using waste streams from the Penticton, B.C. WWTP, and Lulu and Annacis Island WWTPs in Vancouver, B.C., were integral in the progression from batch tests to commercialization of the technology (Britton 2002; Fattah 2004; Forrest 2004).

The goals of the research group have changed and matured from those early days into creating an upstream solution to what has been a downstream problem by recovering nutrients from waste streams and create a full complement fertilizer. Three major nutrients required for plant growth are nitrogen, phosphorus and potassium, with calcium, magnesium and sulphur required as secondary nutrients. This research involved developing fundamental understanding of the processes required to recover phosphorus, nitrogen and potassium in useable forms. Research within the group is also being carried out on further nitrogen recovery, both as a fuel and as a fertilizer. This thesis represents the first project focused on recovery of potassium as K-struvite.

CHAPTER 3
LITERATURE REVIEW

3.1 Introduction to K-struvite

K-struvite ($MgKPO_4:6H_2O$) is a magnesium potassium phosphate hexahydrate, the potassium equivalent of struvite. It is named as such due to the replacement of NH_4^+ by K^+. Natural occurrences have been documented in Switzerland and Austria, as reported by Graeser et al, (2008). K-struvite and struvite are isostructural; what is interesting, for recovery purposes, is that the potassium and ammonium ions have a very similar ionic radius. With potassium being only slightly smaller than ammonium, this substitution creates almost no distortion in the crystal structure (Mathew and Schroeder 1979). It is a white crystalline substance, insoluble in water, although its solubility is slightly higher than that of NH_4-struvite. The general reaction pathway is shown in Equation 1.

$$MgKPO_4: 6H_2O \leftrightarrow Mg^{+2} + K^+ + PO_4^{-3} + 6H_2O$$
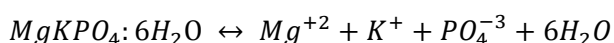
Equation 1

A few important findings were discovered with regard to the chemistry and basics for successful K-struvite recovery. The need for a low NH_4:K ratio, which has recently been confirmed independently in studies from other research groups (Satoshi et al. 2013) is important. K-struvite could form solid solutions with other struvite-type compounds, especially NH_4-struvite, since ammonium and potassium ions have very close ionic radii. The ability of these compounds to form solid solutions has been known for decades (Mathew and Schroeder, 1979). This means that under certain conditions, it should be possible to recover a struvite-based product from wastewater that would have all three nutrients in it, $Mg(NH_4)_xK_{(1-x)}PO_4 \cdot 6H_2O$. The ratio between nitrogen and potassium could be set by the crystallization conditions as noted in Lobanov et al., (2014).

3.1.1 K-struvite morphology and structure

Research previously published has reported that K-struvite forms with an orthorhombic, needle-like structure (Chauhan, Vyas, and Joshi 2011; Mathew and Schroeder 1979; Satoshi et al. 2013; Wilsenach, Schuurbiers, and van Loosdrecht 2007) as seen in Figure 3a, however, different morphologies have been observed under different growth parameters according to supersaturation ratio and pH, as seen in Figure 3b.

As mentioned above, K-struvite and NH_4-struvite have been found to be isostructural, with a K^+ ion replacing the NH_4^+ ion. Similarly to struvite, $Mg(H_2O)_6$ octahedra and PO_4 tetrahedron

groups are held together by a network of hydrogen bonds. The K^+ ion is bonded to five oxygen atoms; one oxygen from the PO_4^{3-} group and four water molecules. The geometry of the K^+ ion coordination can be described as tetragonal pyramidal with the four water molecules at the base and the PO_4 oxygen at the axial position. Mathew & Schroeder (1979) point out that K – O bonds may be weak, though the substitution of K^+ into the structure does not affect the strength of the Mg – O bonds. The structure of K-struvite can be seen in Figure 4.
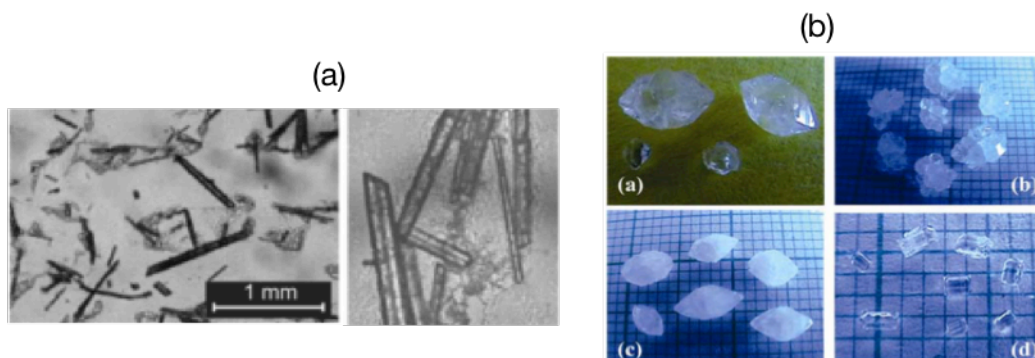
Figure 3 – (a) K-struvite crystals are typically characterized by an orthorhombic, needle-like structure (Wilsenach et al. 2007) **(b) Different morphologies of K-struvite crystals under different growth parameters** (Chauhan et al. 2011)
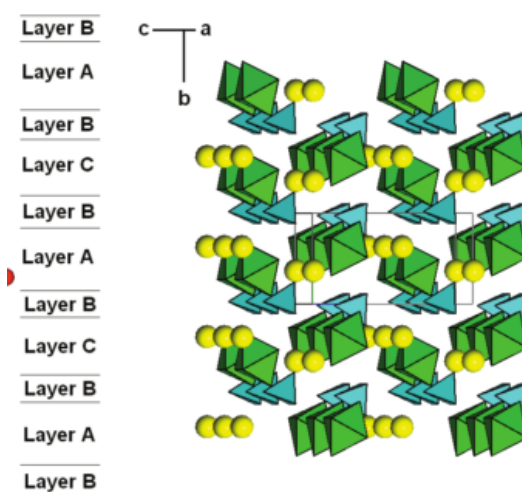
Figure 4 - Crystal structure of K-struvite. Tetrahedra represent PO_4^{3-} groups, octahedral represent Mg(H_2O)_6 groups and spheres, K^+. (Yang and Sun 2004)

3.2 Chemistry of magnesium phosphate compounds

Solutions conducive to precipitating K-struvite will contain potassium, magnesium and orthophosphates. Agricultural wastewaters contain these constituents as well as nitrogen, calcium and other ions. We are interested in producing K-struvite, but a number of other magnesium phosphate crystalline phases such as cattiite, $Mg_3(PO_4)_2$:22H_2O, bobierrite, $Mg_3(PO_4)_2$:8H_2O, newberyite, $MgHPO_4$:3H_2O, or brucite, $Mg(OH)_2$, among others, could form depending on the solution conditions.

K-struvite $\qquad Mg^{2+} + K^+ + PO_4^{3-} + 6H_2O \leftrightarrow MgKPO_4 \vdots 6H_2O$

Cattiite $\qquad 3Mg^{2+} + 2HPO_4^{2-} + 22H_2O \leftrightarrow Mg_3(PO_4)_2 \vdots 22H_2O + 2H^+$ **Equation 2**

Bobierrite $\qquad 3Mg^{2+} + 2HPO_4^{2-} + 8H_2O \leftrightarrow Mg_3(PO_4)_2 \vdots 8H_2O + 2H^+$ **Equation 3**

Newberyite $\qquad Mg^{2+} + H_2PO_4^{2-} + 3H_2O \leftrightarrow MgHPO_4 \vdots 3H_2O + H^+$ **Equation 4**

Brucite $\qquad Mg^{2+} + 2OH^- \leftrightarrow Mg(OH)_2$ **Equation 5**

Hazenite $\qquad 2Mg^{2+} + K^+ + Na^+ + 2PO_4^{3-} + 14H_2O \leftrightarrow Mg_2KNa(PO_4)_2 \text{:} 14H_2O$ **Equation 6**
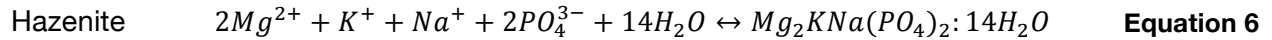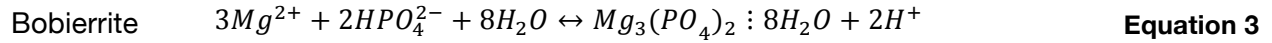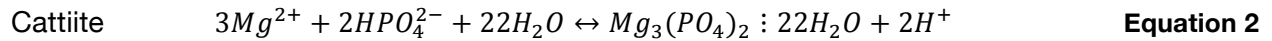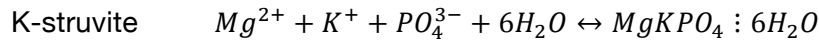
As mentioned previously, struvite will preferentially form if ammonium (NH_4^+) is present in solution, even at low concentrations. Satoshi et al., (2013) found that with ammonia concentrations below 1.1 mM, reductions in potassium, magnesium and orthophosphate almost corresponded to ratios found in K-struvite. Brucite is generally seen only when the pH is greater than 10.

3.2.1 Aqueous equilibria affecting speciation of potassium, magnesium, orthophosphate, and carbonate

Potassium is generally found in its soluble phase and, therefore, does not affect the K-struvite formation through its speciation since equilibrium constants of the formation reactions for potassium complexes are close to unity. Magnesium and orthophosphate ions are involved in a series of complex equilibria and their speciation does affect K-struvite formation. The following equations list some of the aqueous equilibriums that are involved in the formation of magnesium phosphate compounds (Lobanov et al. 2013; USGS 2013).

$$H^+ + OH^- \leftrightarrow H_2O$$

Equation 7

Potassium speciation equations

$$K^+ + HPO_4^{2-} \leftrightarrow KPO_4^{2-} + H^+$$

Equation 8

$$K^+ + HPO_4^{2-} \leftrightarrow KHPO_4^-$$

Equation 9

$$K^+ + H^+ + HPO_4^{2-} \leftrightarrow KH_2PO_4$$

Equation 10

$$2K^+ + HPO_4^{2-} \leftrightarrow K_2PO_4^- + H^+$$

Equation 11

$$2K^+ + HPO_4^{2-} \leftrightarrow K_2HPO_4^-$$

Equation 12

Magnesium speciation equations

$$Mg^{2+} + H_2O \leftrightarrow MgOH^+ + H^+$$

Equation 13

$$Mg^{2+} + 2OH^- \leftrightarrow Mg(OH)_2$$

Equation 14

$$4Mg^{2+} + 4H_2O \leftrightarrow Mg_4(OH)_4^{4+} + 4H^+$$

Equation 15

$$Mg^{2+} + 2HPO_4^{2-} \leftrightarrow Mg(HPO_4)_2^{2-}$$

Equation 16

$$Mg^{2+} + PO_4^{3-} \leftrightarrow MgPO_4^-$$

Equation 17

$$Mg^{2+} + H_2PO_4^- \leftrightarrow MgH_2PO_4^+$$

Equation 18

$$Mg^{2+} + HPO_4^{2-} \leftrightarrow MgPO_4^{-} + H^+$$

Equation 19

$$Mg^{2+} + HPO_4^{2-} \leftrightarrow MgHPO_4$$

Equation 20

$$2Mg^{2+} + 2HPO_4^{2-} \leftrightarrow Mg_2(HPO_4)_2$$

Equation 21

$$Mg^{2+} + 2HPO_4^{2-} + 2H^+ \leftrightarrow Mg(H_2PO_4)_2$$

Equation 22

Phosphate speciation equations

$$HPO_4^{2-} \leftrightarrow H^+ + PO_4^{3-}$$

Equation 23

$$H_2PO_4^- \leftrightarrow H^+ + HPO_4^{2-}$$

Equation 24

$$H_3PO_4 \leftrightarrow 2H^+ + HPO_4^{2-}$$
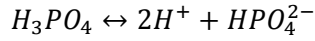
Equation 25

Carbonate speciation
equations
$$CO_2 + H_2O \leftrightarrow H_2CO_3$$

Equation 26

$$H_2CO_3 \leftrightarrow HCO_3^- + H^+$$

Equation 27

$$HCO_3^- \leftrightarrow CO_3^{2-} + H^+$$

Equation 28

$$HCO_3^- + H^+ \leftrightarrow CO_2 + H_2O$$

Equation 29

$$Mg^{2+} + 2HCO_3^- \leftrightarrow Mg(HCO_3)_2$$

Equation 30

$$2Mg^{2+} + HCO_3^- \leftrightarrow Mg_2CO_3^{2+} + H^+$$
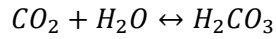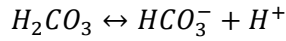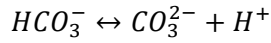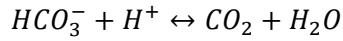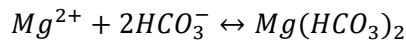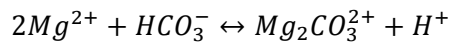
Equation 31

3.2.2 Solubility product (K_{sp})

The solubility product is the equilibrium constant that describes a solid dissolving into its constituent ions. The solubility products of magnesium phosphates vary with temperature according to the Van't Hoff equation (Snoeyink and Jenkins 1980). It depends only on temperature; not pH, concentration, or particle size. An accurate solubility product value helps determine the precipitation potential of K-struvite and helps estimate the supersaturation ratio far more accurately. Since, the supersaturation ratio is the most important parameter in controlling crystallization and, theoretically, if the product of the ionic activity in solution exceeds the solubility product, K-struvite will precipitate. Table 3 lists some experimentally and theoretically determined solubility products measured at 25°C for the solid phases of interest to this research.

Table 3 - Experimentally determined pK$_{sp}$ at 25°C for various magnesium phosphate minerals

Solid phase	pK$_{sp}$ = -logK$_{sp}$	Reference
K-struvite MgKPO$_4$:6H$_2$O	11.00 10.62	Current work A.W. Taylor et al. 1963
NH$_4$-struvite MgNH$_4$PO$_4$:6H$_2$O	13.15 13.26 13.36 13.47	A.W. Taylor et al. 1963 Ohlinger et al. 1998 Bhuiyan et al. 2007 Lobanov et al. 2013
Newberyite MgHPO$_4$:3H$_2$O	5.82 5.88	A W Taylor et al. 1963 Lobanov et al. 2013
Bobierrite Mg$_3$(PO$_4$)$_2$:8H$_2$O	25.20 25.47	A W Taylor et al. 1963 Lobanov et al. 2013

Solid phase	pK_{sp} = -logK_{sp}	Reference
Cattiite $Mg_3(PO_4)_2{:}22H_2O$	23.10	A W Taylor et al. 1963

There are two pK_{sp} for K-struvite reported in the literature. An experimentally determined value of 10.62 at 25°C by Taylor et al., (1963) and a theoretically determined value of 11.67 at 25°C by Luff and Reed (1980) . This is more soluble than struvite with a pK_{sp} of 13.47 (Lobanov et al. 2013). The K_{sp} of K-struvite is defined as:

$$K_{sp} = \gamma[Mg^{+2}] \times \gamma[K^+] \times \gamma[PO_4^{-3}]$$

Equation 32

where: γ : activity coefficient
[x]: concentration (mol/L)

The activity coefficient is determined by the solution ionic strength as discussed in Section 3.3.2. pK_{sp} is the negative log of the solubility product and is defined as:

$$pK_{sp} = -\log_{10}(K_{sp})$$

Equation 33

3.3 Factors affecting K-struvite formation

3.3.1 Supersaturation

A solution's degree of supersaturation with respect to K-struvite will determine whether or not it precipitates. The supersaturation ratio (S) is a measure of the crystallization potential of the solution. A supersaturated solution has an S greater than 1 and predicts precipitation, and an undersaturated solution has an S between 0 and 1, indicating that the precipitate will dissolve and that precipitation is impossible. The degree of supersaturation of K-struvite relative to the supersaturation of other compounds that could form indicates what precipitation will occur.

Variables that affect the K-struvite supersaturation ratio (S_K) include solution ionic strength, pH, and solution temperature. Solution ionic strength affects the activity (y) of a species which is further discussed in Section 3.3.2. The solution pH primarily affects the speciation of orthophosphate and temperature affects the solubility product of K-struvite. The S_K of K-struvite can be written as:

$$S_K = \left(\frac{y[Mg^{2+}]\gamma[K^+]\gamma[PO_4^{-3}]}{K_{sp-K}}\right)^{1/3}$$

Equation 34

The saturation index (SI) is also a term used to describe saturated conditions. A supersaturated solution of K-struvite can be written as:

$$SI = log \left(\frac{\gamma[Mg^{2+}]\gamma[K^+]\gamma[PO_4^{-3}]}{K_{sp-K}} \right)$$ **Equation 35**

Considering a distilled water matrix with magnesium chloride, potassium chloride, potassium phosphate and sodium hydroxide as a pH adjuster. The solid phase reactions shown in Table 3 and the reactions listed below are examples of the competing precipitation reactions taking place.

Potential solid phases:

K-struvite	$MgKPO_4\text{:}6H_2O$
Brucite	$Mg(OH)_2$
Cattiite	$Mg_3(PO_4)_2\text{:}22H_2O$
Bobierrite	$Mg_3(PO_4)_2\text{:}8H_2O$
Newberyite	$MgHPO_4\text{:}3H_2O$
Dimagnesium potassium hydrogen bisphosphate pentadecahydrate (MPHP)	$Mg_2KH(PO_4)_2\text{:}15H_2O$
Hazenite	$Mg_2KNa(PO_4)_2\text{:}14H_2O$
Kovdorskite	$Mg_2PO_4OH\text{:}3H_2O$

Some of these species are more valuable than others for the purpose of creating a slow release fertilizer, recovering potassium and maximizing phosphorus recovery. Three of the magnesium phosphates shown above incorporate potassium into their structures. For example, hazenite and MPHP recover potassium and phosphorus, but at a Mg:K:P molar ratio of 2:1:2, which makes them less desirable than K-struvite, with a Mg:K:P molar ratio of 1:1:1, since only 1 mole of potassium is recovered for every two moles of magnesium and phosphorus. Further little is known about hazenite or MPHP which seem to form under fairly unstable conditions making recovery as hazenite or MPHP difficult.

Therefore, in order to selectively produce K-struvite as opposed to cattiite, newberyite, or other magnesium phosphates, the solution's characteristics need to be optimized which is done through control of the supersaturation ratio. The supersaturation ratio is generally controlled through both the pH and nutrient ratios. pH affects the supersaturation ratio by changing the orthophosphate equilibrium. For example, adding sodium hydroxide, adds hydroxide ions into solution which neutralizes hydrogen ions. This results in a shift from hydrogen phosphate to orthophosphate which can be used in K-struvite formation as demonstrated below.

$$HPO_4^{2-} \leftrightarrow PO_4^{3-} + H^+$$ **Equation 36**

$$Mg^{2+} + K^+ + PO_4^{3-} + 6H_2O \leftrightarrow MgKPO_4{:}6H_2O$$
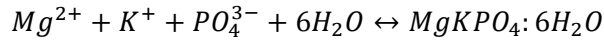
Solution temperature, as mentioned above is also an important variable in the supersaturation ratio since the solubility product is directly dependent on temperature. As temperature increases, we can predict that the solubility product of K-struvite will increase linearly with temperature according to the Van't Hoff relationship (Luff and Reed 1980). An increase in the solubility product, results in a decrease in the K-struvite supersaturation ratio. As has been observed with NH_4-struvite, recovery potential is greater in lower temperature solutions due to its decreased solubility (Lobanov et al. 2013).

The Van't Hoff relationship, Equation 37, relates the change in equilibrium constant to the change in temperature given a standard enthalpy change for the process:

$$\frac{dlnK}{dT} = \frac{H^{\circ}}{RT^2} \quad \rightarrow \quad ln\left(\frac{K_2}{K_1}\right) = -\frac{\Delta H^{\circ}}{R}\left(\frac{1}{T_2} - \frac{1}{T_1}\right) \qquad \textbf{Equation 37}$$

where: $\Delta H°$: enthalpy of reaction, J/mol
R: universal gas constant, 8.314 J/mol•K
T: reaction temperature, K

The supersaturation ratio also influences nucleation, precipitation and resulting crystal growth. This is discussed further in Section 3.4.

3.3.2 Ionic strength and activity

In dilute solutions, we consider activity coefficients to be 1; in more concentrated solutions, this no longer applies because of ionic shielding effects. Therefore, it is important to know the ionic strength of the solution because the ionic strength influences the activity coefficient, affecting the equilibrium constant. The ionic strength of a solution can be calculated as in Equation 38. However, the most commonly used empirical relationship to predict the ionic strength relates ionic strength to electrical conductivity (Russell 1976), as shown in Equation 39.

$$\mu = {}^1/_2 \sum C_i Z_i^2 \qquad \textbf{Equation 38}$$

where: μ : ionic strength
c : concentration of species, i
z : charge of species, i

$$\mu = 1.6x10^{-5} \times EC \qquad \textbf{Equation 39}$$

where: EC: electrical conductivity (μmho/cm)

Once the ionic strength is determined, the activity coefficient can be estimated using the relationships in Table 4.

Table 4 – Common approximations to determine the activity coefficient

Approximation	Equation	Ionic strength range	
Debye-Hückel limiting law approximation	$log\gamma_i = -AZ_i^2\sqrt{\mu}$	$\mu < 0.001$	**Equation 40**
Extended Debye-Hückel approximation	$log\gamma_i = -\dfrac{AZ_i^2\sqrt{\mu}}{1 + B\alpha_i^0\sqrt{\mu}} + b_i\mu$	$\mu < 0.1$	**Equation 41**
Güntelberg approximation	$log\gamma_i = -AZ_i^2\dfrac{\sqrt{\mu}}{1 + \sqrt{\mu}}$	$\mu \sim 0.1 - 0.5$	**Equation 42**
Davies approximation	$log\gamma_i = -AZ_i^2\left(\dfrac{\sqrt{\mu}}{1 + \sqrt{\mu}} + 0.3\mu\right)$	$\mu < 0.5$	**Equation 43**

A, B – constants that depend on solvent and temperature (Snoeyink and Jenkins 1980)
α, b – a constant that relates to the diameter of the hydrated ion; for monovalent ions, usually about 3 to 4Ȧ (Snoeyink and Jenkins 1980)

3.3.4 Influence of ammonium, nitrate and sodium

In the presence of ammonium, struvite is selectively precipitated over K-struvite because kinetics and thermodynamics favour struvite precipitation (Satoshi et al. 2013). However, the same authors report that nitrates present in solution did not hinder K-struvite precipitation.

Some researchers (Xu et al. 2011) have reported that magnesium sodium phosphate ($MgNaPO_4$:$7H_2O$) co-precipitates along with K-struvite when sodium is present in solution, although this research has not found any evidence to support this claim.

3.3.5 Hydrodynamics

There have not been any studies discussing the effects of hydrodynamics on K-struvite formation, so discussed here will be some findings on the influence of hydrodynamics and turbulence on NH_4-struvite precipitation.

Reactor hydrodynamics are believed to play an important role in NH_4-struvite crystallization and, therefore, it is reasonable to expect that hydrodynamics will be important in K-struvite crystallization.

Nucleation and crystal growth are governed by mass transport laws, where different laws govern for crystal nucleation and crystal growth. Ohlinger et al., (1999) demonstrated that a higher mixing speed lowers the induction time for struvite crystal nucleation at the same

supersaturation level. A good correlation between mixing energy and struvite accumulation was also found indicating a transport-controlled process. Crystal nucleation rates tend to increase with increased turbulence, though mixing energy that is too high will result in break up of agglomerates.

With fluidized bed reactors such as the UBC NH_4-struvite crystallizer, turbulence within the reactor is largely dependent on upflow velocity, as well as particle load, particle size and reactor size. A minimum upflow velocity is required for the fluidization of particles and particle mixing with the feed solution; however, an upflow velocity that is too high will result in the loss of fine struvite crystals, in turn, reducing struvite agglomeration rates. Previous results with the UBC-FBR indicate that struvite crystals grown at higher upflow velocities, are larger and denser (Fattah 2004; Huang 2003).

3.3.6 Agglomeration and crystallization

Important processes in crystallization are nucleation, crystal growth, and agglomeration. Agglomeration in precipitation is due to two particles colliding through mixing energy and attractive forces, followed by those two particles staying together through physical forces and crystalline bridges. These steps depend on solution hydrodynamics, electrical and van der Waals forces.

NH_4-struvite crystals were reported to be polar by Romanowski et al., (2010) so, an increase in pH increases surface charge, increasing repelling forces, and thereby reducing agglomeration (Bouropoulos and Koutsoukos 2000; Le Corre et al. 2007). There have been no studies examining the surface charge or the zeta potential of K-struvite in solution and its impact on agglomeration and crystal growth. This kind of work would be useful in helping assess the agglomeration potential of K-struvite.

Ohlinger (1999) found that mixing energy was primarily responsible for controlling struvite growth rate and crystal morphology. Abbona et al., (1985) found that crystal growth and the resulting crystal size are dependent on the supersaturation of the solution. At low supersaturation, larger crystals are generally formed whereas high supersaturation favours formation of fines. Bouropoulos et al., (2000) found that induction times were dependent on supersaturation levels in their work where supersaturation was kept constant. Therefore, there are a number of primary factors controlling agglomeration. Mentioned above are supersaturation and mixing energy, though suspension density, particle size, ionic strength and the presence of impurities are also controlling factors in crystallization and agglomeration. The findings above are likely applicable to K-struvite although similar work has not been done with K-struvite.

3.4 UBC NH$_4$-struvite crystallization process

The UBC fluidized bed reactor (FBR) NH$_4$-struvite crystallizer was designed, developed and tested at UBC through years of research in the UBC Civil Engineering Department, as noted in Section 2.6. The success of this particular design is that hard, 1-2 mm diameter pellets can be formed. Being able to produce pellets is important for a few reasons, namely, (a) pellets are easy to separate from the liquid solution, and require no other drying or processing, and (b) agricultural machinery is designed for conventional fertilizers which are sold in this form. For the struvite product to be adopted, it had to conform to current fertilizer specifications.

The UBC-FBR has only been used to produce NH$_4$-struvite. We do not know how, or if other solid phases, such as K-struvite, will pelletize under the operating parameters used to pelletize NH$_4$-struvite. Therefore, a component of this research was to produce K-struvite in the UBC-FBR to assess its pelletization potential.

The sections below outline the design and operating parameters of the UBC-FBR that have been used for producing NH$_4$-struvite pellets.

3.4.1 Pilot-scale UBC-FBR NH$_4$-struvite crystallizer design

Figure 5 shows the basic design of the UBC-FBR NH$_4$-struvite crystallizer used in initial struvite crystallization trials at UBC by Forrest (2004), Britton (2002), Huang (2003) Fattah (2004) and others. The success of this technology originates from the design of the injection port and the reactor design. The feed, recycle line, magnesium chloride, and caustic are mixed at the injection port causing high turbulence and a high supersaturation ratio resulting in the rapid nucleation of struvite. These nuclei grow into crystals as the fluid flows upward through the reactor. The reactor is made up of four zones of increasing diameter. Starting from the bottom, this includes the harvest zone, active zone, reaction zone, and the seed hopper. The seed hopper has the largest diameter, and acts as a clarifier to retain the small crystals long enough for them grow larger. As zone diameter increases, turbulence decreases due to lower upflow velocities; with the highest upflow velocities found at the injection port. The active zone and harvest zone are characterized by high turbulence and high particle collision frequency. Struvite fines entering these zones agglomerate into larger particles. Over a period of hours to days, these agglomerates grow into round, hard pellets formed by layers of struvite smoothed by attrition and abrasion. The pellets eventually drop into the harvest zone where they can be recovered by draining a portion of the crystallizer. Feed and recycle bypasses allow for continuous operation during harvesting. Orthophosphate residual in the crystallizer effluent can be controlled primarily through recycling. The external clarifier facilitates removal of struvite fines lost to the effluent, while a portion of the supernatant is returned to the crystallizer.

The reactor design used for initial K-struvite trials is similar, with a slight modification to the injection port, as described further in Figure 6.
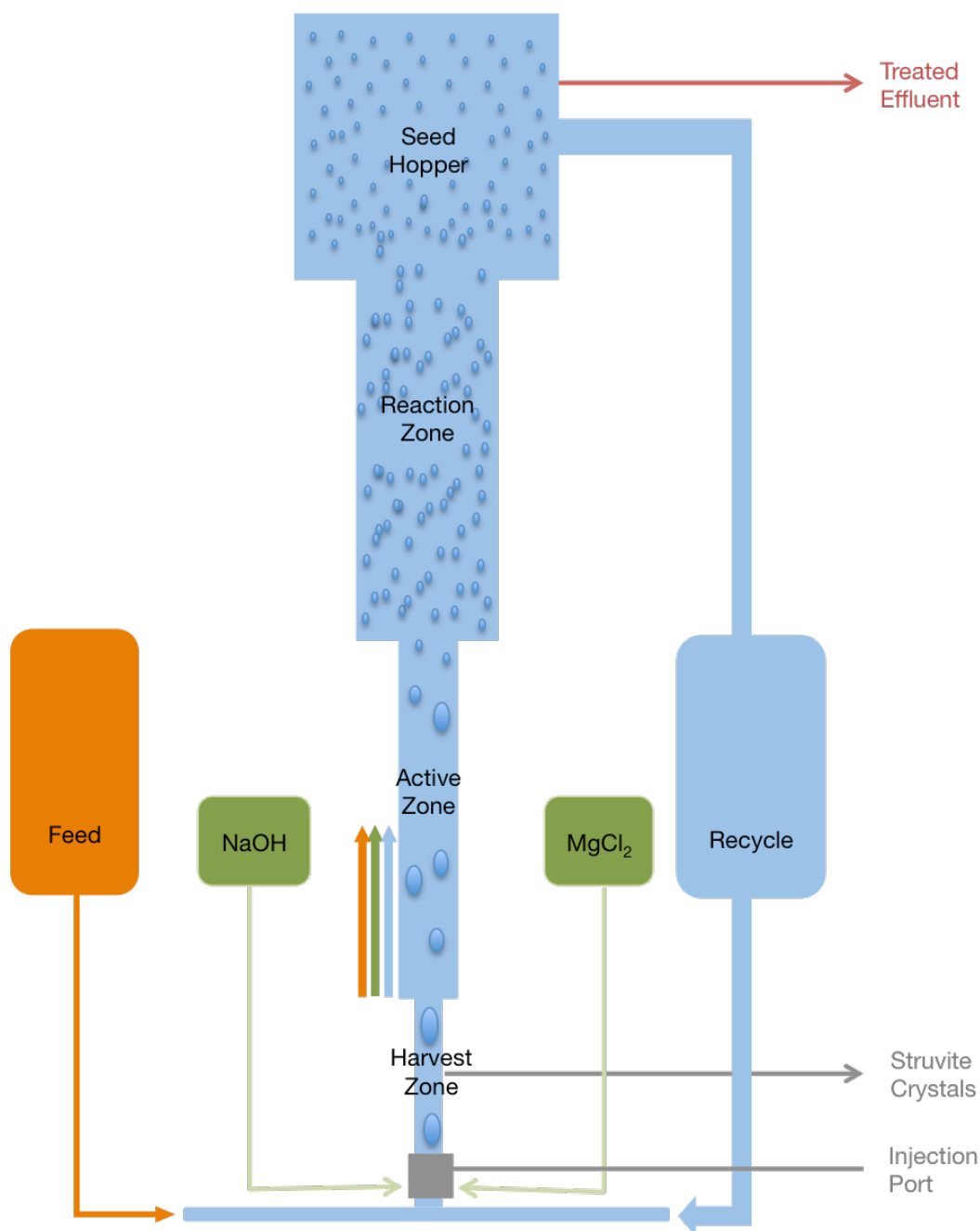
Figure 5 - Design of the UBC-FBR NH$_4$ struvite crystallizer

Figure 6 shows a detailed design of the injection port for NH$_4$-struvite crystallization in the UBC reactor. The injection port was modified for the K-struvite study to have only NaOH injected into the port, as the magnesium was mixed directly into the feed to simulate agricultural wastes.
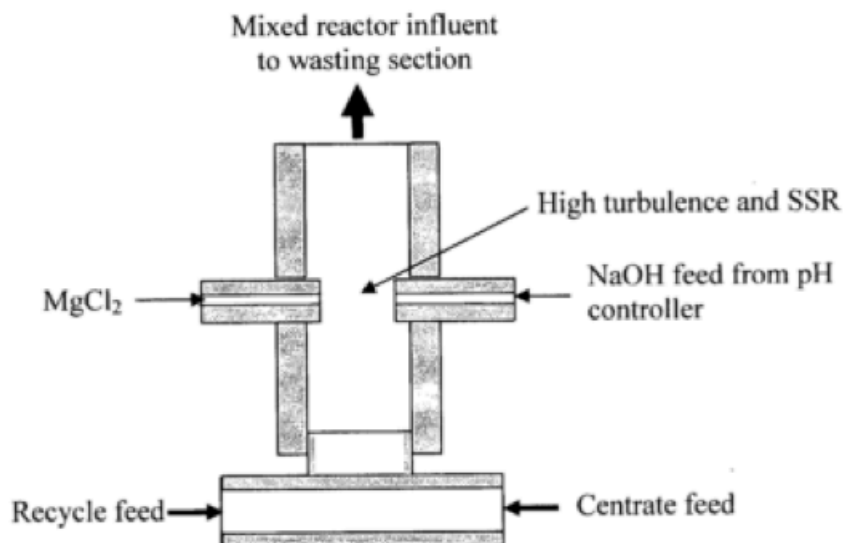
Figure 6 - UBC-FBR NH$_4$-struvite crystallizer injection port design - figure from Fattah (2004)

3.4.2 UBC-FBR NH$_4$-struvite crystallizer operating parameters

NH$_4$-struvite crystallization operational parameters have been widely studied at UBC. A summary of parameters used for successful crystallization and crystal growth experiments is presented in Table 5.

Table 5 – Range of operation and performance for UBC-FBR NH$_4$-struvite crystallizer from pilot studies

Operational Parameter	Britton, 2002 *Penticton digester supernatant*	Huang, 2003 *Lulu & Annacis digester supernatant*	Fattah, 2004 *Lulu dewatering centrate*
[1]Supersaturation ratio	1.1~2.2	1.1~1.9	1.0~1.9
[2]Mg:P molar ratio	1.0~16.9	1.3~3	1.1~30
Temperature (°C)	16-25	10-20	15-29
Total reactor flow (L/min)	2.4~10.2	3.1~4.8	8.3~23.1
[3]Recycle ratio	3.0~23	4.0~10.3	6~12
HRT (min)	Not reported	3.6~9.4	4.0~9.5
[4]CRT (days)	12~47	8~20	Not reported
[5]Upflow velocity (cm/min)	~281	238~541	200~400 (seeded)
Effluent P-PO$_4$ (mg/L)	3.9~43.6	3~13.5	2~54
%PO$_4$ removal	0~91	88~98	24~100
%NH$_4$ removal	0~26	1~22	5~10
Pellet diameter (mm)	0.5~2.1	1.5~3.5	1.4~3.6

1. Cube root of the ratio of conditional solubility product of the solution leaving the injector to that of equilibrium $(P_{S\text{-}reactor}/P_{S\text{-}eq})^{1/3}$
2. Mg:P molar ratio of the solution leaving the injector
3. Recycle flow divided by the influent feed flow
4. The volume of the crystal bed divided by the volumetric rate of crystal harvest
5. Velocity of the total flow measured at the harvest zone

3.5 Previous reports of synthesizing K-struvite in the literature

Table 6 is a summary of experiments in which K-struvite synthesis was reported in the literature. Included in the table are the reported magnesium, potassium, phosphate and ammonia concentrations (if ammonia was used in the research), as well as the pH and the S_K both initially and at equilibrium. The S_K was typically not reported in the study, so it was determined using PHREEQC with the nutrient concentrations and pH given in the literature as model inputs. An S_K greater than 1 initially indicates that the solution is supersaturated with respect to K-struvite, however, this does not indicate whether or not it is supersaturated relative to other potential precipitates. It is also important to examine the S_K at equilibrium to understand what precipitated.

Table 6 - Reported attempts at synthesizing K-struvite in the literature

Study	Initial solution conditions						
	Mg^{2+} (mM)	K^+ (mM)	$P\text{-}PO_4$ (mM)	$N\text{-}NH_3$ (mM)	Mg•K•P molar ratio	pH	S_K initially, S_K at equilibrium[1]
(Li et al. 2015)	212	70.6	212	-	3:1:3	10	13.3, 1
	Study results: Report 53% recovery of potassium as K-struvite from concentrates of landfill leachates nanofiltration. _PHREEQC predicts K-struvite and Cattite formation under these conditions._						
	Mg^{2+} (mM)	K^+ (mM)	$P\text{-}PO_4$ (mM)	$N\text{-}NH_4$ (mM)	Mg•K•P molar ratio	pH	S_K initially and at equilibrium[1]
(Satoshi et al. 2013)	3.1	24.1	7.6	1.1		10	2.41, 0.92
	Study results: Testing influence of ammonium on K-struvite precipitation. Report that decreasing effluent levels correspond to molar ratios in K-struvite when $N\text{-}NH_4$ is below 1.1mM. _PHREEQC predicts precipitation of Cattite under these conditions._						
	Mg^{2+} (mM)	K^+ (mM)	$P\text{-}PO_4$ (mM)	$N\text{-}NH_3$ (mM)	Mg•K•P molar ratio	pH	S_K initially and at equilibrium[1]
(Lin et al. 2012)	16.2	16.2	16.2	0	1•1•1	9	1.93, 0.65

	Study results: Some K-struvite produced though not a pure product. Hypothesized that exopolysaccharides induced K-struvite formation and results showed that ammonium replaced potassium in K-struvite matrix. *PHREEQC predicts precipitation of cattiite under these conditions*.					

	Mg⁺ (mM)	K⁻ (mM)	P-PO₄ (mM)	N-NH₃ (mM)	Mg•K•P molar ratio	pH	S_K initially and at equilibrium[1]
(Xu et al. 2011)	104	52.4	104	0	2•1•2	10	9.42, 1
	Study results: Claiming up to 65% removal of potassium and co-precipitation of K-struvite and magnesium sodium phosphate at pH 10. *PHREEQC predicts precipitation of K-struvite and cattiite under these conditions*						

	Mg⁺ (mM)	K⁻ (mM)	P-PO₄ (mM)	N-NH₃ (mM)	Mg•K•P molar ratio	pH	S_K initially and at equilibrium[1]
(Wilsenach et al. 2007)	13.4	52.4	10.3	2.9	1.3•5•1	9.4	3.39, 0.96
	Study results: Claim that struvite and K-struvite were both produced. Difficult to be certain what was being produced in the experiment. No effluent concentration of potassium is given. No chemical analysis or XRD of precipitate shown. *PHREEQC predicts precipitation of cattiite under these conditions*						

[1] S_k values determined using PHREEQC

There are a couple of takeaways from these papers. A few of the papers used K:P ratios less than 1, perhaps in order to show a high potassium removal. This seems counterproductive for nutrient recovery research as the highest priority for recovery remains, and should remain, phosphorus, not potassium. Adding phosphorus to a potassium rich waste to recover potassium will likely not make any economic sense if one were to analyze the numbers. Secondly, by using the initial solution concentrations and pH, and modeling the reaction in PHREEQC, the initial result was often not pure K-struvite. However, it should be reiterated that the model gives equilibrium predictions which may be different from actual experimental results if equilibrium was not attained in the studies shown.

There are also a number of papers within the concrete literature which discuss using K-struvite in high strength concretes (Chau et al. 2011; Viani et al. 2014); these are not reported here because none of the same parameters (such as nutrient concentrations, pH, supersaturation ratio etc) are reported, thus making any comparisons difficult.

3.5.1 Existing potassium recovery technologies

A few potassium removal technologies, other than crystallization as K-struvite were discussed in the literature.

Some work has been done on recovering potassium from sea brines through precipitation as potassium perchlorate ($KClO_4$), followed by conversion to potassium chloride through anion exchange (Epstein et al. 1975).

A few papers discuss using electrodialysis to remove potassium from solution. Electrodialysis selectively separates anions and cations across an ion exchange membrane driven by an applied field between electrodes. Cationic species (eg. NH_4^+, K^+) move towards the anode, while anionic species move towards the cathode. Mehta et al., (2014) suggests that this process seems to be more applicable for N and K as P can be removed using less expensive methods. This method was been used to recover over 99% of K from winery waste streams and wheat leachates washed from dry wheat biomass, although this technology has yet to be applied at pilot scale.

Decloux et al., (2002) discusses using beet molasses fermentation waste products as organic fertilizers and cattle feed. The fermentation waste products have a high potassium content which is on average, 9.0 g/100g solids as K_2O and must be reduced before it can be used as cattle feed. The author describes results of a project in which potassium concentration of the fermentation waste products was decreased through electrodialysis from about 9 g/L K^+ to about 1 g/L K^+.

3.6 Conclusions for development of present study

What we know from past studies is that chemists and crystallographers know of K-struvite and understand its morphology. However, K-struvite is becoming more frequently referred to in the nutrient recovery literature, and a number of articles reference having synthesized K-struvite. However, the papers published are often lacking in a certain area. Either the articles do not provide detailed methodology on its formation, or evidence that pure K-struvite has been synthesized is lacking. K-struvite can be synthesized under various conditions, but synthesis under conditions similar to typical wastewaters has yet to be reported.

Therefore, there are practical reasons and sufficient interest from the research community to warrant detailed studies of K-struvite synthesis and to develop a more fundamental understanding of this mineral. As well, the interest in K-struvite is derived from the potential to combine it with regular NH_4-struvite; therefore, research into the pelletization potential of K-struvite is in line with current objectives in nutrient recovery.

The ideal waste to recover K-struvite would have high potassium concentrations in the range of potash brine, with phosphate and magnesium concentrations similar to animal wastes. Based on the wastes available with high concentrations of potassium and phosphate, there is no ideal waste for recovering K-struvite.

For nutrient recovery from wastes to become interesting and feasible, a centralized system of dealing with these disparate wastes is needed in order to be able to manage the input nutrient concentration and achieve the necessary supersaturation for crystallization to occur.

Therefore for the present study, this author was interested in laying groundwork for further work in potassium recovery and developing an understanding of how K-struvite forms. To accomplish this, the aqueous equilibrium modeling software PHREEQC was used to estimate synthesis conditions, followed by testing in the lab.

CHAPTER 4
RESEARCH OBJECTIVES

As outlined in Chapter 1, the purpose of this research was to better understand K-struvite chemistry and lay the groundwork for future work in recovering potassium and phosphate as K-struvite. To achieve this, the research was divided up into three separate experiments, each with a separate objective as described below:

1. Define new K_{sp} values for K-struvite at 10, 25 and 35°C. Currently, there is only one published value by Taylor et al., (1963) of 10.62 and it is believed that K-struvite might actually be less soluble than this value indicates.

2. Determine solution conditions required for pure K-struvite synthesis using PHREEQC, and test these conditions in the lab.

3. Assess the pelletization potential of K-struvite through initial runs in the UBC-FBR NH_4-struvite crystallizer.

Each experiment has a chapter devoted to it, starting with defining a new solubility product value for K-struvite, which underlies the modeling work necessary to determine conditions for K-struvite synthesis. Following determination of conditions for K-struvite synthesis, those conditions were applied to initial runs in the UBC-FBR.

CHAPTER 5
EXPERIMENT 1 – K-STRUVITE SOLUBILITY PRODUCT DETERMINATION

5.1 Experimental objectives

The objective of Experiment 1 was to define a new K_{sp} value for K-struvite at 10, 25 and 35°C. There is only one experimental value published for K-struvite by Taylor et al., (1963) of 10.62 at 25°C. It is hypothesized that K-struvite might actually be less soluble than this value indicates because improvements in methods to measure K_{sp} have become more accurate by taking into account the effect of ionic strength on ion activities, and the formation of other magnesium phosphate phases in the equilibrium calculations.

5.2 Materials and methods

Experiments were conducted to determine the solubility product constant, K_{sp-K}. The experiments were designed to establish equilibrium between the component ions in solution and the K-struvite solid phase crystals using a method similar to that of Ohlinger et al., (1998).

5.2.1 Materials and equipment

5.2.1.1 Batch test method and apparatus
Each experiment was run in parallel using two 400 mL, thermostated, stirred, jacketed glass reactors. All parts of the reactor were rinsed with a mild HCl solution followed by distilled and deionized water prior to the start of the experiment.

5.2.1.2 Reagents used
All reagents used were analytical grade chemicals. Distilled and deionized water were used in all experiments.

5.2.1.3 pH monitoring
pH was monitored in both stirred reactors using two Oakton pH 11 Series meters complete with ATC probes. pH meters were calibrated prior to each experiment using standard pH 4, 7 and 10 buffer solutions.

5.2.1.4 Conductivity monitoring
Conductivity was monitored using an Oakton CON 110 meter with ATC probe and calibrated prior to each measurement using a potassium chloride (KCl) standard of similar ionic strengths to that expected in the solution.

5.2.1.5 Sample collection and preservation

All storage vials and collection apparatus were cleaned and rinsed. Liquid samples were collected using a syringe and filtered using a 0.45 µm filter. Liquid samples were preserved with 1-2 drops of concentrated HCl to prevent the formation of solid phases. Solid phase samples were collected using a syringe and filtered with a vacuum using a 0.45 µm filter. The solid sample was rinsed with distilled water and reagent alcohol, left to dry in the ambient, then stored.

5.2.2 Analytical methods

5.2.2.1 Magnesium analysis

Samples were analyzed for magnesium using a Varian Inc. SpectrAA220 Fast Sequential Atomic Absorption spectrophotometer. Samples were diluted to within the calibration range and standards were prepared using $MgCl_2$. A 20 g/L lanthanum solution was prepared from reagent grade lanthanum nitrate, $La(NO_3)_3$ and distilled water to reduce background matrix interference. This was followed by addition of one drop of concentrated nitric acid (HNO_3) to each tube and well-mixed. Prior to each set of analyses, fresh deionized water was provided for auto-sampler rinsing and the magnesium lamp was optimized and warmed up. Each set of samples was analyzed three times at a different flame angle.

5.2.2.2 Phosphate analysis

Samples were analyzed for phosphate by flow injection analysis using the Lachat QuikChem 8000 using Method 4500-NH3 H and 4500-P G from Standard Methods for the Examination of Water and Wastewater (American Public Health Association, American Water Works Association, and Water Environment Federation 2012). Samples were prepared and diluted at a 1:5 volumetric ratio with distilled water. Calibration standard solutions were composed of reagent grade potassium phosphate monobasic (KH_2PO_4) in distilled water.

5.2.2.3 Potassium analysis

Samples were analyzed for potassium using the Varian SpectrAA 220 Fast Sequential Atomic Absorption Spectrophotometer. Samples were diluted to within the calibration range and standards of 0.1, 0.5, 1.0, 2.5, 5.0 10.0 and 15.0 mg/L were prepared using KCl. A 5 g/L Cs^+ solution was prepared as an ionization suppressant. A drop of nitric acid was added to the sample and well-mixed prior to analysis. Prior to each set of analyses, fresh deionized water was provided for auto-sampler rinsing. The potassium lamp was optimized, warmed up and different flame angles were used during the analysis. Each set of samples was analyzed three times.

5.2.2.4 Inorganic carbon analysis

Inorganic carbon analyses were run on the initial and final samples to determine absorption of CO_2 and its resulting influence on pH values. Inorganic carbon was analyzed using the Lachat IL550 TOC-TN analyzer.

5.2.2.5 X-Ray diffraction analysis

Solid samples were analyzed to confirm presence of crystalline phases using a Bruker D8 Advance X-ray diffractometer using CuK α radiation. X-ray diffraction (XRD) output peak patterns were identified using the powder diffraction database file, provided by the International Center for Diffraction Data. This instrument was located in the UBC Department of Chemistry.

5.2.3. Quality assurance & statistical methods

For the K_{sp-K} analyses, each sample was analyzed for magnesium, potassium and phosphate in triplicate and analyzed at three dilutions, giving nine data points per analyte. Data points out of the calibration range, or which appeared to be contaminated were discarded. Experimental blanks were run during experiments and sample blanks were run during chemical analysis to reduce contamination errors and to ensure quality data.

Averages and standard deviations were calculated for analyte concentrations in solid and liquid samples. The average and the standard deviation of the parallel reactors were reported as the result.

5.2.4 Experimental setup

For each experiment, two parallel, jacketed, stirred reactors were used, connected subsequently with a thermostat. Before each experiment, the reactors and its parts were cleaned with a brush, followed by the retention of a mild hydrochloric acid in it for several hours with mixing. After the acid wash, all parts of the reactors, including disassembled agitators, thermometers, and lids, were rinsed with tap, distilled, and deionized water.

5.2.4.1 Formation of synthetic K-struvite for K_{sp-K} determination

K-struvite was prepared according to the following chemical reaction:

$$MgCl_2: 6H_2O_{(aq)} + 3KCl_{(aq)} + K_2HPO_{4(aq)} + KOH_{(aq)} \leftrightarrow MgKPO_4: 6H_2O_{(s)} + 5KCl_{(aq)} + H_2O$$

The initial solution to make 0.25 moles of K-struvite used the following recipe. Dissolve 50.83 g of Magnesium chloride (MgCl$_2$:6H$_2$O) in 200 mL distilled water, dissolve 55.95 g of potassium chloride (KCl) in 200 mL distilled water, and dissolve 43.55 g of potassium phosphate (K$_2$HPO$_4$) in 200 mL distilled water. The initial solution had a S_K of 43 with an Mg:K:P ratio of 1:5:1.

In a stirred one litre reactor, with a pH probe inserted, the potassium phosphate and potassium chloride solutions were mixed until they dissolved. The magnesium chloride solution was added, and the volume brought up to about one litre by adding distilled water. A 2M KOH solution was prepared and added until pH was about 11 and maintained in this range. The mixture was left overnight. The precipitate was then filtered using a vacuum filter, washed with distilled water and reagent alcohol, and left to dry in the ambient.

5.2.4.2 Analysis of synthetic K-struvite

After synthesis, the K-struvite was analyzed for its magnesium, potassium and phosphate content, and XRD analysis was performed. The K-struvite was found to be pure and the results of the analysis can be found in Appendix A.

5.2.4.3 Preparation of KCl solution

Dissolution of K-struvite was done in a 0.1M KCl solution in order to prevent formation of other solid phases. Although this increased the ionic strength (μ) of the solution, which, in turn, can affect the activity coefficients, PHREEQC calculations automatically extrapolate to the true thermodynamic solubility product at μ=0.

This stock solution was prepared in advance, in an amount sufficient for all three temperatures (about three litres). High analytical grade KCl was used to prepare the solution. After preparation, the solution was analyzed for potassium and inorganic carbon.

5.2.4.4 Equipment setup

Before each experiment began, the water bath temperature was set. Both reactors were filled with deionized water, the thermostat and the mixers turned on, and thermometers immersed in both reactors. The reactors were then sealed (with the lids and bungs). The temperature was adjusted until the temperature in the reactors was set for the desired value and was consistent for at least two hours. The thermometer in the reactors was used to check on the actual temperature, not the display of the water bath. In case the temperature in one reactor was slightly different than in the other, the average temperature in the reactors was kept as close to the desired value as possible.

5.2.5 Experimental procedure

Following the experimental setup as described in Section 5.2.4, the water in the reactor was discarded and 400 mL of KCl solution was added to each reactor and brought up to the correct temperature. At the desired temperature, 5 grams of the synthesized K-struvite was added to each reactor. The reactors were then sealed with a lid and bungs to minimize interaction with air. The mixture was retained for 96 hours with the temperature and mixers monitored periodically during this time.

After the retention, a liquid sample was taken using a clean, dry syringe and a 0.45 μm filter. To take the sample, the reactor was unsealed by removing a bung from one side, the tubing immersed while still mixing, and taking a sample from the central part of the reactor. The first sample was taken and disposed of in order to rinse the syringe. The second sample was taken, filtered and poured into a clean container and sealed. The same was done for the second reactor, using a different filter and syringe. The solids retained on the filter paper were disposed of. A 10-time and 100-time dilution was immediately made of the liquid sample in order to prevent precipitation from occurring in the sample. None of the liquid samples were refrigerated to prevent precipitation in the sample.

Following the liquid sample, the lid of the reactor was opened to record pH and conductivity readings. The pH and conductivity probes were first calibrated and rinsed prior to immersion. The probes were then immersed until the reading was constant (approximately 10 minutes). The same probes were used for both reactors. Mixing was maintained during this procedure.

Finally, after collection of the liquid sample and pH and conductivity measurements, the bulk suspension was filtered using a regular vacuum filter. The precipitate was rinsed using deionized water and reagent alcohol. The temperature of the rinsing water and reagent alcohol were of a similar temperature to the experimental temperature. The filtrate was then disposed of, and the precipitate was left to dry in the ambient air before being sealed.

Magnesium, potassium and phosphate analysis of the liquid sample and precipitate was performed, followed by XRD analysis on the precipitate. The undiluted liquid sample was also analyzed for inorganic carbon.

This procedure was repeated for 10, 25 and 35°C

5.2.6 Data treatment for $K_{sp\text{-}K}$ determination

Once all the analytical data were collected and summarized, they were used for equilibrium modeling in PHREEQC, using the same technique as Ohlinger et al., (1998) to determine the $K_{sp\text{-}K}$ value at each temperature. The technique essentially selects a solubility product that best matches the experimental data.

This process requires defining a range of possible $K_{sp\text{-}K}$ values based on the experimental data, then calculating theoretical concentrations for all aqueous magnesium, potassium and phosphate species based on those $K_{sp\text{-}K}$ values chosen and experimental pH. The theoretical species concentrations are summed into total magnesium, potassium and phosphate concentrations, then the $K_{sp\text{-}K}$ value that provides the best match of the of the theoretical concentration values with the experimental data is chosen by minimizing the objective function. The theoretical concentration values were generated using PHREEQC as per Equation 44 and are shown in Appendix A.

$$Objective\ function = \sum \left[\frac{\left(C_{T,Mg}^{theo} - C_{T,Mg}^{meas}\right)^2}{\sigma_{Mg}^2} + \frac{\left(C_{T,K}^{theo} - C_{T,K}^{meas}\right)^2}{\sigma_K^2} + \frac{\left(C_{T,PO_4}^{theo} - C_{T,PO_4}^{meas}\right)^2}{\sigma_{PO_4}^2} \right] \qquad \textbf{Equation 44}$$

To note: each sample was analyzed at three dilutions in triplicate, and measured three times each, giving nine data points per sample. Data points that fell out of the calibration range, or were deemed to be contaminated, were discarded.

5.3 Results and discussion

Figure 13 summarizes the results of the $K_{sp\text{-}K}$ determination at the three temperatures of interest, 10, 25 and 35°C. It was found that K-struvite has a lower solubility product than previously measured by Taylor et al. (1963). making the apparent solubility less than it was previously reported to be. The experimental results fit closely with Van't Hoff's equation, which says that the solubility product is dependent only on temperature.

5.3.1 Experiment 1A: $K_{sp\text{-}K}$ determination at 10°C

The experimental results of solution species concentrations for $K_{sp\text{-}K}$ determination at 10°C can be seen in Table 7. The results of total concentrations for magnesium, potassium and phosphorus were compared against theoretical concentrations generated in PHREEQC. These values were then used to minimize the objective function, Equation 44, for a selected range of possible pK_{sp} values. The objective function essentially selects the pK_{sp} value whose theoretical concentrations best match the experimental conditions.

Figure 8 shows the plot of the objective function versus possible K-struvite pK_{sp} values which were generated from the modeling results for parallel reactors. The objective function was minimized at 11.075 and 11.066 for Reactors A and B, respectively. This gives a pK_{sp} of 11.071±0.006 at 9.7°C. The solid phase produced was confirmed as K-struvite through XRD analysis as seen in Figure 7. The modeling data used to achieve this result can be seen in Appendix A.

Table 7 – Experiment 1A equilibrium results of solution species concentrations at 10°C

Reactor	T (°C)	pH	μ	$C_{T,Mg}^{meas}$ (mM)	$C_{T,K}^{meas}$ (mM)	$C_{T,P\text{-}PO4}^{meas}$ (mM)	Solid phase present
A	9.7	8.72	0.16	2.741	94.756	2.711	K-struvite
B	9.7	8.74	0.16	2.702	98.891	2.684	K-struvite
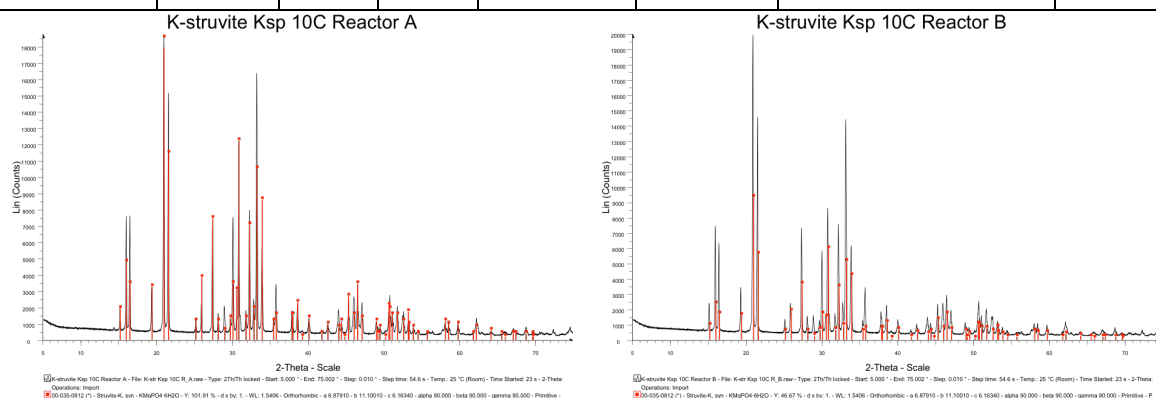
Figure 7 – Experiment 1A: XRD analysis of solid sample for 10°C $K_{sp\text{-}K}$ determination
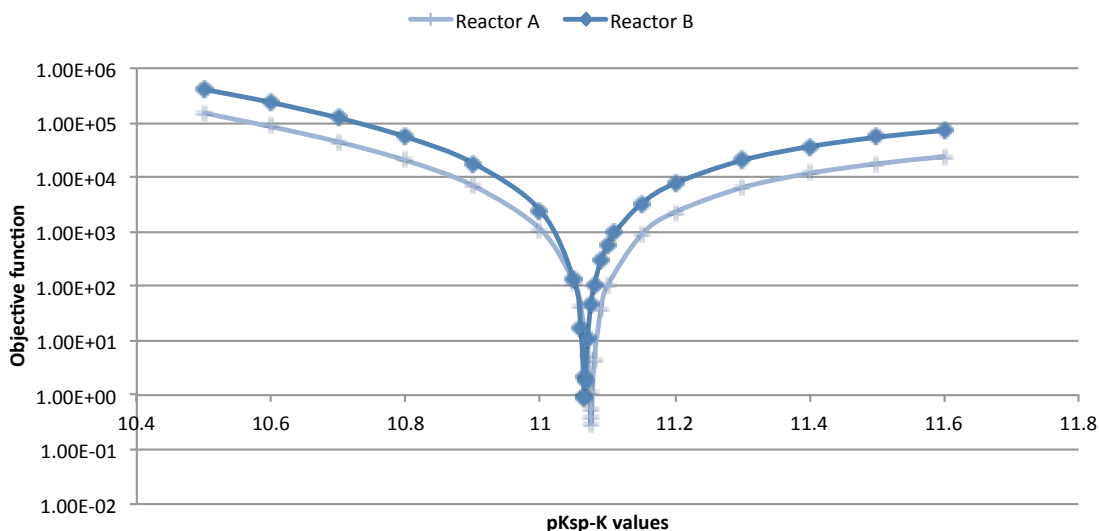
Figure 8 – Experiment 1A: plot of objective function versus possible pK$_{sp-K}$ values for K-struvite at 10°C

5.3.2 Experiment 1B: K$_{sp-K}$ determination at 25°C

The experimental results of solution species concentrations for K$_{sp-K}$ determination at 25°C are shown in Table 8. Figure 9 shows the plot of the objective function versus possible K-struvite pK$_{sp}$ values. The solid phase produced was confirmed as K-struvite through XRD analysis as seen in Figure 10. The objective function was minimized at 10.976 and 11.026 for reactors A and B respectively using the same technique as described in the Section 5.3.1. This gives a pK$_{sp-K}$ of 11.001±0.035 at 25.5°C. The experimental and modeling data can be seen in Appendix A.

Table 8 – Experiment 1B equilibrium results of solution species concentrations at 25°C

Reactor	T (°C)	pH	μ	$C_{T,Mg}^{meas}$ (mM)	$C_{T,K}^{meas}$ (mM)	$C_{T,P-PO4}^{meas}$ (mM)	Solid phase present
A	25.5	8.57	0.12	3.499	98.299	3.346	K-struvite
B	25.5	8.51	0.10	3.546	102.927	3.627	K-struvite
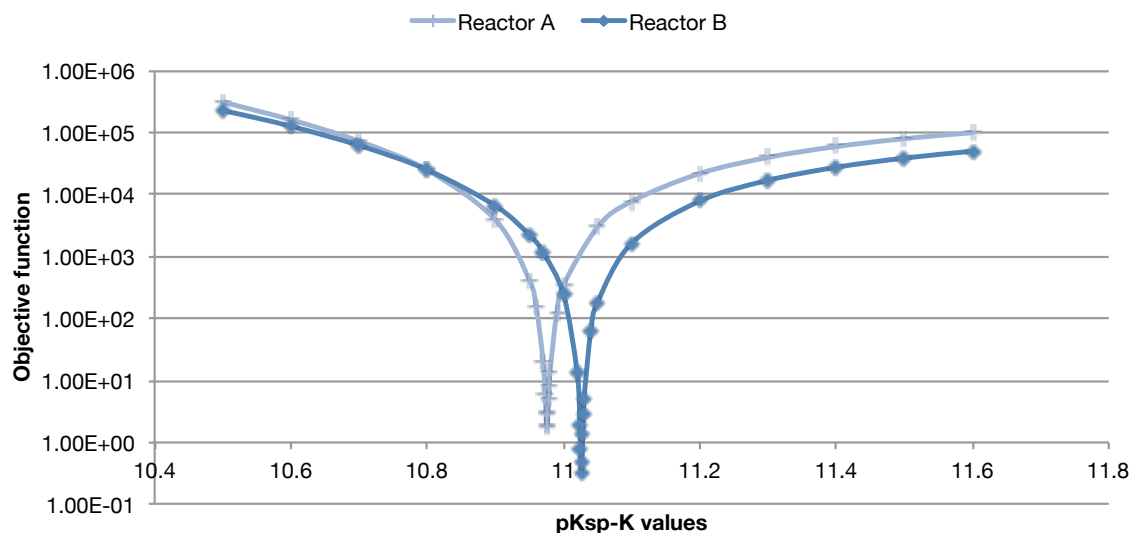
Figure 9 – Experiment 1B: plot of objective function versus possible pK$_{sp-K}$ values for K-struvite at 25°C
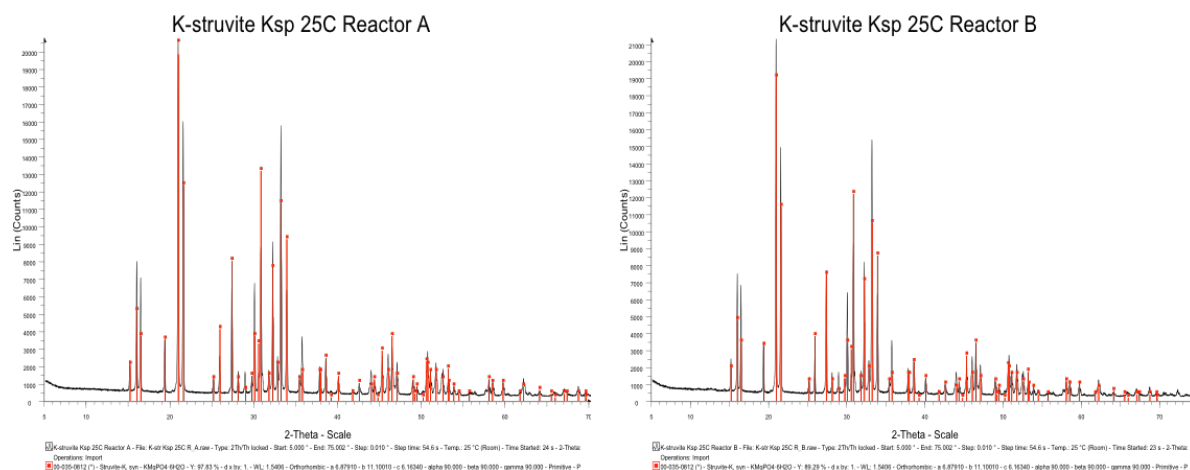
Figure 10 – Experiment 1B: XRD analysis of solid sample for 25°C K$_{sp-K}$ determination

5.3.3 Experiment 1C: K$_{sp-K}$ determination at 35°C

Both K-struvite and bobierrite (Mg$_3$(PO$_4$)$_2$:8H$_2$O) were identified as present in the solid phase, meaning there are now two variables in the determination of K$_{sp-K}$; the K$_{sp-K}$ itself, and the saturation condition of bobierrite. From the XRD analysis shown in Figure 12, we know bobierrite is present in the solid phase, but we do not know how much is present, nor do we know whether it was at equilibrium with the liquid phase.

36

The range of potential pK_{sp-K} values was narrowed to 10.5 – 11.2, and the range of the bobierrite saturation index was set to 1.0 – 2.2 (SI>1 indicates supersaturated conditions). Using the equilibrium solution pH, seen in Table 9, theoretical Mg, K and P-PO$_4$ concentrations were modeled for each condition and the objective function was calculated. Local minimums were found for each set of conditions. The process was repeated at a higher resolution where the lowest minimum was found. The absolute minimum of the objective function as a function of K_{sp-K} and the bobierrite saturation index was determined this way.

Figure 11 shows that the objective function is minimized at for a pK_{sp-K} value of 10.89 and 10.90 for reactors A and B, respectively. This gives a pK_{sp-K} result of 10.895±0.007 at 35.7°C. The data used to generate these figures can be seen in Appendix A.

Table 9 – Experiment 1C equilibrium results of solution species concentrations at 35°C

Reactor	T (°C)	pH	μ	$C_{T,Mg}^{meas}$ (mM)	$C_{T,K}^{meas}$ (mM)	$C_{T,P-PO4}^{meas}$ (mM)	Solid phases present
A	35.7	10.17	0.14	0.0785	117.975	6.377	K-struvite Bobierrite
B	35.7	10.05	0.14	0.0889	121.142	7.168	K-struvite Bobierrite
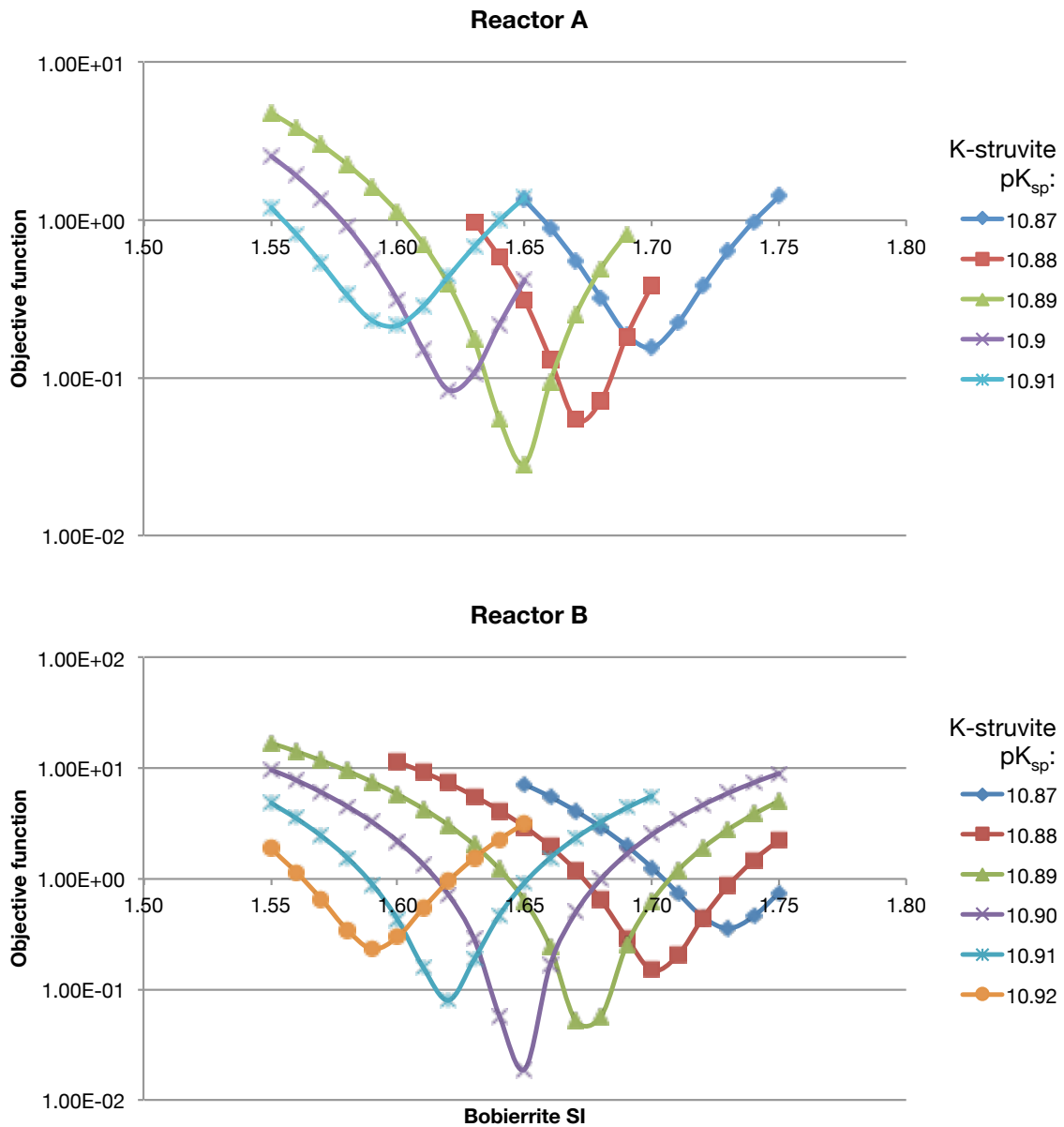
Figure 11 – Experiment 1C: plot of the objective function versus bobierrite saturation index for a range of possible K-struvite K_{sp} values.
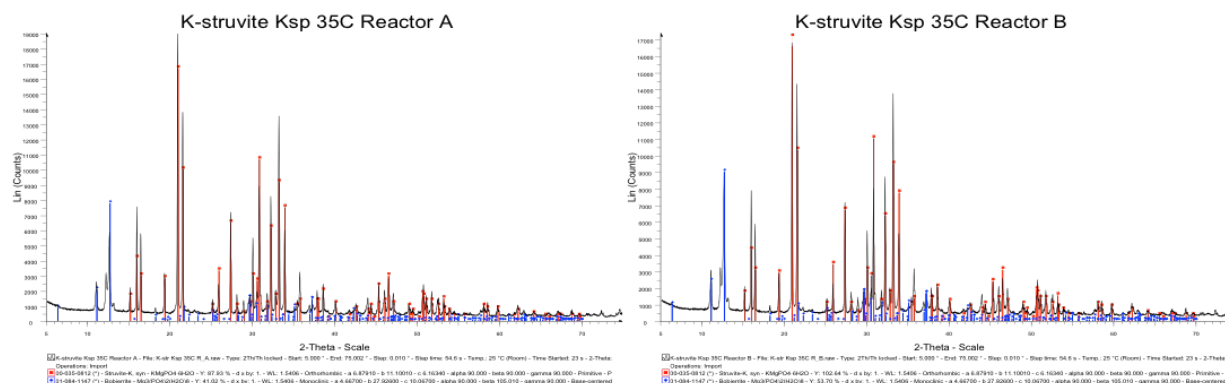
Figure 12 – Experiment 1C: XRD analysis of solid sample for 35°C K$_{sp-K}$ determination

5.4 Conclusions

K-struvite appears to be less soluble than previously reported by Taylor et al. (1963) and the results, as seen in Figure 13 fit the Van't Hoff model. Results for pK$_{sp-K}$ were 11.07, 11.00 and 10.90 at 10, 25 and 35°C, respectively.

Differences between the result presented by Taylor et al. and the result presented here is likely due to several issues: the incorporation of more solid phases into the determination of theoretical magnesium, potassium and phosphate concentrations at equilibrium; as well as upgrading the PHREEQC database with more species, using recently published, critically selected equilibrium constants, and expanding their values in a wide temperature range.

K-struvite experimental solubility product results
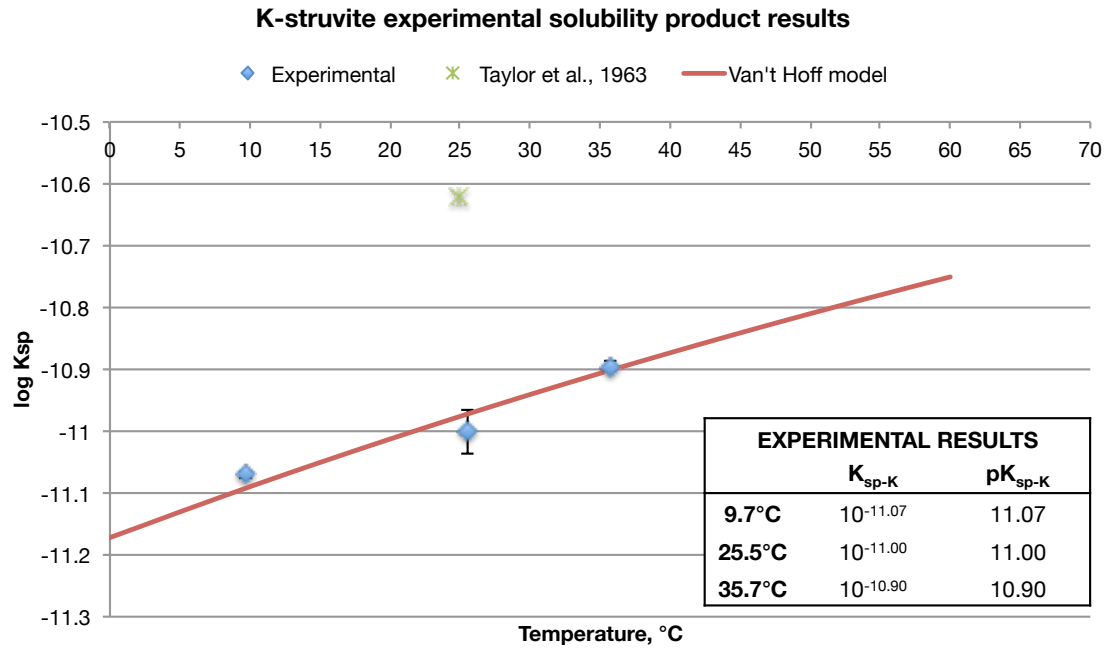
Figure 13 - Summary of experiments 1A, 1B and 1C: K-struvite log K_{sp} values at 10, 25 and 35°C

CHAPTER 6
EXPERIMENT 2 – K-STRUVITE SYNTHESIS

6.1 Experimental objectives

Objectives of this experiment 2 were to identify optimal supersaturation ratios for synthesizing pure K-struvite. Three different supersaturation ratios were tested at different pH's to study the crystallization kinetics of K-struvite.

6.2 Materials and methods

6.2.1 Materials and equipment

Section 5.2.1 provides a full description of reagents and analytical methods used.

6.2.2 Experimental setup

Prior to starting the experiments, reactors were washed with a dilute HCl solution and rinsed with distilled water. Experiments were done parallel stirred reactors, thermostated at 25°C with a pH probe immersed for the duration of the experiment. A 2M NaOH solution was used to control pH.

6.2.3 Experimental procedure

6.2.3.1 High concentration
K-struvite was synthesized using a very high supersaturation ratio in the initial experiment to show that pure K-struvite can be synthesized by the following reaction.

$$MgCl_2:6H_2O_{(aq)} \ + \ K_2HPO_{4(aq)} + \text{KCl}_{(aq)} + \text{NaOH}_{(aq)}$$
$$\leftrightarrow MgKPO_4:6H_2O_{(s)} + 2\text{KCl}_{(aq)} + \text{NaCl}_{(aq)} + H_2O$$
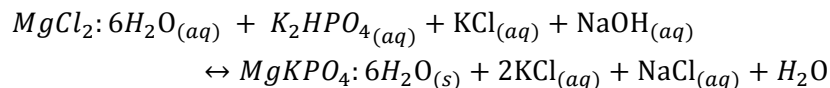
A concentration to give 0.25 moles MgKPO$_4$.6H$_2$O was used with an initial Mg:K:P ratio of 1:3:1. Experiments were repeated at pH's of 10.5, 9.0 and 7.5. The potassium phosphate and potassium chloride solutions were mixed and brought up to 25°C. The magnesium chloride solution was added slowly while stirring. The pH was adjusted using the 2M NaOH solution until pH reached the desired value. The pH was maintained at this level throughout the experiment.

The initial calculated supersaturation ratios, S_K, for this experiment were 33.7, 13.5 and 4.29 for pH's 10.5, 9.0 and 7.5, respectively. Ionic strength was approximately 1.27. Initial concentrations in the reactor were as follows:

Mg	6968 mg/l	or	287 mM
K	29450 mg/l	or	750 mM
P-PO$_4$	7743 mg/l	or	250 mM

Precipitate samples were taken by drawing about 50 mL of well-mixed sample, filtering with a vacuum and 0.45 µm filter, then washing the sample using distilled water followed by ethanol. Samples were then left to dry in the ambient then stored in a sealed container. Samples were taken at the following intervals:

pH 10.5	10 min, 30 min, 1 hr, 3 hr, 6 hr, 24 hr
pH 9.0	10 min, 30 min, 1 hr, 3 hr, 6 hr, 9 hr, 24 hr
pH 7.5	30 min, 3 hr, 6 hr, 9 hr, 24 hr, 48 hr, 72 hr

Precipitate samples were then analyzed for K^+, Mg^{2+} and $P-PO_4^{3-}$ as well as by XRD analysis as described in Section 5.2.2.

6.2.3.2 Low concentration

The experiment for low concentration synthesis used nutrient concentrations similar to those found in dairy waste after nutrient extraction with microwave technology (Zhang 2013) to give a Mg:K:P ratio of 3:11:1. Solution ionic strength was approximately 0.05. Initially calculated supersaturation ratios were 3.64, 1.42 and 0.435 for pH's 10.5, 9.0 and 7.5, respectively. The initial solution concentrations were:

Mg	219 mg/l	9 mM
K	1290 mg/l	33 mM
P-PO$_4$	93 mg/l	3 mM

Precipitate and liquid fraction samples were taken in this experiment. Using a syringe, about 50 mL of well-mixed sample was drawn and filtered using a 0.45 µm filter. The filtrate was collected in a vial and 1-2 drops of concentrated HCl were added to the sample. The precipitate was dried and stored in a sealed container. However, not enough precipitate was produced to analyze, so only the liquid fraction was analyzed. Samples were taken at the following intervals:

pH 10.5	initial, 10 min, 30 min, 1 hr, 3 hr, 6 hr, 24 hr
pH 9.0	initial, 10 min, 30 min, 1 hr, 3 hr, 6 hr, 9 hr, 24 hr
pH 7.5	initial, 30 min, 3 hr, 6 hr, 9 hr, 24 hr, 48 hr, 6 days

Liquid samples were then analyzed for K^+, Mg^{2+} and $P-PO_4^{3-}$ as described in Section 5.2.2.

6.2.3.3 Optimal concentration

Using PHREEQC, it was determined that an optimal Mg:K:P ratio was approximately 3:50:1 for a specific wastewater matrix. The initial S_K was 1.6 and ionic strength was 0.41. Initial concentrations in the reactor were as follows:

Mg	583 mg/l	24 mM
K	13881 mg/l	357 mM
P-PO$_4$	211 mg/l	6.8 mM

This experiment was conducted at pH 8 and precipitate samples were taken at the following intervals: 1 hr, 3 hr, 9 hr and 24 hr. Using a syringe, 100 mL of sample was drawn and filtered using a vacuum and a 0.45 µm filter. The precipitate was washed with distilled water followed by reagent alcohol and left to dry in the ambient. The sample was then stored in a sealed container, ready for analysis.

Precipitate samples were then analyzed for K^+, Mg^{2+} and $P-PO_4^{3-}$, as well as by XRD analysis as described in Section 5.2.2.

6.3 Results and discussion

Table 10 shows a summary of the batch tests performed to synthesize pure K-struvite. Batch tests at high concentrations and the 'optimal' concentration both produced pure K-struvite. In these experiments, the pH's were kept constant at 10.5, 9.0 and 7.5 while supersaturation varied as the solution went to equilibrium.

Table 10 - Summary of experiment 2 parameters for K-struvite synthesis batch tests

Experiment		Mg:K:P molar ratio[1]	Initial solution concentration		pH	Initial S_K	T (°C)	Results of experiment[2]
High concentration	2A	1:3:1	Mg	287 mM	10.5	3.7		See Section 6.3.1
	2B		K	750 mM	9.0	13.5		
	2C		P	250 mM	7.5	4.29		
Low concentration	2D	3:11:1	Mg	9 mM	10.5	3.64	25	See Section 6.3.2
	2E		K	33 mM	9.0	1.42		
	2F		P	3 mM	7.5	0.435		
Optimal concentration	2G	3.5:50:1	Mg	24 mM	8.0	1.60		See Section 6.3.3
			K	357 mM				
			P	6.8 mM				

[1] Initial Mg:K:P molar ratio in solution
[2] Each experiment was performed in parallel

6.3.1 Experiments 2A, B and C: results for high concentration K-struvite synthesis

The high concentration synthesis experiments were performed to show that a pure K-struvite product could be formed and to examine its formation over the reaction time. Three parallel experiments at different pH's were performed as shown in the table below.

Table 11 – Experiments 2A, B, C: solution conditions for high concentration K-struvite synthesis

Experiment	Mg:K:P molar ratio	Initial solution concentration		T (°C)	pH	Initial S_K	Experiment length
2A		Mg	287 mM		10.5	33.7	24 hours
2B	1:3:1	K	750 mM	25	9.0	13.5	48 hours
2C		P	250 mM		7.5	4.29	6 days

Generally, in the batch reactor experiments, supersaturation is initially high and goes to 1 as equilibrium is reached as precipitate is formed. The goal of the experiments with a high supersaturation was to show that pure K-struvite could be synthesized. Table 11 gives details on the experimental and solution conditions for high concentration synthesis. Figure 14 shows results of the synthesis reaction and the molar ratios in the solid. Figure 15 shows select XRD scans of the solid phases produced in the synthesis experiments, which indicates the crystalline phases in the solid.

Figure 14i, at pH 10.5, the initial supersaturation ratio was 33.7 and the mixture was left to react for 24 hours while the pH was maintained. In a pure product we would expect the Mg:K:P molar ratio to be 1:1:1, though these samples show a slight downward trend in the K:P ratio over the course of 24 hours. The K:P ratio was highest at 0.83 at the 10 min sample time and decreased to 0.73 at 24 hours. This was consistent in both reactors. The Mg:P ratio was consistently greater than 1, and showed a slight upward trend over the experiment. Not shown in Figure 14, but the number of waters present based on a mass balance, (assuming the solid phase was pure K-struvite) was also greater than what was expected for the magnesium potassium phosphate hexahydrate. The number of waters was consistently between 6.5 and 7.5. There was likely the formation of an amorphous phase, which could not be identified through XRD analysis, since only crystalline phases can be identified using XRD. However, formation of an amorphous phase with a Mg:P ratio higher than 1 would explain the increasing trend in Mg:P ratio and decreasing trend in K:P ratio. Modeling with PHREEQC predicts K-struvite as the only solid phase under these conditions, so it is unclear as to what the reason may be for the high number of waters present.

Brucite, $(Mg(OH)_2)$, was not observed, though brucite formation is possible at this pH. Xu et al., (2011, 2012) reported that sodium was incorporated into the K-struvite structure above pH 10, but this was not observed in these experiments.

At pH 9.0, the initial supersaturation ratio was 13.5, and the mixture was left to react for 48 hours. K-struvite was the only crystalline phase produced as shown in the XRD scans and as predicted in PHREEQC. Looking at Figure 14(ii), we see Mg:K:P in what is almost a 1:1:1 ratio. The K:P trend is upwards, starting around 0.75, going up to 0.85 as more K is incorporated into the solid phase over the 48 hour reaction. Similarly to the experiments at pH 10.5, the waters are greater than 6, generally around 6.5.

At pH 7.5, the initial supersaturation ratio was 4.29 and the mixture was left to react for 6 days. The results do not fit the model perfectly here. PHREEQC shows that other magnesium phosphates are also initially supersaturated and that newberyite ($MgHPO_4:3H_2O$) is precipitated. However, the XRD results in Figure 15, Experiment 6C, show K-struvite as the only precipitate up until hour 48 of the experiment. After that point, other solid phases are seen, as the dynamic equilibrium of the solution is established. Trace amounts of cattite ($Mg_3(PO_4)_2:22H_2O$) and possibly kovdorskite ($Mg_2PO_4OH:3H_2O$) were identified after 6 days. It is possible that the solution was not yet at equilibrium and if left long enough until equilibrium was reached, newberyite would be produced.

The K:P ratio trend is generally upwards until 48 hours for both reactors, starting around 0.7 and reaching 0.8 at 48 hours, before dropping at the 6 day sample. The waters of hydration in the solid sample are consistently around 6 based on the mass balance of the sample.

As a summary of this set of experiments, K-struvite was the only solid phase identified in samples at pH 9.0 and 10.5. Other solid phases were identified at pH 7.5. The K:P ratio was consistently less than 1, while waters were consistently greater than 6.
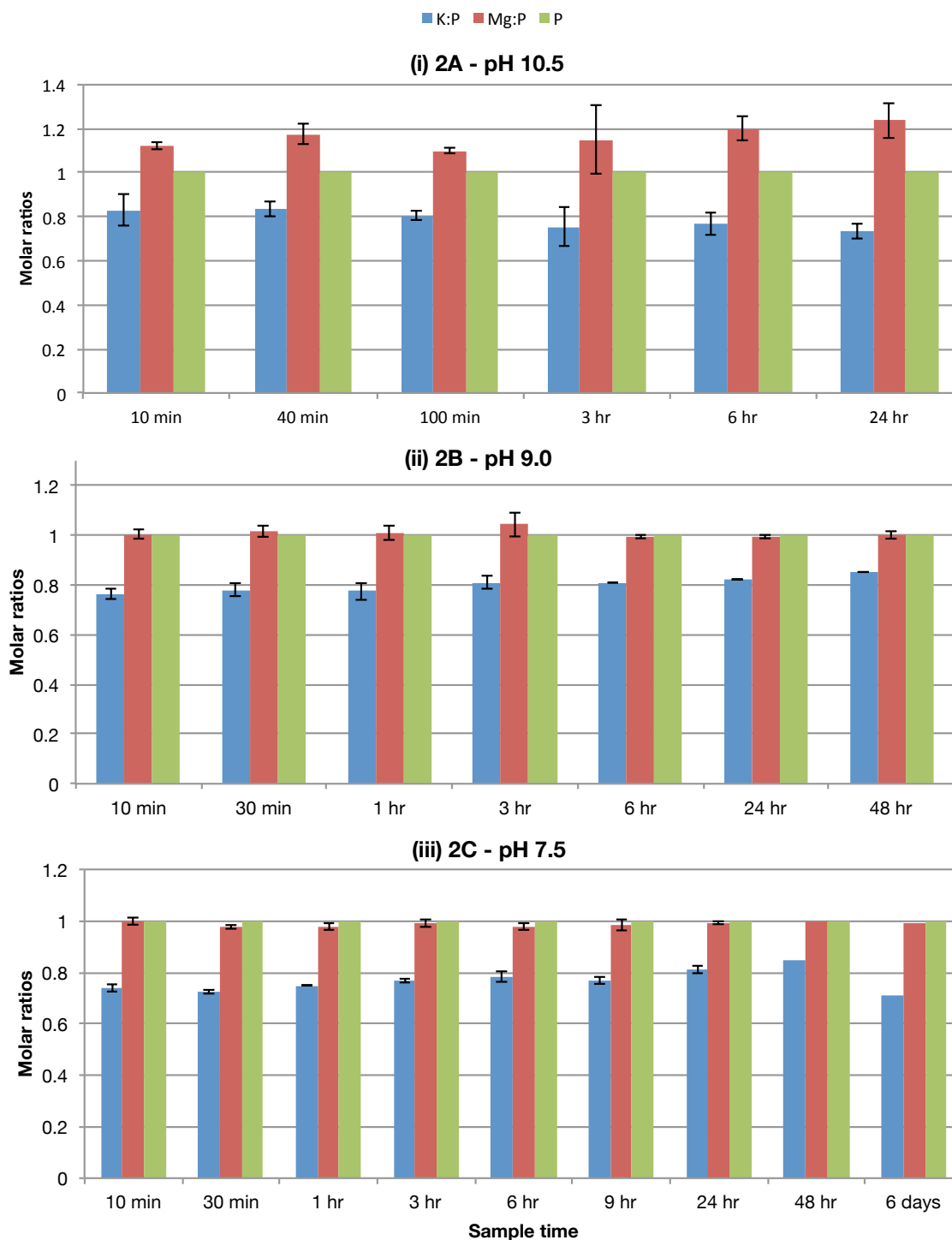
Figure 14 – Molar ratios in solid phase at high S_K for (i) experiment 2A at pH 10.5 (ii) experiment 2B at pH 9.0 and (iii) experiment 2C at pH 7.5
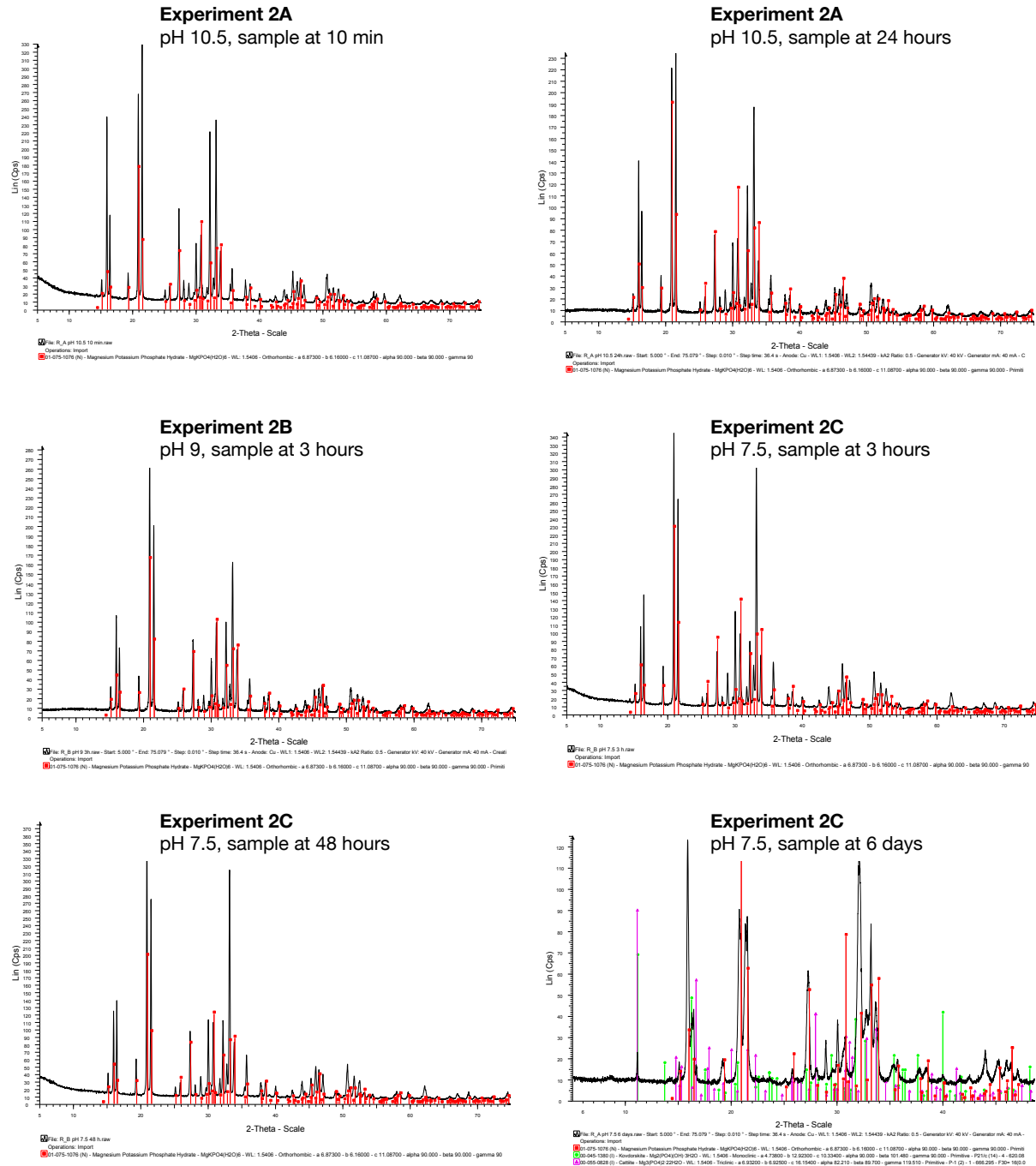
Figure 15 - XRD scans of samples synthesized at high S_K for experiment 2A at pH 10.5, experiment 2B at pH 9.0, and experiment 2C at pH 7.5

6.3.2 Experiments 2D, E and F: results for low concentration K-struvite synthesis

The concentrations used in the high concentration synthesis experiments were higher than what will likely be seen in any naturally occurring waste or material from which K-struvite could be synthesized. Therefore, the following experiments used concentrations found in dairy cow manure from the UBC Dairy Education and Research Centre in Agassiz, BC (Zhang 2013).

This set of synthesis experiments was conducted to test potassium, magnesium and phosphate concentrations seen in dairy cow manure. Initial concentrations were as described in Section 6.2 and are summarized in Table 12.

Table 12 – Experiment 2D, E, F: solution conditions for low concentration K-struvite synthesis

Experiment	Mg:K:P molar ratio	Initial solution concentrations		pH	Initial S_K	Experiment length
2D		Mg	9 mM	10.5	3.64	24 hours
2E	3:11:1	K	33 mM	9.0	1.42	4 days
2F		P	3 mM	7.5	$4.35E^{-1}$	13 days

A solid sample could not be collected because not enough precipitate was formed in the 400 mL reactors. Therefore, samples of the liquid fraction were collected and analyzed. Instead of looking at the solid composition, which was the method used in the high concentration synthesis experiments; the change in solution concentration over time was analyzed. However, the error on the potassium measurements was high because of the dilution required to analyze it. Precipitate was formed in the reactor, but from modeling results, the low supersaturation ratio, and experimental results it is unlikely that K-struvite was the only precipitate observed in the reactor.

At pH 10.5, in Figure 16(i), we see that the K:P reduction ratio increases up until the 1 hour sample time, then starts to decrease. This indicates that potassium was incorporated into the solid phase, and K-struvite was produced initially, but starts to dissolve as equilibrium is established. These results fit with PHREEQC's modeled results. PHREEQC models an initial supersaturation ratio of 3.64 for these solution conditions, although it predicts brucite and cattiite precipitates at equilibrium. If left for a longer period of time, the K-struvite produced in the reactor would have dissolved and the K:P molar reduction ratio would likely have gone to 0.

At pH 9.0, the initial modeled supersaturation ratio is greater than 1. Figure 16(ii) shows K:Mg:P ratios at 10, 30 and 60 minutes indicating rapid K-struvite formation. However, after 1 hour, the K:P ratio decreases to 0 at the 96 hour sample time, indicating that the K-struvite has redissolved. The Mg:P ratio is about 1.3:1 at 96 hours indicating formation of a magnesium phosphate. PHREEQC predicts cattiite precipitation at that equilibrium.

At pH 7.5, Figure 16(iii) shows negative K:P ratio results because the measured concentration of potassium in solution was greater than the initial measured concentration, even though it was a closed system and no potassium was added. This is likely due to analytical error caused

by high dilutions. However, we can still make a couple of conclusions and say that no potassium was incorporated into the solid phase under the experimental conditions and initial supersaturation ratio less than 1. PHREEQC predicted newberyite precipitation under these solution conditions.
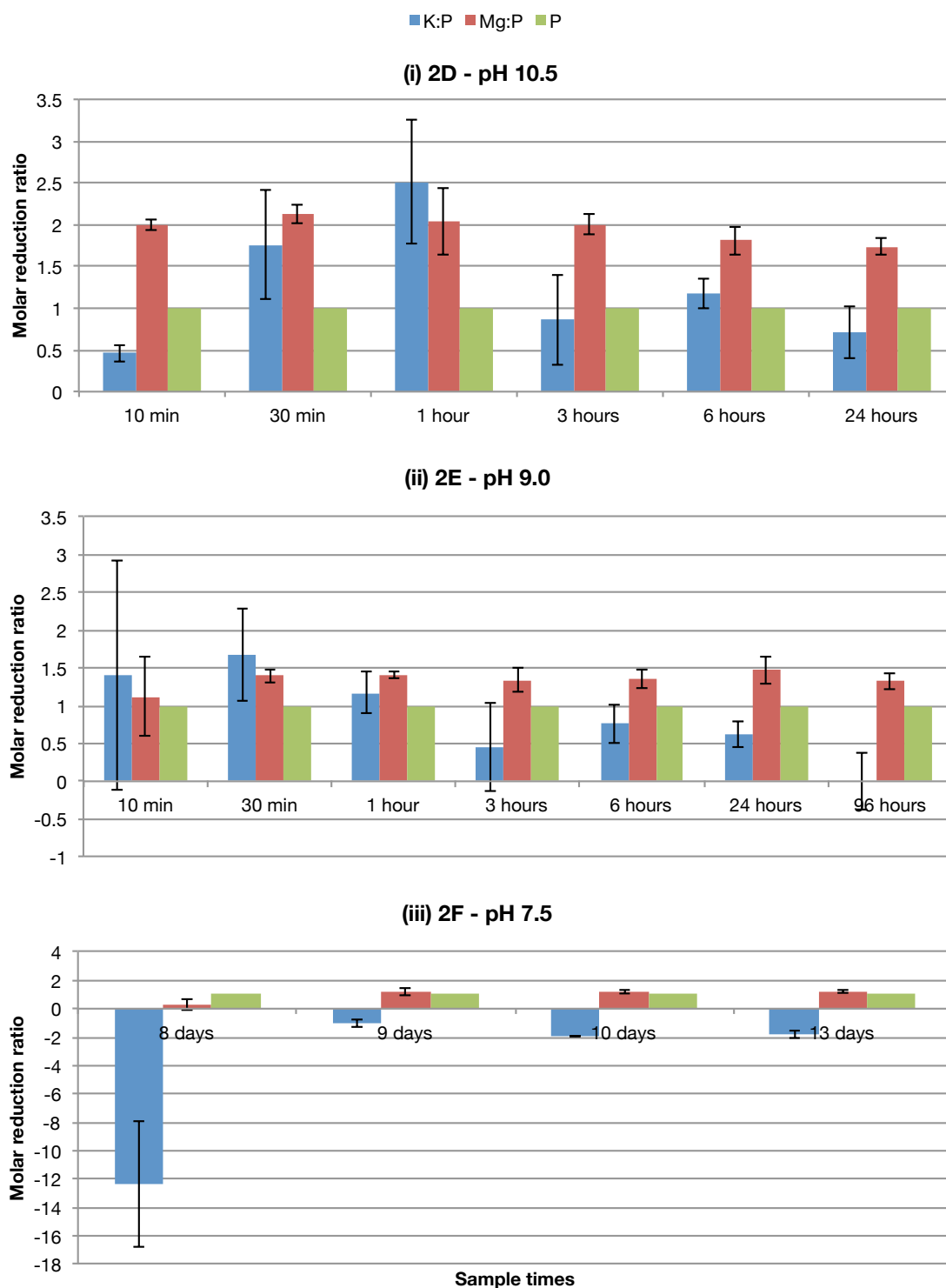
Figure 16 – Molar ratios of reduction of analyte in solution at low S_K for (i) experiment 2D at pH 10.5 (ii) experiment 2E at pH 9.0 and (iii) experiment 2F at pH 7.5

6.3.3 Experiment 2G: results for optimal concentration K-struvite synthesis

It was found that pure K-struvite was produced at relatively high concentrations, as seen in Section 6.3.1. However at lower Mg, K and P concentrations such as those naturally found in wastes, in Section 6.3.2, solution conditions are not naturally optimized for K-struvite precipitation.

To successfully synthesize K-struvite at lower concentrations, solution equilibrium modeling with PHREEQC was used to determine the conditions required for recovery for a certain wastewater matrix. This wastewater matrix included a relatively low P concentration, around 8 mM, Mg:P ratio of 3:1 and pH 8. The phosphorus concentration was chosen to be relatively similar to animal wastes, while the Mg:P ratio was chosen similarly. The pH was chosen to minimize caustic costs, and because much below pH 8, K-struvite is undersaturated.

Using these criteria, PHREEQC was used to determine optimal conditions for K-struvite precipitation, the results of which are shown in Figure 17. The results indicated that cattiite, is the primary 'competition' for K-struvite precipitation. The K:P ratio in solution must be very high at this pH, approximately 50:1 at a minimum, for K-struvite to precipitate

Optimizing the K:P ratio for low concentration K-struvite synthesis
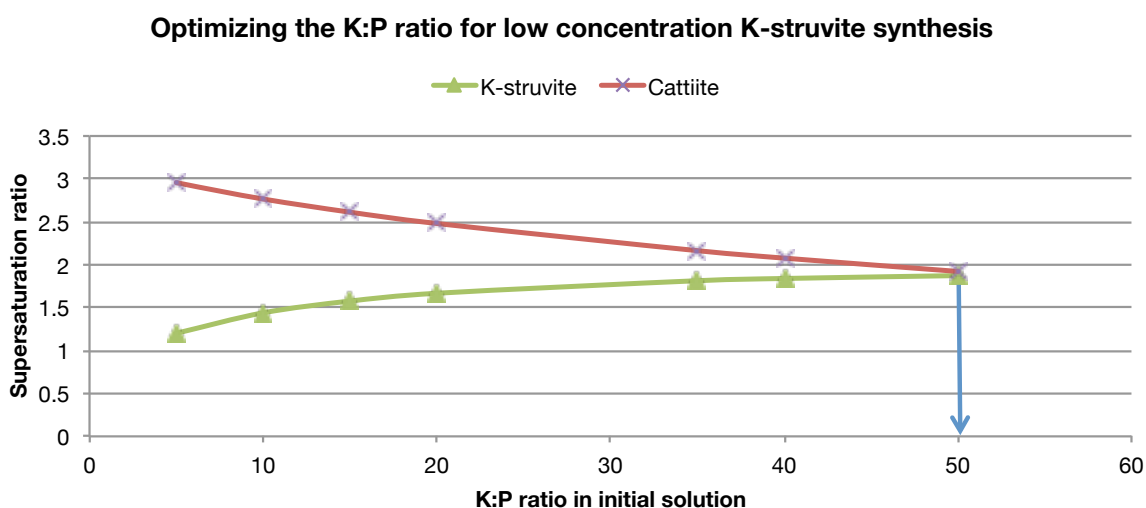
Figure 17 - Optimizing the K:P ratio for low concentration K-struvite synthesis at pH 8.0, [P-PO$_4$] = 8 mM

This experiment showed that pure K-struvite could be formed at lower concentrations, similar to those which might be found in animal manures. The initial supersaturation ratio for this experiment was 1.6, with a high K:P ratio of about 50:1.

As seen in Figure 18 the K:P trend is steadily upwards, reaching an average of 0.92 at 24 hours, which is greater than what was observed under highly supersaturated conditions in Section 6.3.1. The Mg:P ratio remained close to 1 as expected. From XRD scans in Figure 19,

we see that at the 3 hour sample time, the peaks are stronger than at the 1 hour sample time but do not get much stronger after that point.
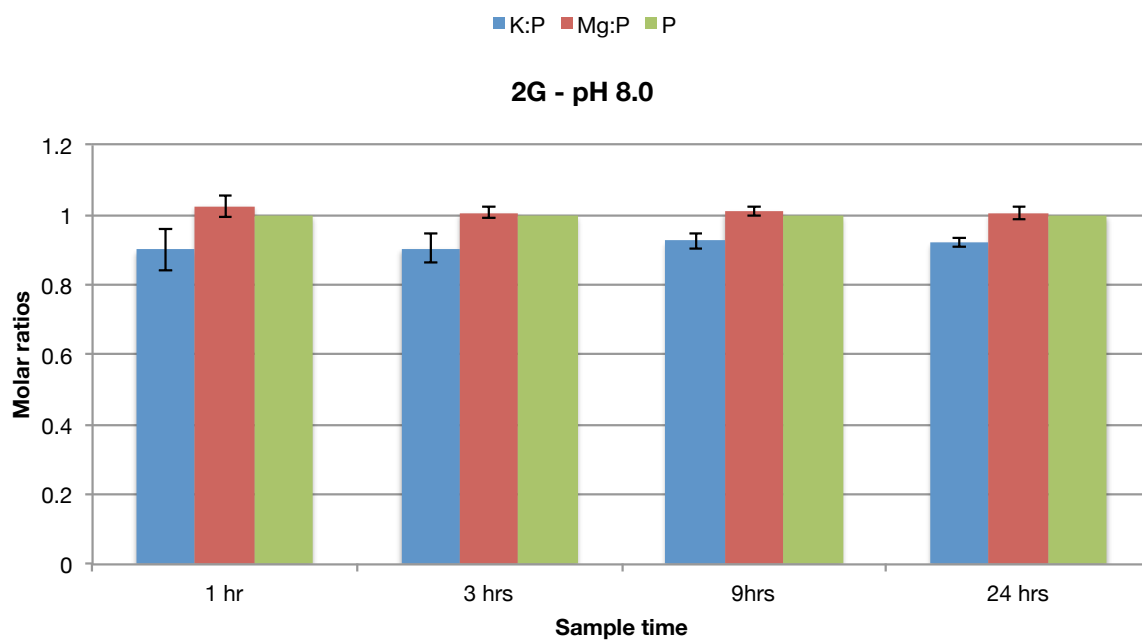
Figure 18 – Experiment 2G: molar ratios in solid phase at optimal S_K
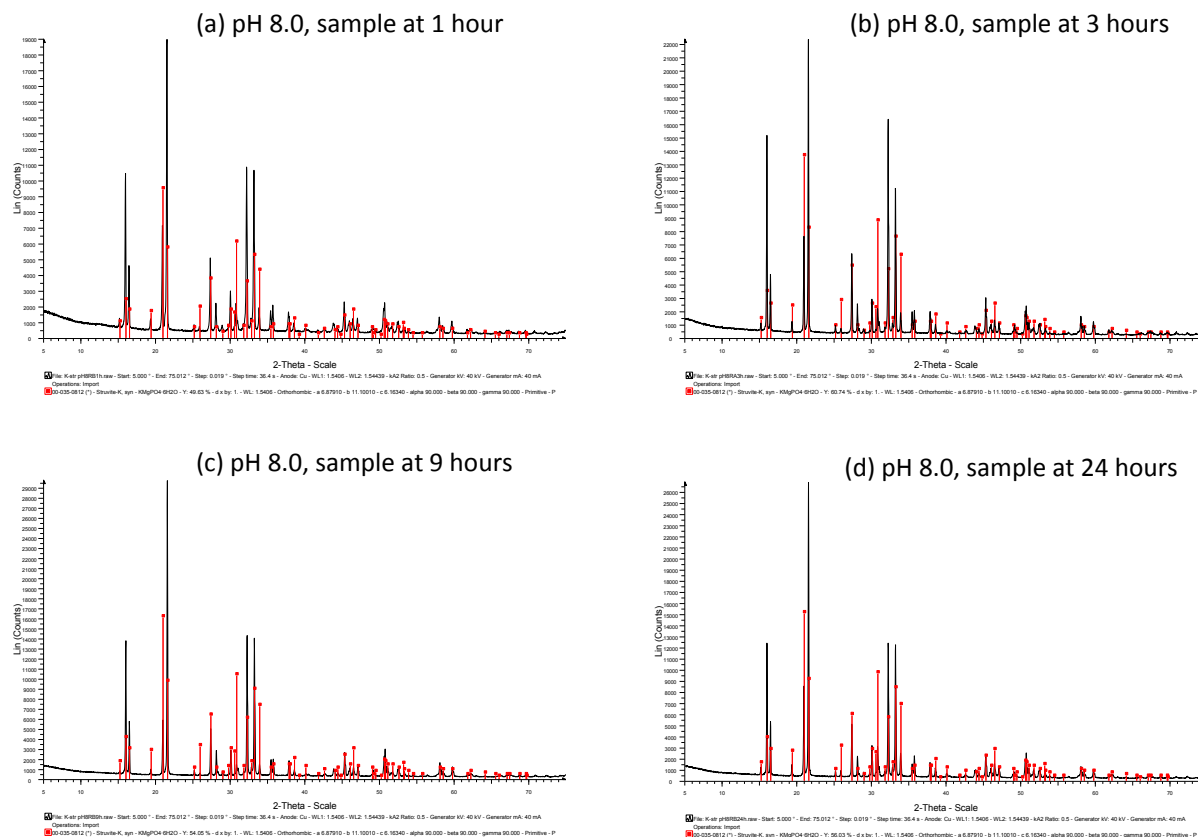
Figure 19 – Experiment 2G: XRD scans of solid phases synthesized at optimal K-struvite S_K at (a) 1 hour (b) 3 hours (c) 9 hours and (d) 24 hours for experiment 2G

6.4 Conclusions

Previous reports in the literature of synthesizing K-struvite did not always form a pure product and these studies used concentrations that were unlikely to be seen in animal manures and other waste products. This work demonstrates that forming a pure product is possible under certain conditions, when the K-struvite supersaturation ratio is greater than 1, and greater than the supersaturation ratio of other magnesium phosphates (such as cattiite).

It was found that a pure product was formed at high supersaturation ratios, yet those concentrations are unlikely to be found in wastes. A minimum K:P of approximately 50:1 is necessary to increase the supersaturation ratio of K-struvite relative to cattiite, and for synthesis of pure K-struvite given a wastewater matrix with pH 8, P-PO_4 concentration around 8 mM and Mg:P ratio of 3:1.

CHAPTER 7
EXPERIMENT 3 – MAKING K-STRUVITE IN THE UBC-FBR

7.1 Experimental objectives

The objective of this experiment was to produce pure K-struvite and assess the pelletization potential of K-struvite through initial runs in the UBC-FBR struvite crystallizer using synthetic feed.

This experiment represents the first attempt to produce something other than NH_4-struvite in this patented reactor. It follows from the batch reactor synthesis experiments at which the optimal concentration and S_K were determined to produce pure K-struvite at low P concentrations and pH 8.

7.2 Materials and methods

7.2.1 Experimental setup

This experiment took the results of the most recent batch reactor experiment and use similar concentrations. A pilot scale UBC-FBR was set up at the UBC Pilot Plant facility (UBC Staging Environmental Research Centre) and was operated with recycle with the goal of maintaining a constant and predictable supersaturation ratio in the reactor.

Before starting the experiment the reactor, feed and effluent tanks were cleaned. Large tanks, able to hold approximately 2000 L of solution were used in order to have enough feed for several days.

The reactor setup was modified slightly from the typical setup to simulate conditions which may be typical for treating wastes high in potassium, such as animal wastes. For this reason, magnesium chloride was not contained and injected separately, rather it was mixed directly into the feed. To prevent crystallization in the feed tank, the pH of the feed was kept low to maintain undersaturated conditions. The total volume of the reactor was about 6.5 L. A diagram showing basic reactor configuration is shown in Figure 20 andFigure 21.

A Masterflex feed pump and a Moyno 500 recycle pump were selected to maintain flows of about 0.2 L/min and 1.8 L/min, respectively. This gave the potential for a total flow of 2 L/min giving an upflow velocity of approximately 400 cm/min for a 1" (25.4mm) diameter at the

harvest zone. This upflow velocity has been shown to be very successful in NH_4-struvite pelletization (Bhuiyan et al. 2008; Fattah 2004; Huang 2003).

A BLX pH/M metering pump and pH probe within the active zone were installed to maintain the pH at a constant value using 0.2M NaOH. The reactor temperature was not controlled and was left at ambient temperature.
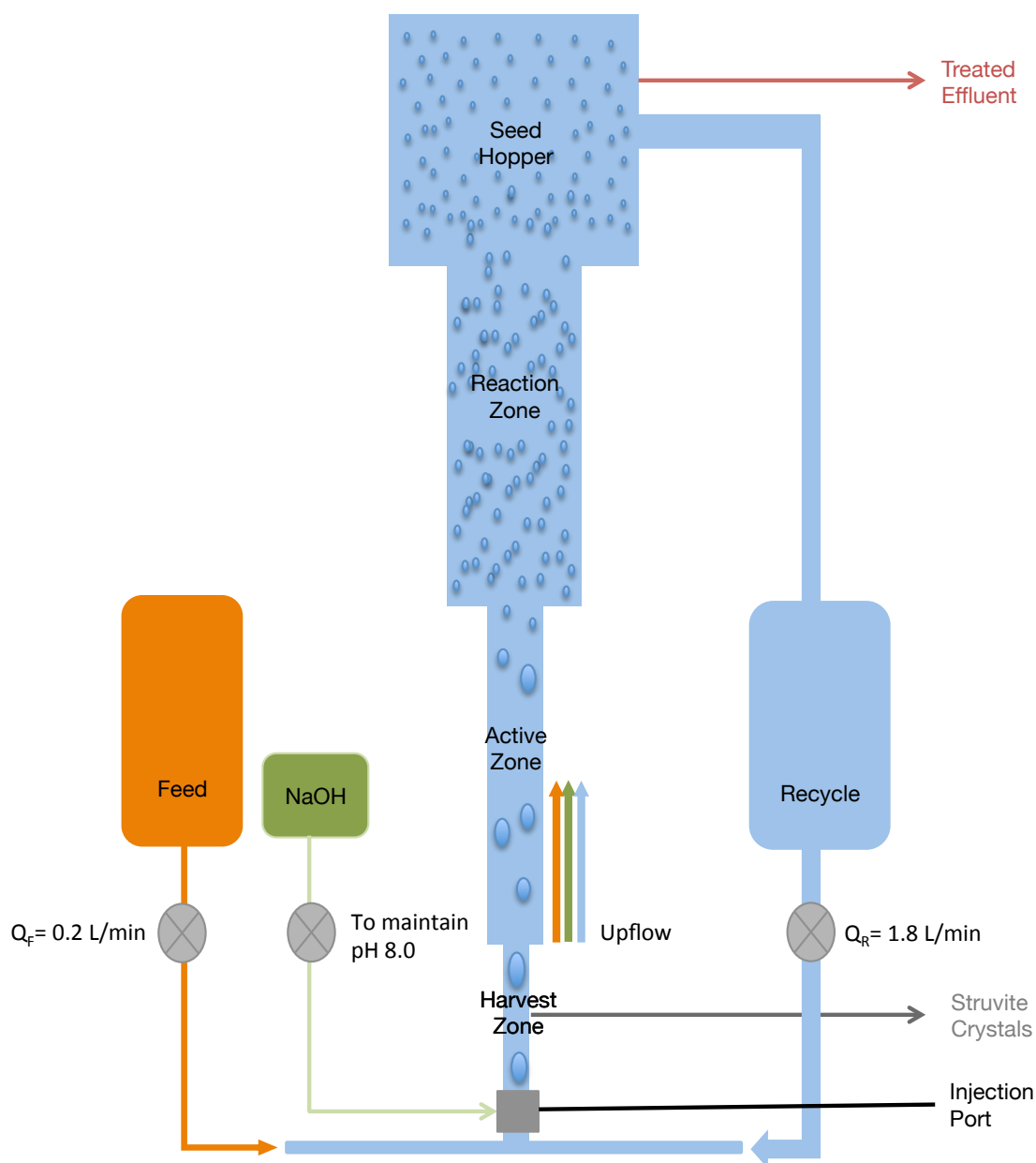
Figure 20 – General schematic of the UBC-FBR NH_4-struvite crystallizer modified for K-struvite production
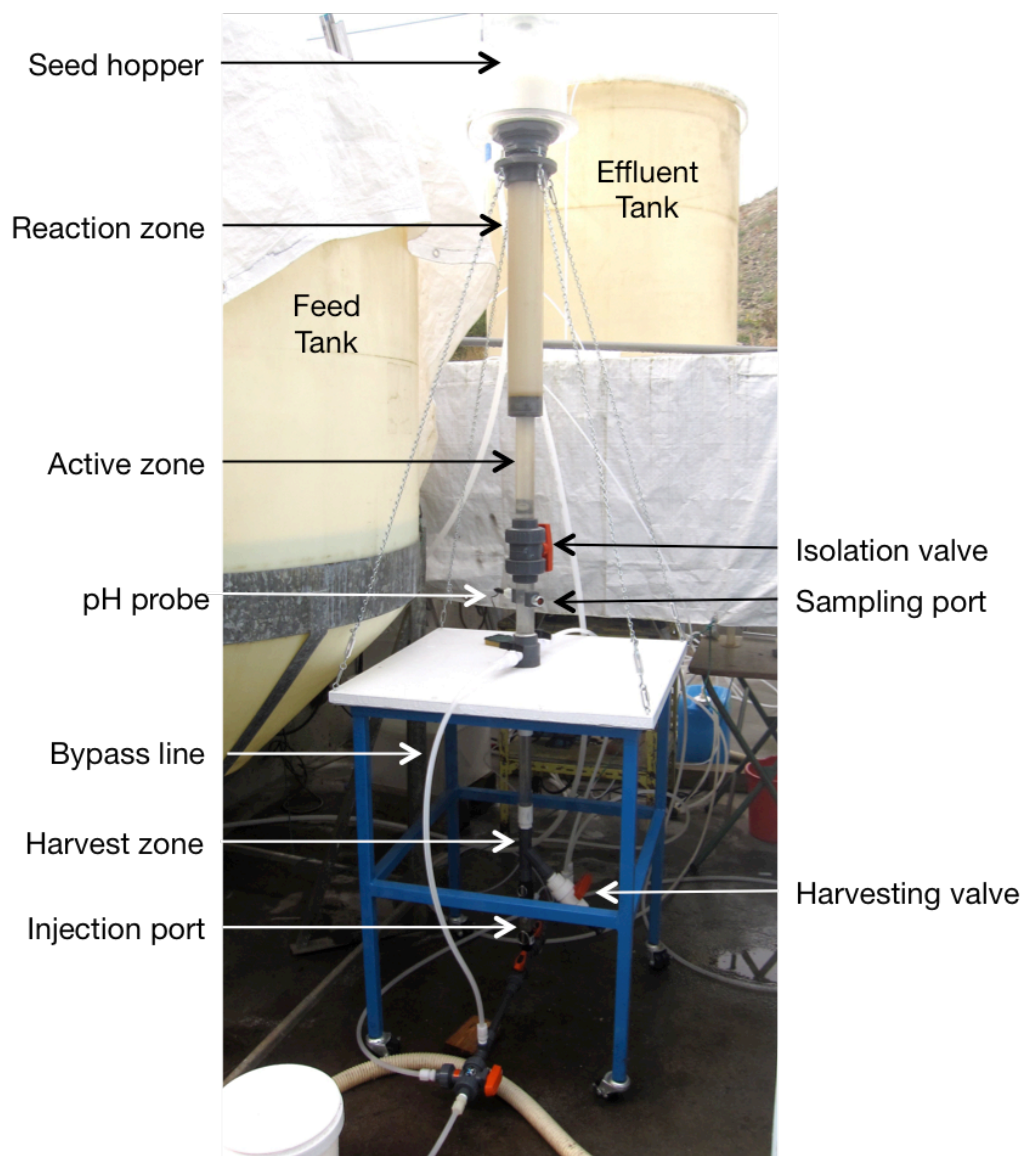
Figure 21 – Experimental setup with the UBC-FBR NH$_4$-struvite crystallizer modified for K-struvite production

7.2.1.1 Synthetic feed composition

Synthetic feed was made up with a Mg:K:P ratio of about 3:42:1. Magnesium chloride was used as the magnesium source, phosphoric acid as a phosphorus source and muriate of potash as the potassium source. The pH of the feed was approximately 2.3 and the ionic strength was about 0.3. Enough feed for approximately 2 weeks of continuous operation at 0.2 L/min was made up using these concentrations:

P	241 mg/L	or	8 mmol/L
Mg	535 mg/L	or	22 mmol/L
K	13099 mg/L	or	335 mmol/L

7.2.2 Reactor operation

The reactor was operated continuously for 12 days using synthetic feed, with recycle as described above in Section 7.2.1.

Reactor startup involved filling the reactor and clarifier with feed before turning on the recycle pump. Once full, the pH pump was turned on and set to maintain a pH of 8, the feed pump was set to a low flow rate of 0.05 L/min, and to maintain a recycle ratio of 10, the recycle pump was set to 0.5 L/min. The flow rates were kept low initially to prevent the precipitate being washed out of the reactor. Flow rates were slowly increased over the course of the reactor operation to increase the upflow velocity to the desired value. It should be noted here that the operational parameters were not kept constant due to a number of factors discussed further in Section 7.3. Table 13 gives the operational parameters desired based on the literature and previous successful pelletization attempts, and contrasts them with the range of operational parameters that were achieved.

Table 13 - Desired vs achieved reactor operational parameters

Operational parameters	Desired range	Range achieved
[1]Supersaturation ratio in reactor	1.6	$1.7E^{-4}$ to 9.7 1.58 on average
[2]K:P molar ratio	50	~41 in feed 24 to 7600 in-reactor
Reactor pH	8	1.52 to 13.23 ~8.1 on average
Temperature, °C	n/a	11.7 to 22 °C ~17°C on average
Total reactor flow (L/min)	2	0.4 to 1.38 ~ 1 L/min on average
[3]Recycle ratio	10	5 to 15 ~10 on average
[4]Upflow velocity (cm/min)	400	75 to 300 ~200 cm/min on average
Crystal retention time	8-20	Not measured

1. Cube root of the ratio of solubility product of the solution at the sampling port to that at equilibrium $(K_{K-reactor}/K_{K-eq})^{1/3}$
2. K:P molar ratio of the solution leaving the injector
3. Recycle flow divided by the influent feed flow
4. Velocity of the total flow measured at the harvest zone

The reactor was monitored twice daily and sampled once daily. Monitoring the reactor involved monitoring feed and recycle flows, taking pH measurements in the feed, reactor, seed hopper and clarifier, taking temperature and conductivity measurements in the feed, and clarifier, and monitoring caustic levels. Liquid samples of the feed, in-reactor, seed hopper and effluent were taken. Feed samples were taken from the feed tank, in-reactor samples were taken from the reactor sampling port, seed hopper samples were taken from the seed hopper and effluent samples were taken from the clarifier. Samples were filtered with a 0.45 µm filter and preserved

with 1-2 drops of HCl. Samples of precipitate were also taken through the harvest port, rinsed with distilled water and left to dry in the ambient. Chemical analyses of the liquid samples was performed for potassium, magnesium and phosphate using the analytical methods described in Section 5.2.2.

Other reactor maintenance also included cleaning the injection port from precipitate buildup, draining fines from the clarifier, and calibrating the in-reactor pH probe.

7.3 Results and discussion

The objective of this experiment was to produce pure K-struvite in the UBC reactor by going from a batch process which had an initial S_K of 1.6 that goes to 1 at equilibrium, to a continuous process that maintains a constant S_K of 1.6. This researcher wanted to see if the K-struvite would agglomerate and form pellets. It should be noted that the goals of this experiment were not to optimize the recovery of either potassium or phosphorus.

The easiest way to maintain a constant S_K is to maintain constant Mg, K, PO_4 concentrations and pH in the reactor. The obvious way to do this is to have a constant feed, without recycle. However, to obtain the desired upflow velocities to induce the necessary turbulence would require huge quantities of feed solution for a continuous process, requiring large tanks, pumps which will not corrode on contact with acidic solutions, and expensive quantities of chemicals. These operational parameters were not feasible; and therefore, a recycle line was introduced. The recycle line introduced difficulties in maintaining a constant supersaturation ratio in the reactor because the reactor effluent was not constant due to the varying pH in reactor, making it difficult to stabilize. Given a long enough run, the system should theoretically stabilize, and the data was starting to stabilize near the end of the 12 days.

Another goal of the experiment was to observe whether or not K-struvite would agglomerate and form pellets. From work with NH_4-struvite, it was known that a high supersaturation ratio results in a high nucleation rate producing lots of fines, while a low supersaturation ratio encourages crystal growth (Abbona and Boistelle 1985). However, growing crystals from nuclei can take several days, even weeks.

K-struvite crystals were not available with which to seed the reactor, meaning that pellets would have to agglomerate from the fines produced, (which could be a lengthy process). This constraint also required that recycle and feed flows be slowly increased as crystals grew, to prevent fines from being washed out of the reactor due to a strong upflow. Time constraints and low upflow velocities made it difficult to stabilize conditions in the UBC-FBR, and made it difficult to assess the pelletization potential of K-struvite.

The expected operational parameters and the achieved operational parameters can be seen in Table 13 above. The upflow velocity stayed fairly low, between 75 and 300 cm/min, averaging

about 200 cm/min. It was never able to approach the 400 cm/min due to the threat of K-struvite fines being washed out from the reactor.

The pH averaged a value around 8, but in reality, it was subject to sharp increases and drops due to the how the inline pH pump operates. Once the pH probe, located just below the isolation valve read a value below pH 8, the pump would send sharp bursts of caustic into the reactor. The time delay between the caustic entering the reactor and the injection port and the pH probe reading the increased pH, was long enough such that the pH of the reactor was subject to increases of up to 10 and 11. A higher upflow velocity would have reduced this issue because there would not have been that long delay between caustic entering the reactor and the pH probe registering the reading. There were also issues encountered with the pH probe losing its calibration, causing the reactor to go acidic, and issues with peristaltic pump losing its prime, also causing the reactor to go acidic.

The supersaturation ratio was also quite variable, ranging from $1.7E^{-4}$ when the pH in the reactor dropped to 1.5, and went as high as 9.7 when the pH spiked to 11.7. Given the correct operating conditions, we may have expected constant supersaturation in the reactor, reaching equilibrium, with a S_K of 1 in the seed hopper. The supersaturation values in the feed, reactor, seed hopper and effluent can be seen in Appendix B.

Despite these setbacks, there are a few results from this experiment to note. Generally, the recovery of phosphorus was quite high when the process was operating smoothly. Recovery of potassium was also evident, with between 5 and 20% of potassium being recovered as K-struvite, as seen in Table 14. Where we can see zero recovery for magnesium and phosphate, and very little for K, the pH in the reactor dropped to 1.5 and was due to an issue with the inline pH monitoring pump. This resulted in several hours where no caustic was being added to the system, causing the pH to drop; this created undersaturated conditions and dissolved some of the precipitate in the reactor.

Pure K-struvite was produced during the process, as can be seen in the XRD analysis of the precipitate in Figure 23. This represents the first time that K-struvite has been produced in the UBC-FBR; it was uncertain whether the hydraulic retention time through the reactor would be sufficient for K-struvite to precipitate. In the XRD, it seems that KCl is present in the solid, however, the likeliest explanation is that residual KCl dried on the precipitate sample due to inadequate rinsing, and should be disregarded. The samples were rewashed and reanalyzed, so the chemical analyses are true, and do not overestimate the potassium content of the precipitate. The K-struvite produced was quite pure, according to the chemical analysis, with a K:Mg:P ratio of almost 1:1:1 as seen in Figure 23.

It was possible to recover a small sample of crystals from the reactor, primarily crystals which had formed on the inside of the injection port. Upon analysis of the crystals it was found that they were not pure K-struvite. Chemical analysis indicated a K:Mg:P ratio of approximately 0.5:3.5:1 (Figure 22a) and the XRD analysis showed that the crystal was composed of K-struvite, cattite and brucite (Figure 23a). This is likely due to the fact that pH and the

supersaturation at the injection port was unstable and often very high. The occasionally high pH at the injection port due to the unstable nature of pH pumping as described above encouraged formation of brucite, As well, the high K:P ratio at the injection port also increased the supersaturation of K-struvite. The data for the in-reactor conditions can be seen in Appendix B.

Table 14 – Experiment 3: recovery of K, Mg and P during initial UBC-FBR run

Sample Date	K recovery (mM)	Mg recovery (mM)	P-PO₄ recovery (mM)	% K recovery	% Mg recovery	% P- PO₄ recovery
14-09-11	75.76	8.88	7.75	22.4	41.6	99.7
14-09-12	26.62	1.83	6.35	7.9	8.6	81.1
14-09-14	30.14	8.00	7.85	9.4	37.6	99.4
14-09-15	19.23	0	0	5.9	0.0	0.0
14-09-16	14.70	9.21	7.54	4.8	43.4	99.5
14-09-17	35.85	7.21	6.93	10.9	34.5	89.6
14-09-18	30.25	2.10	1.71	9.5	10.2	22.0
14-09-19	34.91	4.61	3.75	10.9	21.6	47.4
14-09-20	14.17	7.34	5.57	4.4	33.9	81.8
14-09-21	42.01	8.66	7.46	12.5	39.8	92.7
14-09-22	64.25	6.63	5.47	18.9	30.6	67.9

(a) Chemical analysis of precipitates recovered

(b) 10x magnification of crystal recovered from injection port
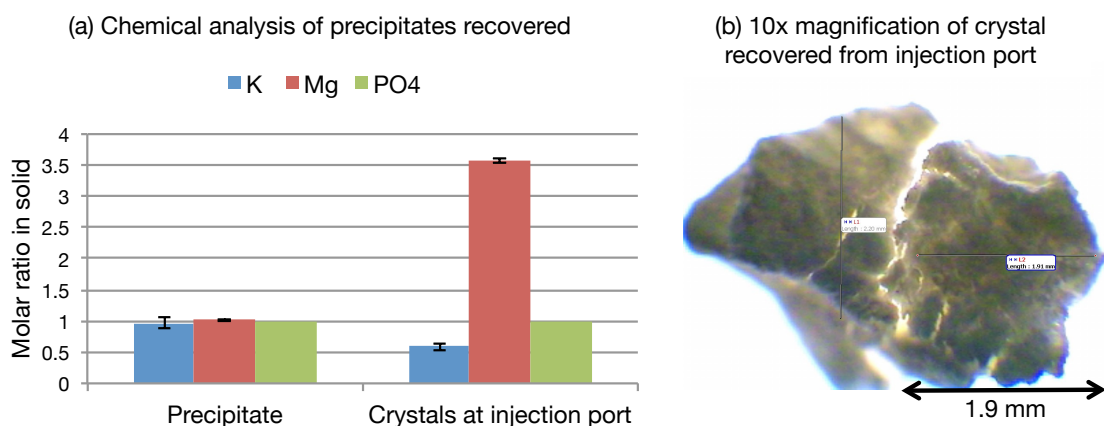
Figure 22 – Experiment 3: (a) chemical analysis of precipitate and crystals at Injection port, and (b) 10x magnification of crystal recovered from the injection port
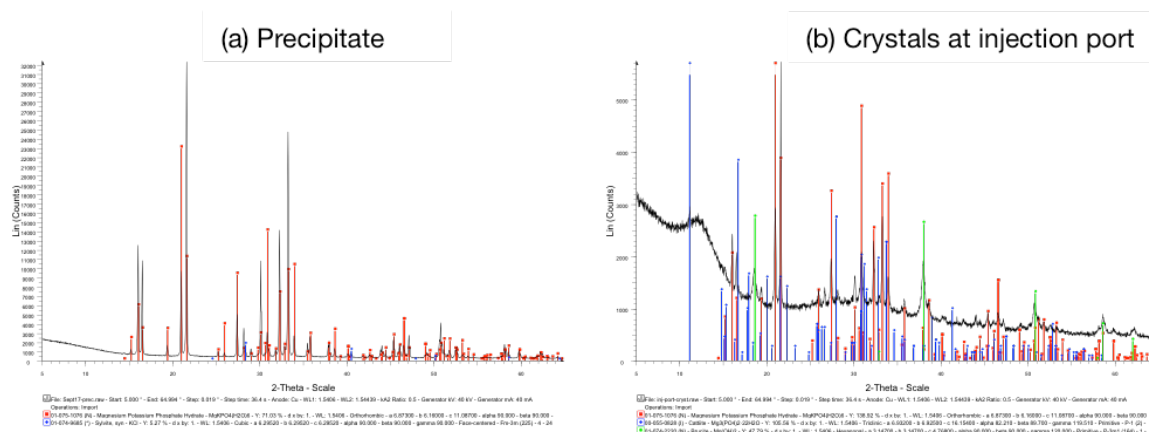
Figure 23 – Experiment 3: XRD scan of (a) precipitate and (b) crystals recovered from injection port of the UBC-FBR

7.4 Conclusions

Pure K-struvite can be produced in the UBC-FBR. However, the main objective of this experiment, which was to assess the pelletization potential of K-struvite, remains unanswered.

More work needs to be done in determining the appropriate supersaturation ratio of K-struvite for the UBC-FBR and creating stable conditions to better assess its potential. As well, it is recommended to seed the reactor to better compare K-struvite crystallization with the results observed in struvite crystallization. Struvite crystals could be used as seed material, although this may introduce complexities by way of ammonium introduction in the matrix.

CHAPTER 8
CONCLUSIONS AND RECOMMENDATIONS

The title of this thesis is *'Potential for potassium recovery as K-struvite'* can be thought of as a question. Looking at the drivers for potassium recovery, it is evident that there is a need for a slow release potassium based fertilizer; a full complement fertilizer with both NH_4-struvite and K-struvite would be very interesting, particularly if derived from waste products. However, without a need to recover potassium to supplement potash reserves or legislative drivers to recover potassium, it is uncertain that this kind of work will gain much commercial traction at this time.

8.1 Conclusions

The conclusions from this research, based on the experimental objectives are as follows:

1. Determining a new K_{sp-K} value for K-struvite:

    K-struvite was found to be less soluble than previously reported with results for pK_{sp-K} were 11.07, 11.00 and 10.90 at 10, 25 and 35°C respectively. Differences between the result presented by Taylor et al. (1963) and the result presented here is the likely the incorporation of more solid phases into the determination of theoretical magnesium, potassium and phosphate concentrations at equilibrium as well as updating equilibrium constants in the PHREEQC database.

2. Determining optimal conditions for K-struvite synthesis:

    Previous reports in the literature for synthesizing K-struvite did not always form a pure product and used concentrations that were unlikely to be seen in animal manures and other waste products. These experiments demonstrate that forming a pure product can occur under certain conditions when the K-struvite supersaturation ratio is greater than 1, and greater than the supersaturation ratio of other magnesium phosphates (such as cattiite).

    It was found that a pure product was formed at very high supersaturation, yet those concentrations were unlikely to be found in wastes. A minimum K:P of approximately 50:1, giving a $S_{K-Struvite} > S_{cattiite}$ was found to be optimal for pure K-struvite synthesis, given a wastewater matrix with pH 8, P-PO_4 concentration around 8 mM and Mg:P ratio of 3:1.

3. Pelletization potential of K-struvite in the patented UBC-FBR NH_4-struvite crystallizer:

   Pure K-struvite can be produced in the reactor. However, the objective of this experiment, which was to assess the pelletization potential of K-struvite, is left unanswered. More work needs to be done in determining the appropriate supersaturation ratio of K-struvite for the UBC-FBR and creating stable conditions to better assess pelletization potential.

8.2 Recommendations for future work

Based on the conclusions of the experimental work and the observations made during the work, the following are recommendations for further research avenues into potassium recovery as K-struvite:

1. Further studies with the UBC struvite crystallizer using struvite as seed material would be interesting. This would introduce nitrogen into the system, providing information as to how K-struvite forms in the reactor once nitrogen is in the system, as well as how well K-struvite pelletizes once reactor conditions are similar to reactor operating parameters for NH_4-struvite.

2. Satoshi et al., (2013) studied the effect of ammonium on K-struvite formation and found that, as expected, struvite preferentially forms when ammonium is present, though they conclude that K-struvite will form when the ammonium concentration is below 1.1 mM. Although it seems that nitrates do not impact the formation of K-struvite, studying this further and better understanding how much nitrogen can be present in solution to would be valuable to the research body of nutrient recovery from wastewater.

3. Lin et al., (2012) confirmed through experimental results, that ammonium replaces potassium in the K-struvite matrix, as originally hypothesized by Mathew & Schroeder (1979). Those familiar with K-struvite believe that forming solid solutions of K-struvite and NH_4-struvite will be the key to studying K-struvite and effectively recovering potassium as part of a full complement fertilizer. Studying this further through ion exchange experiments or formation of solid solutions, would provide some important initial findings into the feasibility of this process.

REFERENCES

Abbona, F., and R. Boistelle. 1985. "Nucleation of Struvite (MgNH4PO4:6H2O) Single Crystals and Aggregates." *Crystal Research and Technology* 20(2): 133–40.

Adeoye, G. O., M. K. C. Sridhar, and R. R. Ipinmoroti. 2001. "Potassium Recovery from Farm Wastes for Crop Growth." *Communications in Soil Science and Plant Analysis* 32(15-16): 2347–58. http://www.tandfonline.com/doi/abs/10.1081/CSS-120000377 (December 4, 2014).

Ahmad, A. L., and C. Y. Chan. 2009. "Sustainability of Palm Oil Industries: An Innovative Treatment via Membrane Technology." *Journal of Applied Sciences* 9(17): 3074–79.

American Public Health Association, American Water Works Association, and Water Environment Federation. 2012. *Standard Methods for the Examination of Water and Wastewater*. 22nd editi. eds. Eugene W. Rice, Rodger B. Baird, Andrew D. Eaton, and Lenore s. Clesceri. Washington, DC: American Public Health Association.

American Society of Agricultural Engineers. 2003. *Manure Production and Characteristics*. http://www.manuremanagement.cornell.edu/Pages/General_Docs/Other/ASAE_Manure_Production_Characteristics_Standard.pdf.

Bhuiyan, M I H, D S Mavinic, and F a Koch. 2008. "Phosphorus Recovery from Wastewater through Struvite Formation in Fluidized Bed Reactors: A Sustainable Approach." *Water Science & Technology* 57(2): 175–81. http://www.ncbi.nlm.nih.gov/pubmed/18235168 (March 18, 2013).

Bhuiyan, MIH, DS Mavinic, and RD Beckie. 2007. "A Solubility and Thermodynamic Study of Struvite." *Environmental Technology* 28(9): 1015–26. http://www.ncbi.nlm.nih.gov/pubmed/17910254.

Bouropoulos, Nicolaos Ch, and Petros G Koutsoukos. 2000. "Spontaneous Precipitation of Struvite from Aqueous Solutions." *Journal of Crystal Growth* 213(3-4): 381–88. http://linkinghub.elsevier.com/retrieve/pii/S0022024800003511.

Brady, Nyle C., and Ray R. Weil. 2008. "Potassium: Nature and Ecological Roles." In *The Nature and Properties of Soils*, ed. Vernon R. Anthony. USA: Pearson Education Inc.

Braunschweig, LC von. 1986. "Types of K-Fertilizers in the K-Replacement Strategy." In *Nutrient Balances and the Need for Potassium*, Reims.

Britton, A. 2002. "Pilot Scale Struvite Recovery Trials from a Full Scale Anaerobic Digester Supernatant at the City of Penticton Advanced Wastewater Treatment Plant." University of British Columbia.

Britton, A, FA Koch, DS Mavinic, A Adnan, WK Oldham, and B Udala. 2005. "Pilot-Scale Struvite Recovery from Anaerobic Digester Supernatant at an Enhanced Biological Phosphorus Removal Wastewater Treatment Plant." *Journal of Environmental Engineering and Science* 4(4): 265.

Canadian Council of Ministers of the Environment. 2014. "Canadian Environmental Quality Guidelines Summary Table."

Cerrillo, Míriam, Jordi Palatsi, Jordi Comas, Jaume Vicens, and August Bonmatí. 2014. "Struvite Precipitation as a Technology to Be Integrated in a Manure Anaerobic Digestion Treatment Plant - Removal Efficiency, Crystal Characterization and Agricultural Assessment." *Journal of Chemical Technology & Biotechnology* (April): n/a – n/a. http://doi.wiley.com/10.1002/jctb.4459 (August 13, 2014).

Chau, C.K., Fei Qiao, and Zongjin Li. 2011. "Microstructure of Magnesium Potassium Phosphate Cement." *Construction and Building Materials* 25(6): 2911–17. http://linkinghub.elsevier.com/retrieve/pii/S0950061810007130 (January 27, 2014).

Chauhan, C. K., P. M. Vyas, and M. J. Joshi. 2011. "Growth and Characterization of Struvite-K Crystals." *Crystal Research and Technology* 46(2): 187–94. http://doi.wiley.com/10.1002/crat.201000587 (March 5, 2013).

Le Corre, Kristell S., Eugenia Valsami-Jones, Phil Hobbs, Bruce Jefferson, and Simon a. Parsons. 2007. "Agglomeration of Struvite Crystals." *Water Research* 41: 419–25.

Decloux, Martine, Andre Boriesb, Richard Lewandowski, Claire Fargues, Amel Mersad, Marie Laure Lameloisea, Frdric Bonnet, Bertrand Dherbecourt, and Leandro Nieto Osuna. 2002. "Interest of Electrodialysis to Reduce Potassium Level in Vinasses. Preliminary Experiments." *Desalination* 146: 393–98.

Epstein, J A, D Altaras, E M Feist, and J Rosenzweig. 1975. "The Recovery of Potassium Chloride from Dead Sea Brines by Precipitation and Solvent Extraction." *Hydrometallurgy* 1: 39–50.

FAO. 2015. *World Fertilizer Trends and Outlook to 2018*. Rome.

Fattah, Kazi Parvez. 2004. "Pilot Scale Struvite Recovery Potential from Centrate at Lulu Island Wastewater Treatment Plant." University of British Columbia.

Forrest, Alexander Lebaron Alexaner. 2004. "Process Optimization of a Technical Scale Phosphorus Recovery System Through Struvite Crystallization at the City of Penticton Advanced Wastewater Treatment Plant." University of British Columbia.

Garrett, Donald E. 1996. *Potash: Deposits, Processing, Properties and Uses*. 1st ed. London: Chapman & Hall.

Godwin, Jonathan. 2014. "Personal Communication."

Graeser, Stefan, Walter Postl, Hans-Peter Bojar, Peter Berlepsch, Thomas Armbruster, Thomas Raber, Karl Ettinger, and Franz Walter. 2008. "Struvite-(K), the Potassium Equivalent of Struvite – a New Mineral." *European Journal of Mineralogy* 20(4): 629–33. http://openurl.ingenta.com/content/xref?genre=article&issn=0935-1221&volume=20&issue=4&spage=629 (April 12, 2013).

Huang, Hui. 2003. "Pilot Scale Phosphorus Recovery from Anaerobic Digester Supernatant." University of British Columbia.

Jasinski, Stephen. 2010. "Potash." *Mining Engineering* 62(6).

———. 2012. "Potash." (703). http://minerals.usgs.gov/minerals/pubs/commodity/potash/mcs-2012-potas.pdf.

———. 2014. *Phosphate Rock*. http://minerals.usgs.gov/minerals/pubs/commodity/phosphate_rock/mcs-2014-phosp.pdf.

———. 2015a. "Phosphate Rock." http://minerals.usgs.gov/minerals/pubs/commodity/phosphate_rock/mcs-2015-phosp.pdf.

———. 2015b. "Potash." http://minerals.usgs.gov/minerals/pubs/commodity/potash/mcs-2015-potas.pdf.

Li, Xinyang, Wei Zhu, Yue Wu, Chengwen Wang, Jianzhong Zheng, Kangning Xu, and Jiyun Li. 2015. "Recovery of Potassium from Landfill Leachate Concentrates Using a Combination of Cation-Exchange Membrane Electrolysis and Magnesium Potassium Phosphate Crystallization." *Separation and Purification Technology*. http://linkinghub.elsevier.com/retrieve/pii/S1383586615000647.

Lin, Y M, J P Bassin, and M C M van Loosdrecht. 2012. "The Contribution of Exopolysaccharides Induced Struvites Accumulation to Ammonium Adsorption in Aerobic

Granular Sludge." *Water Research* 46(4): 986–92.
http://www.ncbi.nlm.nih.gov/pubmed/22209260 (April 12, 2013).

Lobanov, Sergey, Frederic Koch, and Donald Mavinic. 2013. "The Implication of Aqueous Equlibrium Modelling to Evaluate the Potential for Nutrient Recovery from Wastewater Streams." In *WEF/IWA Nutrient Removal and Recovery: Trends in Resource Recovery and Use,*.

———. 2014. "Nutrient Recovery from Wastewater Streams by Crystallisation." *Journal of Environmental Engineering and Science* 9(3): 151–54.

Luff, Basil B, and Robert B Reed. 1980. "Thermodynamic Properties of Magnesium Potassium Orthophosphate Hexahydrate." *Journal of Chemical Engineering Data* 312(3): 310–12.

Lunt, Owen R., Anton M. Kofranek, and Sylvester B. Clark. 1964. "Availability of Minerals from Magnesium Ammonium Phosphates." *Journal of Agriculture and Food Chemistry* 12(6): 497–504.

MacDonald, Graham K, Elena M Bennett, Philip a Potter, and Navin Ramankutty. 2011. "Agronomic Phosphorus Imbalances across the World's Croplands." *Proceedings of the National Academy of Sciences of the United States of America* 108(7): 3086–91. http://www.pubmedcentral.nih.gov/articlerender.fcgi?artid=3041096&tool=pmcentrez&rendertype=abstract (October 20, 2014).

Manning, David A C. 2011. "Mineral Sources of Potassium for Plant Nutrition." *Sustainable Agriculture Volume* 2(2010): 281–94.

Mathew, B Y M, and L W Schroeder. 1979. "Crystal Structure of a Struvite Analogue , MgKPO4:6H20." *Acta Cryst* B35: 11–13.

Mavinic, Donald. 2015. "Personal Communication with Dr. Mavinic (UBC Civil Engineering), April 2015."

Mehta, Chirag M., Wendell O. Khunjar, Vivi Nguyen, Stephan Tait, and Damien J. Batstone. 2014. "Technologies to Recover Nutrients from Waste Streams: A Critical Review." *Critical Reviews in Environmental Science and Technology* (May 2014): 00–00. http://www.tandfonline.com/doi/abs/10.1080/10643389.2013.866621 (May 23, 2014).

Ohlinger, By Kurt N, Student Member, Thomas M Young, Associate Member, Edward D Schroeder, and Kurt N Ohlinger. 1999. "Kinetics Effects on Preferential Struvite Accumulation in Wastewater." *Journal of Environmental Engineering* 125(August): 730–37.

Ohlinger, K.N., T.M. Young, and E.D. Schroeder. 1998. "Predicting Struvite Formation in Digestion." *Water Research* 32(12): 3607–14. http://linkinghub.elsevier.com/retrieve/pii/S0043135498001237.

Pew Research Center. 2014. *Attitudes about Aging: A Global Perspective*. http://www.pewglobal.org/2014/01/30/attitudes-about-aging-a-global-perspective/.

Romanowski, Zbigniew, Paweł Kempisty, Jolanta Prywer, Stanisław Krukowski, and Agnieszka Torzewska. 2010. "Density Functional Theory Determination of Structural and Electronic Properties of Struvite." *Journal of Physical Chemistry* 114: 7800–7808.

Römheld, Volker, and Ernest a. Kirkby. 2010. "Research on Potassium in Agriculture: Needs and Prospects." *Plant and Soil* 335(1-2): 155–80. http://www.springerlink.com/index/10.1007/s11104-010-0520-1 (February 27, 2013).

Russell, L.L. 1976. "Chemical Aspects of Groundwater Recharge with Wastewaters." University of California, Berkeley.

Salutsky, Murrell L, and Ronald P Steiger. 1964. "Properties of Fertilizer Materials: Metal Potassium Phosphates." *Agricultural and Food Chemistry* 12(6): 486–91.

Satoshi, Yamaguchi, Ohura Seichiro, Harada Hiroyuki, Akagi Kotaro, Yoshiharu Mitoma, Kawakita Hidetaka, and Biplob K. Biswas. 2013. "Simultaneous Crystallization of Phosphate and Potassium as Magnesium Potassium Phosphate Using Bubble Column Reactor with Draught Tube." *Journal of Environmental Chemical Engineering*: 1–5. http://dx.doi.org/10.1016/j.jece.2013.08.032.

Schmidt, Orlando, and Geoff Hughes-Games. 2010. *Potassium Considerations for Nutrient Management*. http://www2.gov.bc.ca/gov/DownloadAsset?assetId=58B437F50CC543ABB90B06F818A737F1&filename=631500-5_potassium_considerations.pdf.

Schuiling, R.D., and A. Andrade. 1999. "Recovery of Struvite from Calf Manure." *Environmental Technology* 20(7): 765–68. http://www.tandfonline.com/doi/abs/10.1080/09593332008616872 (April 12, 2013).

Sheldrick, William F, J.Keith Syers, and John Lingard. 2003. "Soil Nutrient Audits for China to Estimate Nutrient Balances and Output/input Relationships." *Agriculture, Ecosystems & Environment* 94(3): 341–54. http://linkinghub.elsevier.com/retrieve/pii/S0167880902000385.

Shu, L, P Schneider, V Jegatheesan, and J Johnson. 2006. "An Economic Evaluation of Phosphorus Recovery as Struvite from Digester Supernatant." *Bioresource Technology* 97(17): 2211–16. http://www.ncbi.nlm.nih.gov/pubmed/16364632 (December 3, 2014).

Smil, Vaclav. 1999. "Crop Residues: Agriculture's Largest Harvest." *Biosciences* (April): 299–308.

Snoeyink, Vernon L., and David Jenkins. 1980. *Water Chemistry*. USA: John Wiley & Sons Inc.

Statistics Canada. 2013. *A Geographical Profile of Livestock Manure Production in Canada, 2006*.

Tallin, JE, DE Pufahl, and SL Barbour. 1990. "Waste Management Schemes of Potash Mines in Saskatchewan." *Canadian Journal of Civil Engineering* 17: 528–42.

Taylor, A W, A W Frazier, E L Gurney, and J P Smith. 1963. "Solubility Products of Di- and Trimagnesium Phosphates and the Dissociation of Magnesium Phosphate Solutions." *Transactions of the Faraday Society* 59: 1585. http://xlink.rsc.org/?DOI=tf9635901585.

Taylor, A.W., A.W. Frazier, and E.L. Gurney. 1963. "Solubility Products of Magnesium Ammonium and Magnesium Potassium Phosphates." *Transactions of the Faraday Society* 59: 1580. http://xlink.rsc.org/?DOI=tf9635901580.

Tilley, E, J Atwater, and D Mavinic. 2008. "Effects of Storage on Phosphorus Recovery from Urine." *Environmental Technology* 29(7): 807–16. http://www.ncbi.nlm.nih.gov/pubmed/18697522 (October 1, 2013).

UN News Centre. 2013. *World Population Projected to Reach 9.6 Billion by 2050*. http://www.un.org/apps/news/story.asp?NewsID=45165#.VPd1E0LVmoU.

USGS. 2013. "PHREEQC (Version 3) - A Computer Program for Speciation, Batch-Reaction, One-Dimension Transport and Inverse Geochemical Calculations." http://wwwbrr.cr.usgs.gov/projects/GWC_coupled/phreeqc/index.html.

Viani, Alberto, Marta Perez-Estebanez, Simone Pollastri, and Alessandro F. Gualtieri. 2014. *Hydration Reaction Kinetics of Magnesium Potassium Phosphate Cements (chemically Bondend Magnesium Phosphate Ceramics)*.

Wang, Yujue, Xinyang Li, Limin Zhen, Heqing Zhang, Ying Zhang, and Chengwen Wang. 2012. "Electro-Fenton Treatment of Concentrates Generated in Nanofiltration of Biologically Pretreated Landfill Leachate." *Journal of Hazardous Materials* 229-230: 115–21. http://dx.doi.org/10.1016/j.jhazmat.2012.05.108.

Wilsenach, J.A., C.A.H. Schuurbiers, and M.C.M. van Loosdrecht. 2007. "Phosphate and Potassium Recovery from Source Separated Urine through Struvite Precipitation." *Water Research* 41(2): 458–66. http://www.ncbi.nlm.nih.gov/pubmed/17126877 (March 18, 2013).

Xu, Kangning, Chengwen Wang, Haiyan Liu, and Yi Qian. 2011. "Simultaneous Removal of Phosphorus and Potassium from Synthetic Urine through the Precipitation of Magnesium Potassium Phosphate Hexahydrate." *Chemosphere* 84(2): 207–12. http://www.ncbi.nlm.nih.gov/pubmed/21596418 (September 17, 2013).

Xu, Kangning, Chengwen Wang, Xiaoxue Wang, and Yi Qian. 2012. "Laboratory Experiments on Simultaneous Removal of K and P from Synthetic and Real Urine for Nutrient Recycle by Crystallization of Magnesium-Potassium-Phosphate-Hexahydrate in a Draft Tube and Baffle Reactor." *Chemosphere* 88(2): 219–23. http://www.ncbi.nlm.nih.gov/pubmed/22445958 (January 17, 2014).

Yang, Hexiong, and Henry J. Sun. 2004. "Crystal Structure of a New Phosphate Compound, Mg2KNa(PO4)2·14H2O." *Journal of Solid State Chemistry* 177(9): 2991–97. http://linkinghub.elsevier.com/retrieve/pii/S0022459604002142 (January 31, 2014).

Zeng, Le, and Xiaomei Li. 2006. "Nutrient Removal from Anaerobically Digested Cattle Manure by Struvite Precipitation." *Journal of Environmental Engineering Science* 294(November): 285–94.

Zhang, Hui. 2013. "Pilot Scale Application of Microwave Technology for Dairy Manure Treatment and Nutrient Recovery through Struvite Crystallization." University of British Columbia.

APPENDICES

Appendix A: Experiment 1: K-Struvite solubility product determination

This section references the work done in Chapter 5.

A1. Analysis of K-struvite for K_{sp-K} determination

Figure 24 and Figure 25 indicate that the K-struvite used for K_{sp-K} determination was pure with an Mg:K:P ratio of 1.02: 0.93:1 and a K-struvite being the single crystalline phase identified under XRD analysis.
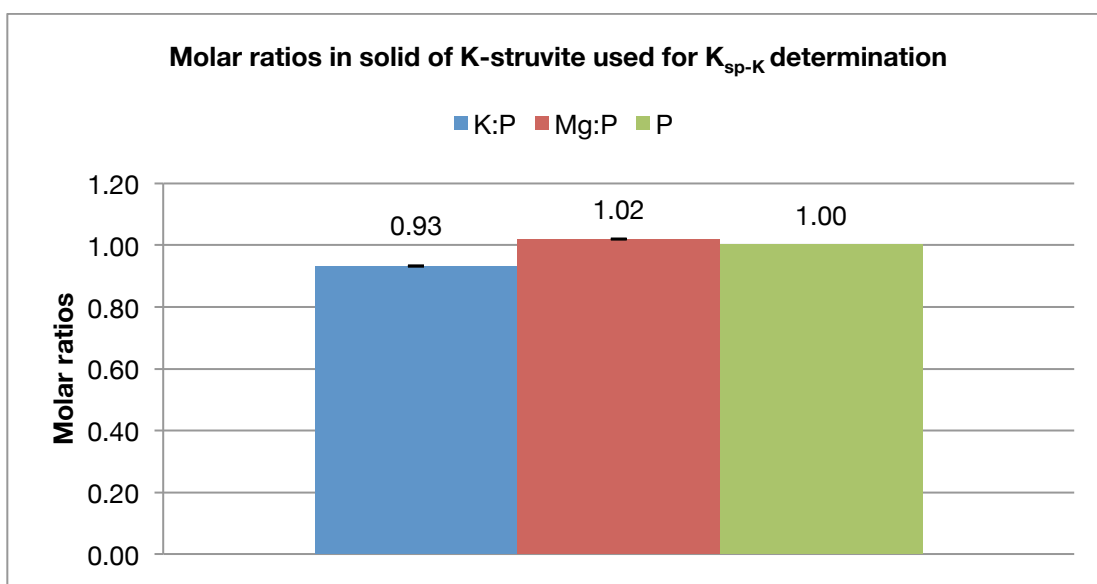
Figure 24 – Experiment 1: chemical analysis of K-struvite used for K_{sp-K} determination

K-struvite for Ksp

File: K-str Aline.raw - Start: 5.000 ° - End: 75.012 ° - Step: 0.019 ° - Step time: 36.4 s - Anode: Cu - WL1: 1.5406 - WL2: 1.54439 - kA2 Ratio: 0.5 - Generator kV: 40 kV - Generator mA: 40 mA - Creation
Operations: Import
01-075-1076 (N) - Magnesium Potassium Phosphate Hydrate - MgKPO4(H2O)6 - WL: 1.5406 - Orthorhombic - a 6.87300 - b 6.16000 - c 11.08700 - alpha 90.000 - beta 90.000 - gamma 90.000 - Primiti
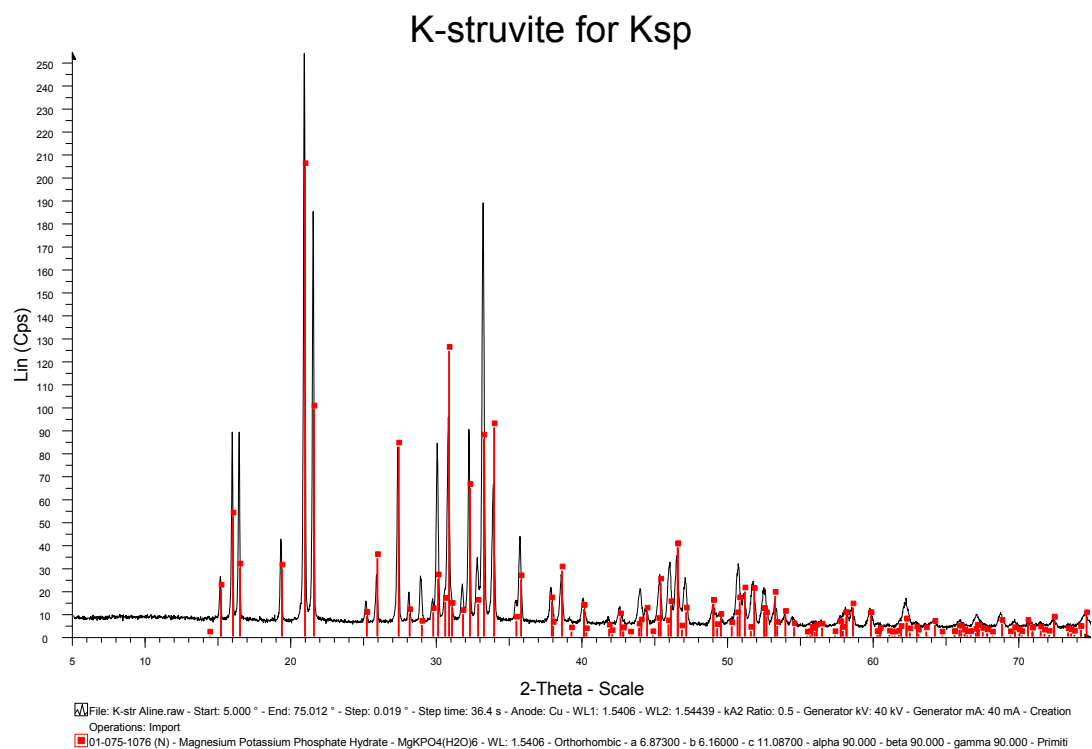
Figure 25 – Experiment 1: XRD analysis of K-struvite used for K_{sp-K} determination

A2. K_{sp-K} experimental data

The data in Table 15, Table 16 and Table 17 were generated in the K_{sp-K} experiments described in Chapter 5 and are given here for reference.

A2.1 Experiment 1A: K_{sp-K} experimental data at 10°C

Table 15 - Experiment 1A: K_{sp-K} experimental data at 10°C

K_{sp-K} experimental data at 10°C				
REACTOR A - SOLID SAMPLE COMPOSITION				
K:P	**Mg:P**	**P**	**Solid phases present**	
0.84	0.98	1.00	K-struvite	

REACTOR A - SOLUTION SPECIES CONCENTRATIONS (C_T^{meas})

Solution characteristics	P-PO$_4$		K		Mg	
	mM		**mM**		**mM**	
pH = 8.72	2.928	$C_{T, P-PO4}^{meas}$	85.623	$C_{T, K}^{meas}$	2.748	$C_{T, Mg}^{meas}$
T = 9.7 °C	2.922	2.711	82.270	94.756	2.774	2.741
EC = 9.9 mS/cm	2.922		82.508		2.783	
	2.483	σ^2	104.414	σ^2	2.679	σ^2
	2.479	0.05484	103.235	81.063	2.640	0.008854
	2.531		103.455		2.621	
			96.567		2.679	
			98.209		2.698	
			96.521		2.711	
					2.949	
					2.853	
					2.853	
					2.770	
					2.832	
					2.781	
					2.738	
					2.602	
					2.623	

REACTOR B - SOLID SAMPLE COMPOSITION				
K:P	**Mg:P**	**P**	**Solid phases present**	
0.83	0.98	1.00	K-struvite	

REACTOR B - SOLUTION SPECIES CONCENTRATIONS (C_T^{meas})					
Solution characteristics	**P-PO$_4$**		**K**		**Mg**	
	mM		**mM**		**mM**	
pH = 8.74	2.896	$C_{T, P-PO4}^{meas}$	101.780	$C_{T, K}^{meas}$	2.694	$C_{T, Mg}^{meas}$
T = 9.7 °C	2.889	2.684	99.902	98.891	2.684	2.702
EC = 9.9 mS/cm	2.889		98.854		2.715	
	2.483	σ^2	101.526	σ^2	2.664	σ^2
	2.495	0.05170	98.191	8.00161	2.638	0.005031
	2.453		99.734		2.653	
			101.281		2.613	
			94.534		2.641	
			94.222		2.668	
					2.910	
					2.809	
					2.703	
					2.687	
					2.737	
					2.752	
					2.747	
					2.648	
					2.680	

A2.2 Experiment 1B: K_{sp-K} experimental data at 25°C

Table 16 – Experiment 1B: K_{sp-K} experimental data at 25 °C

K_{sp-K} experimental data at 25°C					
REACTOR A - SOLID SAMPLE COMPOSITION					
K:P	**Mg:P**	**P**	**Solid phases present**		
0.86	0.98	1.00	K-struvite		

REACTOR A - SOLUTION SPECIES CONCENTRATIONS (C_T^{meas})					
Solution characteristics	**P-PO$_4$**		**K**		**Mg**	
	mM		**mM**		**mM**	
pH = 8.57	3.681	$C_{T, P-PO4}^{meas}$	86.552	$C_{T, K}^{meas}$	3.472	$C_{T, Mg}^{meas}$
T = 25.5 °C	3.649	3.346	85.209	98.299	3.497	3.499
EC = 7.3 mS/cm	3.649		84.344		3.532	
	3.119	σ^2	108.688	σ^2	3.498	σ^2
	2.964	0.121	107.361	102.927	3.367	0.00632
	3.013		106.085		3.499	

		106.156	3.476
		100.345	3.479
		99.954	3.437
			3.637
			3.536
			3.654
			3.540
			3.512
			3.560
			3.542
			3.396
			3.355

REACTOR B - SOLID SAMPLE COMPOSITION

K:P	Mg:P	P	Solid phases present
0.85	0.99	1.00	K-struvite

REACTOR B - SOLUTION SPECIES CONCENTRATIONS (C_T^{meas})

Solution characteristics	P-PO$_4$		K		Mg	
	mM		mM		mM	
pH = 8.51	4.004	$C_{T, P\text{-}PO4}^{meas}$	88.912	$C_{T, K}^{meas}$	3.602	$C_{T, Mg}^{meas}$
T = 25.5 °C	3.972	3.627	87.253	97.958	3.568	3.546
EC = 6.5 mS/cm	3.972		85.165		3.570	
	3.261	σ^2	107.896	σ^2	3.519	σ^2
	3.294	0.152	104.187	74.027	3.492	0.00858
	3.261		105.980		3.422	
			102.831		3.471	
			99.230		3.507	
			100.164		3.480	
					3.767	
					3.646	
					3.525	
					3.609	
					3.601	
					3.653	
					3.553	
					3.433	
					3.403	

A2.3 Experiment 1C: K_{sp-K} experimental data at 35°C

Table 17 - Experiment 1C: K_{sp-K} experimental data at 35°C

K_{sp-K} experimental data at 35°C						
REACTOR A - SOLID SAMPLE COMPOSITION						
K:P	**Mg:P**	**P**		**Solid phases present**		
0.64	1.11	1.00		K-struvite, Bobierrite		
REACTOR A - SOLUTION SPECIES CONCENTRATIONS (C_T^{meas})						
Solution characteristics	**P-PO$_4$**		**K**		**Mg**	
	mM		**mM**		**mM**	
pH = 10.17	7.0714	$C_{T, P-PO4}^{meas}$	111.9392	$C_{T, K}^{meas}$	0.0616	$C_{T, Mg}^{meas}$
T = 35.7°C	7.0714	6.3771	105.5092	117.9753	0.0615	0.0785
EC = 8.8 mS/cm	7.0714		107.4454		0.0611	
	5.6829	σ^2	126.3645	σ^2	0.0041	σ^2
	5.6829	0.5783	124.2289	59.6787	0.0000	0.008125
	5.6829		123.4104		0.0008	
			123.0140		0.0844	
			118.7861		0.0857	
			121.0804		0.0854	
					0.2624	
					0.2587	
					0.2633	
					0.0622	
					0.0594	
					0.0592	
					0.0000	
					0.0037	
					0.0000	
REACTOR B - SOLID SAMPLE COMPOSITION						
K:P	**Mg:P**	**P**		**Solid phases present**		
0.62	1.15	1.00		K-struvite, bobierrite		
REACTOR B - SOLUTION SPECIES CONCENTRATIONS (C_T^{meas})						
Solution characteristics	**P-PO$_4$**		**K**		**Mg**	
	mM		**mM**		**mM**	
pH = 10.05	7.7817	$C_{T, P-PO4}^{meas}$	114.3153	$C_{T, K}^{meas}$	0.0716	$C_{T, Mg}^{meas}$

T = 35.7 °C	7.7494	7.1682	108.5912	121.1420	0.0705	0.0889
EC = 8.9 mS/cm	7.7494		105.3174		0.0713	
	6.5870	σ^2	132.4518	σ^2	0.0148	σ^2
	6.5547	0.4208	127.0065	91.3577	0.0074	0.009175
	6.5870		129.4951		0.0000	
			126.2648		0.0967	
			125.3721		0.0953	
			121.4640		0.0957	
					0.2904	
					0.2723	
					0.2847	
					0.0717	
					0.0716	
					0.0728	
					0.0000	
					0.0000	
					0.0140	

A3. K_{sp-K} equilibrium concentrations data generated with PHREEQC

A3.1 Experiment 1A: equilibrium concentrations data generated with PHREEQC at 10°C

For reactor A, the objective function was minimized at pK_{sp-K} =11.075. For reactor B, the objective function was minimized at pK_{sp-K} =11.066.

Table 18 - Experiment 1A: K-struvite theoretical solution equilibrium concentration data generated with PHREEQC at 10°C for parallel reactors

K_{sp-K} model data at 10°C				
REACTOR A - SOLUTION SPECIES CONCENTRATIONS				
pK_{sp-K} range	$C_{T, P-PO4}^{theo}$ (mM)	$C_{T,K}^{theo}$ (mM)	$C_{T,Mg}^{theo}$ (mM)	Objective Function
10.5	6.1059	95.657	6.1059	1.48E+05
10.6	5.2855	94.845	5.2855	8.48E+04
10.7	4.5856	94.152	4.5856	4.46E+04
10.8	3.9868	93.559	3.9868	2.03E+04
10.9	3.4733	93.05	3.4733	7.03E+03
11	3.0319	92.613	3.0319	1.11E+03
11.05	2.8346	92.418	2.8346	1.16E+02
11.06	2.7969	92.38	2.7969	4.20E+01
11.07	2.7597	92.343	2.7597	5.14E+00
11.073	2.7486	92.332	2.7486	1.16E+00

11.074	2.745	92.329	2.745	5.62E-01
11.075	**2.7413**	**92.325**	**2.7413**	**3.02E-01**
11.076	2.7376	92.322	2.7376	3.99E-01
11.08	2.723	92.307	2.723	4.28E+00
11.09	2.6869	92.271	2.6869	3.78E+01
11.1	2.6513	92.236	2.6513	1.04E+02
11.15	2.481	92.067	2.481	8.81E+02
11.2	2.3226	91.91	2.3226	2.29E+03
11.3	2.0378	91.628	2.0378	6.46E+03
11.4	1.7905	91.384	1.7905	1.18E+04
11.5	1.5754	91.171	1.5754	1.78E+04
11.6	1.3879	90.985	1.3879	2.39E+04

REACTOR B - SOLUTION SPECIES CONCENTRATIONS				
pK_{so^*} range	$C_{T,\text{P-PO4}}^{theo}$ (mM)	$C_{T,K}^{theo}$ (mM)	$C_{T,Mg}^{theo}$ (mM)	Objective Function
10.5	5.9308	95.589	5.9308	4.16E+05
10.6	5.1363	94.802	5.1363	2.36E+05
10.7	4.458	94.13	4.458	1.23E+05
10.8	3.8776	93.555	3.8776	5.50E+04
10.9	3.3795	93.062	3.3795	1.83E+04
11	2.9511	92.638	2.9511	2.46E+03
11.05	2.7596	92.448	2.7596	1.30E+02
11.06	2.7229	92.412	2.7229	1.72E+01
11.064	2.7084	92.398	2.7084	2.11E+00
11.065	2.7048	92.394	2.7048	9.69E-01
11.066	**2.7012**	**92.39**	**2.7012**	**8.60E-01**
11.067	2.6976	92.387	2.6976	1.78E+00
11.07	2.6868	92.376	2.6868	1.08E+01
11.075	2.669	92.358	2.669	4.58E+01
11.08	2.6512	92.341	2.6512	1.06E+02
11.09	2.6162	92.306	2.6162	2.99E+02
11.1	2.5816	92.272	2.5816	5.85E+02
11.11	2.5476	92.238	2.5476	9.59E+02
11.15	2.4162	92.108	2.4162	3.27E+03
11.2	2.2622	91.956	2.2622	7.73E+03
11.3	1.9854	91.682	1.9854	2.05E+04
11.4	1.745	91.444	1.745	3.66E+04
11.5	1.5358	91.236	1.5358	5.43E+04
11.6	1.3533	91.056	1.3533	7.26E+04

A3.2 Experiment 1B: equilibrium concentrations data generated with PHREEQC at 25°C

For reactor A, the objective function was minimized at pK_{sp-K} =10.976. For reactor B, the objective function was minimized at pK_{sp-K} =11.026.

Table 19 – Experiment 1B: K-struvite theoretical solution equilibrium concentration data generated with PHREEQC at 25°C for parallel reactors

K_{sp-K} model data at 25°C			
REACTOR A - SOLUTION SPECIES CONCENTRATIONS			
pK_{sp-K} range	$C_{T, P-PO4}^{theo}$ (mM)	$C_{T,K}^{theo}$ (mM)	$C_{T,Mg}^{theo}$ (mM)	Objective Function
10.5	6.99	96.284	6.99	3.06E+05
10.6	6.0163	95.32	6.0163	1.59E+05
10.7	5.1909	94.502	5.1909	7.18E+04
10.8	4.4896	93.808	4.4896	2.46E+04
10.9	3.8922	93.216	3.8922	3.88E+03
10.95	3.627	92.953	3.627	4.13E+02
10.96	3.5764	92.903	3.5764	1.52E+02
10.97	3.5266	92.854	3.5266	2.08E+01
10.973	3.5119	92.839	3.5119	5.81E+00
10.974	3.5069	92.834	3.5069	3.19E+00
10.975	3.502	92.83	3.502	1.85E+00
10.976	**3.4971**	**92.825**	**3.4971**	**1.71E+00**
10.977	3.4922	92.82	3.4922	2.77E+00
10.978	3.4874	92.815	3.4874	4.98E+00
10.979	3.4825	92.81	3.4825	8.43E+00
10.98	3.4776	92.805	3.4776	1.31E+01
10.99	3.4293	92.758	3.4293	1.23E+02
11	3.3818	92.711	3.3818	3.46E+02
11.05	3.1548	92.486	3.1548	2.97E+03
11.1	2.9446	92.278	2.9446	7.71E+03
11.2	2.5692	91.906	2.5692	2.17E+04
11.3	2.2458	91.586	2.2458	3.94E+04
11.4	1.9666	91.309	1.9666	5.89E+04
11.5	1.7249	91.07	1.7249	7.90E+04
11.6	1.5152	90.862	1.5152	9.88E+04

	REACTOR B - SOLUTION SPECIES CONCENTRATIONS			
pK_{sp-K} range	$C_{T, P-PO4}^{theo}$ (mmol/L)	$C_{T,K}^{theo}$ (mmol/L)	$C_{T,Mg}^{theo}$ (mmol/L)	Objective Function
10.5	7.6519	97.344	7.6519	2.30E+05
10.6	6.5774	96.28	6.5774	1.25E+05
10.7	5.6677	95.379	5.6677	6.14E+04
10.8	4.8958	94.615	4.8958	2.48E+04
10.9	4.2391	93.964	4.2391	6.55E+03
10.95	3.948	93.676	3.948	2.20E+03
10.97	3.8378	93.567	3.8378	1.16E+03
11.00	3.6789	93.409	3.6789	2.41E+02
11.02	3.577	93.309	3.577	1.34E+01
11.024	3.557	93.289	3.557	1.95E+00
11.025	3.5521	93.284	3.5521	8.04E-01
11.026	**3.5471**	**93.279**	**3.5471**	**3.09E-01**
11.027	3.5421	93.274	3.5421	4.96E-01
11.028	3.5372	93.269	3.5372	1.34E+00
11.029	3.5322	93.264	3.5322	2.88E+00
11.03	3.5273	93.259	3.5273	5.04E+00
11.04	3.4783	93.211	3.4783	6.27E+01
11.05	3.4301	93.163	3.4301	1.83E+02
11.1	3.1998	92.935	3.1998	1.63E+03
11.2	2.7888	92.528	2.7888	7.82E+03
11.3	2.4354	92.178	2.4354	1.68E+04
11.4	2.1307	91.876	2.1307	2.73E+04
11.5	1.8673	91.615	1.8673	3.84E+04
11.6	1.639	91.389	1.639	4.96E+04

A3.3 Experiment 1C: equilibrium concentrations data generated with PHREEQC at 35°C

The data generated in PHREEQC for K_{sp-K} experiment at 35°C is presented slightly differently from the data at 10 and 25°C because of the two solid phases present in solution, K-struvite and bobierrite, at the end of the retention time. This introduces two variables, the K_{sp-K}, and the saturation condition of bobierrite. The objective function becomes a three dimensional function and needs to be minimized for both those variables.

The range of potential pK_{sp-K} was narrowed to between 10.87 and 10.92 through analyzing local minimums of the objective function. Table 20 below gives the objective function as a function of the pK_{sp-K} and the saturation index of bobierrite for this range. Each potential pK_{sp-K} value has a local minimum at a certain saturation condition for bobierrite. We are interested in the absolution minimum, indicating K-struvite in equilibrium with the solution. For Reactor A, there

is an absolute minimum at OF=2.86E^{-2} where the pK$_{sp-K}$ is set to 10.89. For Reactor B, there is an absolute minimum at OF=1.91E^{-2} where the pK$_{sp-K}$ is set to 10.90.

These tables were used to generate the figures in Chapter 5, section 5.3.3.

Table 20 – Experiment 1C: objective function calculated as a function of bobierrite SI and K-struvite pK$_{sp-K}$ for theoretical equilibrium concentrations data generated with PHREEQC at 35°C for parallel reactors

K$_{sp-K}$ model data at 35°C					
REACTOR A - SOLUTION SPECIES CONCENTRATIONS					
Bobierrite SI	**Range of potential pK$_{sp-K}$ values**				
	10.87	**10.88**	**10.89**	**10.9**	**10.91**
1.55		-	4.82E+00	2.58E+00	1.21E+00
1.56	**OBJECTIVE FUNCTION**	-	3.86E+00	1.92E+00	8.22E-01
1.57	-	-	3.01E+00	1.37E+00	5.32E-01
1.58	-	-	2.27E+00	9.17E-01	3.36E-01
1.59	-	-	1.64E+00	5.65E-01	2.31E-01
1.6	-	-	1.12E+00	3.10E-01	**2.15E-01**
1.61	-	-	7.07E-01	1.51E-01	2.85E-01
1.62	-	-	3.92E-01	**8.38E-02**	4.41E-01
1.63	-	9.64E-01	1.75E-01	1.07E-01	6.79E-01
1.64	-	5.85E-01	5.48E-02	2.19E-01	9.99E-01
1.65	1.34E+00	3.09E-01	**2.86E-02**	4.17E-01	1.40E+00
1.66	8.96E-01	1.32E-01	9.45E-02	-	-
1.67	5.56E-01	**5.42E-02**	2.51E-01	-	-
1.68	3.22E-01	7.19E-02	4.95E-01	-	-
1.69	1.89E-01	1.83E-01	8.26E-01	-	-
1.7	**1.56E-01**	3.87E-01	-	-	-
1.71	2.21E-01	-	-	-	-
1.72	3.81E-01	-	-	-	-
1.73	6.35E-01	-	-	-	-
1.74	9.82E-01	-	-	-	-
1.75	1.42E+00	-	-	-	-

REACTOR B - SOLUTION SPECIES CONCENTRATIONS						
Bobierrite SI	**Range of potential pK$_{sp-K}$ values**					
	10.87	**10.88**	**10.89**	**10.90**	**10.91**	**10.92**
1.55		-	1.71E+01	9.86E+00	4.87E+00	1.86E+00
1.56	**OBJECTIVE FUNCTION**	-	1.43E+01	7.84E+00	3.55E+00	1.16E+00

1.57	-	-	1.18E+01	6.08E+00	2.45E+00	6.55E-01
1.58	-	-	9.53E+00	4.56E+00	1.57E+00	3.49E-01
1.59	-	-	7.55E+00	3.27E+00	8.96E-01	**2.32E-01**
1.6	-	1.15E+01	5.82E+00	2.20E+00	4.29E-01	2.99E-01
1.61	-	9.28E+00	4.32E+00	1.35E+00	1.59E-01	5.43E-01
1.62	-	7.33E+00	3.07E+00	7.19E-01	**7.97E-02**	9.59E-01
1.63	-	5.63E+00	2.04E+00	2.89E-01	1.86E-01	1.54E+00
1.64	-	4.18E+00	1.23E+00	5.77E-02	4.71E-01	2.29E+00
1.65	7.20E+00	2.96E+00	6.31E-01	**1.91E-02**	9.29E-01	3.19E+00
1.66	5.54E+00	1.97E+00	2.42E-01	1.67E-01	1.56E+00	-
1.67	4.12E+00	1.20E+00	**5.23E-02**	4.96E-01	2.35E+00	-
1.68	2.94E+00	6.41E-01	5.73E-02	1.00E+00	3.30E+00	-
1.69	1.99E+00	2.94E-01	2.51E-01	1.68E+00	4.40E+00	-
1.7	1.26E+00	**1.50E-01**	6.27E-01	2.51E+00	5.65E+00	-
1.71	7.54E-01	2.01E-01	1.18E+00	3.52E+00	-	-
1.72	4.53E-01	4.43E-01	1.91E+00	4.67E+00	-	-
1.73	**3.57E-01**	8.70E-01	2.80E+00	5.98E+00	-	-
1.74	4.58E-01	1.48E+00	3.85E+00	7.43E+00	-	
1.75	7.52E-01	2.26E+00	5.07E+00	9.03E+00	-	

Appendix B: Experiment 3: K-struvite reactor data

This section references the work done in Chapter 7.

B1. K-struvite reactor run results

Table 21 - Experiment 3: feed K, Mg and P solution concentrations, pH and S_K

Sample date	K (mM)	Mg (mM)	P-PO$_4$ (mM)	pH	S_K
Sep 11 AM	338.56	21.38	7.77	2.32	7.37E^{-4}
Sep 12 AM	335.49	21.39	7.82	2.29	7.37E^{-4}
Sep 13 AM	319.53	21.29	7.89	2.27	7.11E^{-4}
Sep 14 AM	326.40	21.70	7.99	2.28	7.37E^{-4}
Sep 15 AM	309.68	21.23	7.59	2.38	7.18E^{-4}
Sep 16 AM	327.35	20.89	7.74	2.40	7.37E^{-4}
Sep 17 AM	319.32	20.59	7.74	2.19	7.11E^{-4}
Sep 18 AM	321.29	21.37	7.91	2.31	7.11E^{-4}
Sep 19 AM	318.88	21.67	6.81	2.35	7.11E^{-4}
Sep 20 PM	335.16	21.77	8.06	2.26	7.37E^{-4}
Sep 21 AM	339.25	21.65	8.05	2.37	7.37E^{-4}

Table 22 – Experiment 3: in-reactor K, Mg and P solution concentrations, pH and S_K

Sample date	K (mM)	Mg (mM)	P-PO$_4$ (mM)	pH	S_K
Sep 10 PM	307.22	13.65	1.38	8.80	1.52
Sep 11 AM	288.48	8.53	0.03	8.00	2.04E^{-1}
Sep 11 PM	300.18	14.14	0.04	10.90	1.68
Sep 12 AM	313.93	20.30	4.07	8.23	1.46
Sep 13 AM	318.91	26.75	13.23	8.45	2.70
Sep 14 AM	290.20	14.25	0.10	8.59	5.42E^{-1}
Sep 15 AM	305.03	21.97	9.00	1.52	1.73E^{-4}
Sep 16 AM	305.31	14.01	1.12	7.85	6.70E^{-1}
Sep 17 AM	300.65	12.08	0.08	7.80	2.60E^{-1}
Sep 18 AM	296.86	19.04	6.40	7.75	1.15
Sep 19 AM	296.15	17.96	4.80	7.66	9.74E^{-1}
Sep 20 PM	318.87	16.20	2.45	8.29	1.28
Sep 21 AM	297.62	11.68	0.09	8.96	6.66E^{-1}
Sep 22 AM	297.14	16.01	3.60	7.66	8.64E^{-1}

Table 23 – Experiment 3: seed hopper K, Mg and P solution concentrations, pH and S_K

Sample Date	K (mM)	Mg (mM)	P-PO$_4$ (mM)	pH	S_K
Sep 10 PM	268.68	17.87	4.04	9.9	2.23
Sep 11 AM	295.11	11.33	0.03	10.12	0.91
Sep 11 PM	295.92	11.98	0.06	10.34	1.33
Sep 12 AM	317.92	13.39	0.03	7.13	1.23
Sep 13 AM	313.43	20.94	4.49	5.58	0.63
Sep 14 AM	318.86	22.72	9.22	10.3	0.13
Sep 15 AM	280.12	13.18	0.03	3.1	1.18
Sep 16 AM	312.78	22.20	8.52	10.5	$2.80E^{-3}$
Sep 17 AM	299.56	12.21	0.03	8.52	1.30
Sep 18 AM	292.79	13.59	0.73	7.47	0.98
Sep 19 AM	292.73	19.13	6.47	7.63	0.93
Sep 20 PM	291.55	17.31	4.48	8.29	0.92
Sep 21 AM	293.43	13.85	0.96	8.96	0.91
Sep 22 AM	293.01	12.88	0.33	7.66	1.05

Table 24 – Experiment 3: effluent K, Mg and P solution concentrations, pH and S_K

Sample Date	K (mM)	Mg (mM)	P-PO$_4$ (mM)	pH	S_K
Sep 10 PM	270.28	11.66	0.12	9.9	0.27
Sep 11 AM	262.80	12.49	0.03	10.16	1.44
Sep 11 PM	310.28	11.43	0.02	10.37	1.07
Sep 12 AM	308.87	19.56	1.48	7.55	1.06
Sep 13 AM	332.37	28.14	14.04	5.57	0.63
Sep 14 AM	289.39	13.29	0.04	10.4	0.15
Sep 15 AM	307.17	22.18	9.22	3.09	1.38
Sep 16 AM	294.98	12.02	0.04	10.45	$2.82E^{-3}$
Sep 17 AM	291.50	13.68	0.80	8.37	1.39
Sep 18 AM	289.07	18.50	6.04	7.47	0.90
Sep 19 AM	286.38	16.77	4.16	7.64	0.90
Sep 20 PM	304.71	14.34	1.24	8.25	0.91
Sep 21 AM	293.15	13.11	0.59	8.74	0.98

Table 25 - Experiment 3: recovery of K, Mg and P during initial UBC-FBR run

Sample Date	K (mM)	Mg (mM)	P-PO$_4$ (mM)	%K recovery	%Mg recovery	%P recovery
Sep 11 AM	75.76	8.88	7.75	22.38	41.56	99.65
Sep 12 AM	26.62	1.83	6.35	7.93	8.56	81.15
Sep 14 AM	30.14	8.00	7.85	9.43	37.59	99.44
Sep 15 AM	19.23	0	0	5.89	0.00	0.00
Sep 16 AM	14.70	9.21	7.54	4.75	43.37	99.45
Sep 17 AM	35.85	7.21	6.93	10.95	34.50	89.64
Sep 18 AM	30.25	2.10	1.71	9.47	10.18	22.03
Sep 19 AM	34.91	4.61	3.75	10.87	21.56	47.41
Sep 20 PM	14.17	7.34	5.57	4.44	33.85	81.76
Sep 21 AM	42.01	8.66	7.46	12.53	39.79	92.65
Sep 22 AM	64.25	6.63	5.47	18.94	30.61	67.88

Appendix C: Potash mining

This section is additional to the information presented in Chapter 2.

C1. Potash mining

Production of phosphorus and potassium rely on mining ore deposits from the earth's crust whereas production of nitrogen fertilizers relies on fixing elemental nitrogen from the atmosphere through the Haber-Bosch process. Potash ore is extracted from two major ore deposit types: deeply buried marine deposits that typically range from 400 to 1000 metres below the surface, and surface brine deposits associated with saline water bodies. The world mine production of potash for 2011 was 37,000,000 tonnes. Most potash is extracted through conventional underground methods. Solution mining is used when underground deposits are irregular and very deep. Evaporation of brine in shallow salt lakes is also used to harvest potassium minerals. Solution mining is currently used at a number of North American operations, which rely on the differences in solubility of KCl compared to NaCl. Solution mining allows extraction at greater depths than conventional underground mining methods.

Saskatchewan potash mines have a recovery rate of approximately 80-85% (Godwin 2014). Potash ore is predominantly NaCl (halite), KCl (sylvite) and 1-5% insolubles. For everyone tonne of KCl that is refined, two tonnes of NaCl are produced (Tallin, Pufahl, and Barbour 1990). With reserves lasting hundreds of years, in Canada alone, this produces a serious brine issue. The major constituents of brine recovered from potash operations are Na, K, and Cl with lesser amounts of Ca, Mg, HCO_3 and SO_4. The brines from mines extracting the Esterhazy Member ore are significantly richer in Mg because of the presence of carnallite. Ca, Mg, HCO_3 and SO_4 are derived from partial solution of minerals such as dolomite, anhydrite and gypsum found in potash ores.

Brines are made up of coarse and fine tailings. The coarse tailings account for about 45% of total tailings, and are primarily made up of NaCl. Fine tailings account for about 55% of tailings and are made up of about 35-45% NaCl, 40-50% anhydrite and other silicates, and 10-20% KCl (Godwin 2014).

There are brine sources that contain commercial tonnages of potash, but potash tailings brine can contain anywhere from 1-10% KCl depending on your source, which is quite dilute and any recovery of potash from the brine tailings requires a further concentrating step such as solar evaporation (Garrett 1996).

C2. Composition of potash tailings

Potash tailings are potentially interesting as a potassium source for K-struvite production. Tailings composition data was collected through personal communication with Jonathan Godwin (2014) (Process Engineer for Teck Resources) and the Saskatchewan Ministry of Environment, as well as using engineering estimates where required.

The major constituents of brine recovered from potash operations are sodium, potassium, and chloride with lesser amounts of calcium, magnesium, bicarbonates and sulfates. The brines from mines extracting the Esterhazy member ore are significantly richer in magnesium because of the presence of Carnallite. Calcium, magnesium, HCO_3 and SO_4 are derived from partial solution of minerals such as dolomite, anhydrite and gypsum found in potash ores.

We can calculate the potassium concentration in the tailings by knowing a few numbers and making a few engineering estimates.
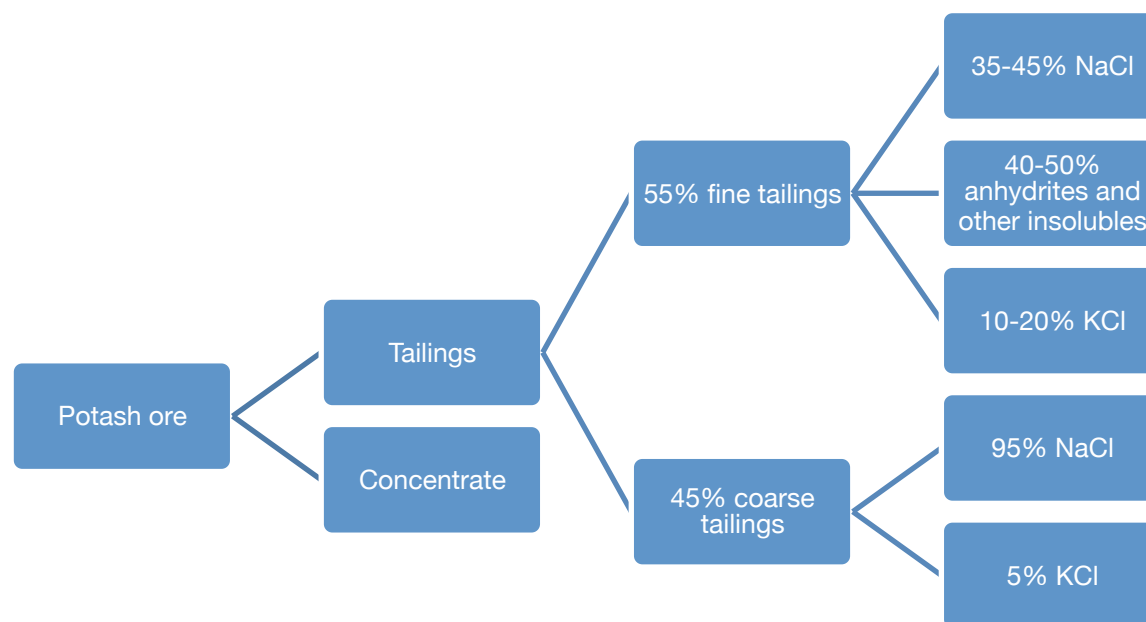

Figure 26 - Potash tailings composition for mines in Saskatchewan

The numbers:

- Fine tailings are approximately 35 weight% solids
- KCl density = 1.98 g/cm^3
- NaCl density = 2.16 g/cm^3
- Anhydrite density = 2.97 g/cm^3

Engineering assumptions:

- Assume soluble potassium would be in the fine tailings, since in the coarse tailings it would likely not be liberated from the ore material
- Calculate the potassium concentration as potassium in the fines, not overall tailings, since they are separated at a number of mining operations
- Fine tailings are like a 'slurry,' therefore we do not need a bulk density measurement, rather an overall solids density
- Use 40% NaCl, 15% KCl and 45% anhydrites as average 'fine tailings composition'

Given these numbers and assumptions we can calculate:

Density of solids component of fine tailings:

$$(0.15 \times 1.98) + (0.40 \times 2.16) + (0.45 \times 2.97) = 2.49 \ g/cm^3$$

Overall density of fine tailings:

$$(0.65 \times 1.0) + (0.35 \times 2.49) = 1.52 \ g/cm^3$$

With the density, we can estimate the volume of fine tailings we would have given initial 1000t of tailings:

$$\frac{(1000t \ tailings)(55\% \ fines)(1000 \frac{kg}{t})}{1.52 \ kg/L} = 3.6 \times 10^5 \ L$$

We can further estimate K⁺ concentration in the fine tailings:

$$\frac{(15t)\left(1000\frac{kg}{t}\right)\left(1000\frac{g}{kg}\right)(1000\frac{mg}{g})}{3.6 \times 10^5 \ L} = 4.2 \times 10^4 \frac{mg}{L}$$

The calculations estimate an average potassium concentration of 4.2×10^4 mg/L in the fine tailings. This is assuming that all the potassium is in soluble form in the tailings and fine and coarse tailings are separated.